Stony Brook University

Photo Cleavable Polymers for Tissue Engineering

A Dissertation Presented

By

Monica Apostol

The Graduate School

In Partial Fulfillment of the

Requirements

For the Degree of

Doctor of Philosophy

In

Material Science and Engineering

Stony Brook University

May 2011

Stony Brook University

The Graduate School

Monica Apostol

We, the dissertation committee for the above candidate for the

Doctor of Philosophy degree, hereby recommend

acceptance of this dissertation.

Dr. Miriam Rafailovich-Dissertation Advisor
Professor-Department of Material Science

Dr. Vladimir Jurukov-Chairperson of Defense
Adjunct Professor-Department of Material Science

Dr. Nadine Pernodet
Executive Director-Estee Lauder Companies, Inc.

Dr. Liliana George
Executive Director-Estee Lauder Companies, Inc.

This dissertation is accepted by the Graduate School

Lawrence Martin
Dean of the Graduate School

Abstract of the Dissertation

Photo Cleavable Polymers for Tissue Engineering

by

MONICA APOSTOL

Doctor of Philosophy

in

Materials Science and Engineering

Stony Brook University

2011

We have found that P_4VP and PMMA thin films can be etched with UVA radiation. Furthermore, we also found that dermal fibroblasts could be cultured successfully on the P_4VP polymer, with a doubling time comparable to tissue culture Petri dish standards. Consequently we were able to grow tissue on P_4VP substrates which could easily be lifted using UVA radiation. The cells that were removed were then re-plated at a lower density and a series of assays was performed at 3 and 6 days. While only a small amount of damage was discernable at day 3 nearly complete recovery was observed at day 6. The technique was also used to pattern areas within the tissue, where other types of cells could be inserted. In order to demonstrate the technique, a hybrid tissue layer was produced, where the dermal fibroblasts in a circular area at the center of the sample were removed via exposure through a mask. A keratinocyte layer was inserted which adhere to the fibroblast layer forming a tissue with integrated layers of two distinct cell types.

We also investigated the effects of coated TiO_2 particles on cells exposed to UVC. We found that as expected, cells were adversely affected by exposure to UVC and died even after exposure to as little as 3.5 J/cm^2. Addition of 0.4mg/ml TiO2 particles that were uncoated did not provide protection, and the cells died at the same rate. Addition of 4mg/ml of coated TiO_2 on the other hand, did not affect cell viability in the absence of UV light and increased the viability after exposure to UVC radiation. In fact the cells containing the

coated particles were indistinguishable for the unexposed control samples even after exposure to as much as 7.1J/cm^2 of UVC.

Table of Contents

LIST OF FIGURES

square of the photosensitive polymer removed by UV light. After 4 hours exposure the polymer removed was 38nm.

Figure2.8: EDAX composition of tri-block copolymer:
(a) AFM shows the uniform patterns of the mask transferred onto the polymer coated silica wafer.
(b) Different regions analyzed by EDAX, imaged by AFM.
(1, 2, 3) SEM determines the composition of the polymer in three different areas:
1) In the exposed aria where the polymer was reacting under UVC light, the spectrum indicates very low carbon and oxygen peak.
2) The aria near the aria covered by TEM grid shows small carbon, oxygen peak.
3) The aria covered by TEM grid shows the presence of photo-sensitive polymer. The spectrum indicates large carbon and oxygen peak comparable with the unexposed sample as references.

Figure2.9: SEM Analysis of UV-Exposed PS Films **a**) unexposed photosensitive polymer coated silica wafer shows a large oxygen peak at 0,5keV.This is the control data. b) The PS film on top of photosensitive polymer coated silica wafer indicates that a small oxygen peak is visible at 0.5keV. c) Un-flipped PS film after exposure to UVC light shows no oxygen peak at 0.5keV. Un-flipped PS film means that after exposure to UV light, the PS film was lifted exact as it was and floated onto a clean Si wafer.d) Flipped PS film after exposure to UVC light shows no oxygen peak at 0.5keV. Flipped PS film means that after exposure to UV light, the PS film was flipped, so the bottom was facing upwards. These results show that no residue of PMMA was left on the polystyrene film.

Figure 3.1: Etching rate of PMMA, P_4VP, and P_4VP/PMMA polymers exposed to the following radiation: (a) 3.98mW/cm2 of UVC, (b) 1.44 mW/cm2 of UVA and (c) contact angle of P_4VP surfaces exposed to different UVA doses.

Figure 3.2: Neonatal dermal fibroblast were plated with an initial density of 3000 cells/cm^2 on P_4VP, PMMA, P_4VP/PMMA substrates and the control sample was plated on tissue culture Petri dish plastic. (a) The growth curves obtained on the different substrates and (b) the doubling time calculated from the data in (a).

Figure 3.3: Confocal microscope images of the neonatal dermal fibroblast obtained on day three after platting 3000 cell/cm^2. The actin fibers were stained with Alexaflour Phalloidin 488 and the nuclei are stained with Propidium Iodide. The cells were plated on different substrates (a) PMMA, (b) P_4VP, (c) P_4VP/PMMA and (d) Tissue Culture Petri Dish.

Figure 3.4: (a) Proliferation of neonatal dermal fibroblasts plated on P_4VP at a density of 10^5cells/cm2 and irradiated with 1.44mW/cm2 of UVA for 15 minutes (1.3J/cm2), 30 minutes (2.6J/cm2) and 60 minutes (5.2J/cm2). The control sample was not irradiated. Confocal microscopy images of the cells, stained with Alexaflour Phalloidin 488 and Propidium iodide. Phase-contrast (top view) microscopy image of the sheet of neonatal dermal fibroblasts detached after (b) 5 minutes of UVA exposure and (c) 30 minutes of UVA exposure. (d) Confocal microscope picture of the cell sheet removed after 30 minutes UVA exposure.

Figure 3.5: Schematic of the experimental sequence designed to measure the effects of 30 minutes exposure to UVA radiation (2.6 J/cm2) on cell proliferation, cells viability, mitochondrial function, ROS production and apoptosis.

Figure 3.6: Apoptosis detection assay of the cells according to schematic in figure 5 after incubation of day1 (a) unexposed sample, (b) sample exposed to 1.3J/cm^2 and (c) sample exposed to 2.6 J/cm^2. Cells viability was assayed by flow cytometry after annexinV-FITC/propidium iodide staining. Numbers indicated express viable cells (lower left quadrant) as a percentage of total cells.

Figure 3.7: Neonatal dermal fibroblasts plated on a P_4VP surface, lifted following exposure and then replated at a density of 12,500 cells/cm2, according to the schematic shown in fig 5. (a) Growth curve of the control (un-exposed sample) versus the samples exposed to UV irradiation. Confocal microscopy images of the cells stained with Alexaflour Phalloidin 488 and Propidium iodide and imaged on day 0 and day 6 following exposure; (b ,c) Unexposed control and (d, e) exposed for 30 minutes.

Figure 3.8: Alamar blue viability assays of the neonatal dermal fibroblast cells, removed from the P4VP surface via UVA exposure, re-plated according to fig 5 , measured on days (a) one (b) three and (c) six. The corresponding proliferation curve (d) and the doubling time (e).

Figure 3.9: Mitochondrial activity assays of the cells according to the schematic in figure 5 after incubation of (a) day 1 and (b) day 6.

Figure 3.10: Assay of ROS product formation of the cells according to schematic in figure 5 measured after (a) day 1 (b) day 2 and (c) day 6.

Figure 3.11: (a) Schematic of the experimental protocol used to produce tissue with adjacent areas composed of two distinct cell populations. Confocal images of a patterned tissue containing a central area of keratinocytes surrounded by dermal fibroblasts. (b) The dermal fibroblast area imaged immediately after removal of the circular central area, as shown in part a. (c) The central portion of the tissue imaged 24 hours after plating keratinocytes. Interfacial region between the two types of tissue is showing attachment of the keratinocytes to the dermal fibroblast layer. (d) High magnification image (63X) of figure (11c) presenting the keratinocytes plated on the UVA exposed area.

Figure 4.1 SEM images of rutile TiO2 nanoparticles.

Figure 4.2. Confocal Microscope pictures of neonatal dermal fibroblast coated with (a) 0.4mg/ml, (b) 0.8 mg/ml, (c) 4mg/ml, (d) 10mg/ml, (e) 40mg/ml and (f) 80mg/ml. (g) Proliferation of neonatal dermal fibroblast incubated with 4mg/ml rutile TiO2 nanoparticle versus un-coated control sample.

Figure 4.3 Confocal images of neonatal dermal fibroblast plated at the density of 100,000 cells/sample and incubated for 24 hours: a) control, unexposed sample versus b) exposed sample to 3.5J/cm2UV light.

Figure 4.4 Neonatal dermal fibroblast incubated for 24 hours with different concentrations of polymeric coated TiO2 a) 0.4mg/ml b) 0.8mg/ml, c) 4mg/ml, d) 10mg/ml,e) 40mg/ml, f) 80mg/ml exposed to 3.5J/cm2 UV light. (g) Unexposed sample at 4 mg/ml. The best concentration of polymeric TiO_2 is 4mg/ml.

Figure 4.5 Alamar blue of neonatal dermal fibroblast on (a) day1, (b) day4, and (c) day7 after UV light exposure. The samples were coated with 0.8mg/ml regular TiO_2 and 4mg/ml polymeric TiO_2. High concentration of polymeric coated particles protects the cells in the culture from UVC irradiation.

Figure 4.6 Alamar Blue of different concentration of neonatal dermal fibroblast coated with 10mg/ml polymeric TiO2 and irradiated with 30' UVC irradiation at 50cm and 6.5cm away from lamp. (a) day1, (b) day4 and (c) day7 after irradiation.

Figure 4.7 Alamar Blue of different concentration of neonatal dermal fibroblast coated with 0.4mg/ml polymeric TiO2 and irradiated with 30' UVC irradiation at 50cm and 6.5cm away from lamp. (a) day1, (b) day4 and (c) day7 after irradiation.

LIST OF SCHEMES:

List of Abbreviation

NIH	National Institute of Health
AHDF	Adult human dermal fibroblast
DMEM	Dulbecco's modified eagle's medium
ECM	Extracellular matrix
P_4VP	Poly (4-vinyl pyridine)
P_4VP-PMMA	Poly [4-vinylpyridine]- poly [methyl methacrylate]
PVPK	Poly (vinyl phenyl ketone)
PMMA	Poly (methyl methacrylate)
P_4VP-PVPK-PMMA	Poly [4-vinylpyridine]-poly(phenylvinylketone)- poly [methylmethacrylate]
UV/VIS	Ultraviolet/Visible
UVA, UVB, UVC	Ultraviolet A, B, C
TiO_2	Titanium dioxide
NH_4OH	Ammonium Hydroxide
H_2O_2	Hydrogen Peroxide
HF	Hydrofluoric acid
H_2SO_4	Sulfuric Acid
DMF	Dimethylformamide
TEM	Transmission Electronic Microscope
SEM	Scanning Electronic Microscope

ACKNOWLEDGEMENT

Be humble and perseverant!

This is the greatest lesson which I have learned during the PhD program at Stony Brook University. Over the past five years in Stony Brook, many of the greatest people have inspired me to perform valuable work. First, my advisor, Professor Miriam Rafailovich, is my mentor for knowledge, creativity and research guidance. I sincerely thank Dr. Rafailovich for the opportunity to be her PhD student.

Next, I thank Dr. Nadine Pernodet for her mentoring and her guidance during my research. Thank you for giving me the honor in working with her.

I greatly thank Dr. Liliana George for her generous assistance, discussions and suggestions during my research as well as her support. I thank my laboratory members and colleagues for their constant help and encouragement Kathy Kretzschmar and Craig Tadlock, Dr. Marina Sokolinsky, Dr. Vasile Ionita-Manzatu, Terry Azer, Saul Micklean.

My special thanks go to Tatsiana Mironava and Dr. Jim Queen for their technical training and support.

Finally, I would like to thank my husband and my parents for their support, love and encouragement. I especially thank my husband for his love, consideration, patience and support and my son Cristinel who is the best gift I ever got in my life. My husband is my best of best friend and companion in life. Since his love and encouragement have driven a completion of my dissertation, I hereby dedicate this dissertation to my husband, Cristian.

Chapter 1

Introduction

1.1 Background

Tissue engineering is used to mimic natural biological organ functions by combining biology, materials science in order to replace damaged tissues or improve their functions.

A commonly applied definition of tissue engineering as stated by Lander and Vacanti, is an interdisciplinary field that applies the principles of engineering and life science toward the development of biological substitutes that restore, maintain, or improve tissue function or a whole organ [Langer, et.al 1993]. Tissue engineering has also been defined as understanding the principles of tissue growth, and applying this to produce functional replacement tissue for clinical use [Macarthur, et.al 2005].

National Institute of Health (NIH) defines tissue engineering/regenerative medicine like an emerging multidisciplinary field involving biology, medicine, and engineering that is likely to revolutionize the ways we improve the health and quality of life of millions of people worldwide by restoring, maintaining, or enhancing tissue and organ function.

Tissue engineering is used extensively in clinical procedures today. Probably the world's most successful tissue engineering work is based on the findings of Dr. Stephen Badylak. He demonstrated that sub mucosa derived from porcine small intestine or urinary bladder can be the source of scaffold material [Badylak, et.al 1993] [McPherson, et. al 1998].

Tissue engineering is based on a culture of cells or tissue isolated from an organism. Cell and tissue culture refer to the culturing of cells in vitro. Cell or tissue culturing is carried out under precisely controlled conditions, and generally requires the use of a growth medium [Madigan, et.al 2005]

There are different types of cells categorized by their source: autologous (cells are obtained from the same individual to which they will be re-implanted), allergenic (cells come from the body of a donor of the same species), xenogenic (cells are these isolated from individuals of another species), syngenic or isogenic (cells are isolated from genetically

identical organism, such as twins), primary (cells are from an organism), secondary (cells are from a cell bank) and stem cells (undifferentiated cells with the ability to divide in culture and give rise to different forms of specialized cells). Stem cells due to their pluri-potentiality and unlimited capacity for self-renewal, may allow significant advances for distinct reconstructive and cosmetic procedures. This review aims at outlining the principles of tissue engineering, focusing on the use of adult-derived stem cells as applied to the research and practice of plastic surgery [Hendrick, et.al 2003]

Also, by using autologous cells as well as stem cells to replace a tissue in the same person, we will avoid rejection of the implants or new organs and that will be associated to many other benefits (health care cost). Organ transplantation replaces a recipient's damaged or failing organ with functional tissue from a donor site. However, the critical shortage of organ donors, as well as, the risk of host rejection in patients who do receive organ transplants, had limited the medical practice of organ transplantation for decades [Yang, et. al 2005]. Engineering the production of transplantable tissues to replace donated organs would help reduce the massive death rate of patients on organ transplant waiting lists.

Various methods of isolating cells for ex-vivo culture are known. These include: purifying white blood cells from blood [Kanof, et.al 2001]; breaking down extracellular matrix with enzymes (mononuclear cells) [Celentano, et. al 1997].

Cells in culture may be manipulated to various ends, by various methods. At some point, some cells may be removed from the culture. The particular manipulation depends on whether the culture is in suspension or adherent. Some cells live without attaching to a surface and may be cultured in suspension. Cells of the blood stream are one example. The extraction is more difficult for the cells derived from solid tissues. Adherent cells require the breaking of bonds between identical cells or different types of cells and the proteins, and possibly, between the cells themselves.

First, the field of tissue engineering proposed to entirely replace the method of organ transplantation with artificially produced tissues [Langer and Vacanti, et. al 1993], and relies heavily on the use of biodegradable scaffolds [Griffith and Naughton, et. al 2002].

Based on the concept that cells seeded on these structures would regenerate native tissue in accordance with scaffold biodegradation, the re-creation of some tissues such as bone, heart valves, and cartilage has been successfully facilitated [Yang, et. al

2005].However, despite the successes yielded from seeding cells into scaffolds, there remain many limitations to this technique. We need a biodegradable scaffold, but also a scaffold that gives the right organization to the cells. For example, in the heart, cells are organized at 120 degrees orientation from one layer to another, and this has been a big challenge to reproduce. This is even without considering that there are different kinds of cells in an organ such as the heart (fibroblasts, cardiomyocytes) with a dense connective tissue [Shimizu, et. al 2002].

Furthermore, cell necrosis has been observed at the center of larger constructs, due to limits on the diffusion of nutrients and waste products [Yang, et. al 2005]. This is a critical issue in myocardial tissue engineering, where a sufficient supply of oxygen and nutrition is necessary to produce functional heart tissue [Shimizu, et. al 2003]. However, the biggest disadvantage to the use of biodegradable scaffolding is the strong, non-specific host inflammatory response that is induced upon biodegradation. It has been shown that the implantation of nearly all polymer materials will induce this response [Ronneberger, et. al 1990].

Another shortcoming of conventional tissue engineering methods is the loss of differentiated cell functions during cell harvesting. Typical cell harvesting techniques use proteolytic enzymes such as trypsin or dispase [Ito, et. al 1961] [Lorette, et.al 1999], which irreversibly damage cell surface proteins such as growth factor receptors, ion channels, and cell-to-cell junction proteins [Yang, et. al 2007].This result is an inability to build up constructs from differentiated cells. To challenge these shortcomings, cell sheet engineering has been proposed as a novel methodology to facilitate the non-invasive harvest of cultured cells as intact cell sheets (Yamato and Okano, 2004). Since the cell sheets harvested through this technique are recovered with intact cell-to-cell junctions and deposited extracellular matrix ,(ECM), whole cell sheets can be transferred to other tissue surfaces to produce versatile 2-D or 3-D tissues [Ng, et. al 2005]. Single cell sheets may be transferred directly to the host tissue to replace damaged skin or corneal tissue. Homogeneous cell sheets can be layered to create thick tissues such as myocardium, and heterogeneous cell sheets can be layered to form complex organs composed of various layers of highly differentiated tissue, such as the liver.

Cell sheet engineering advanced rapidly with the development of culture dishes covalently grafted with temperature-responsive polymers. According to the method of

Rheinwald and Green, keratinocytes are proliferated and made a multilayer on the grafted surfaces at 37°C. The multilayered keratinocytes sheets were detached from the grafted surfaces only by reducing temperature to 20°C without need of dispase [Masayuki, et. al 2001]. These culture surfaces allowed whole, contiguous cell sheets to spontaneously detach from the surface with a simple decrease in temperature [Kwon, et. al 1999]. This technique has been used to culture four layers of cardiomyocytes which successfully formed pulsatile myocardial tissue *in vitro* and *in vivo* [Shimizu, et. al 2002]. Also, epidermal keratinocytes have shown the maintenance of differentiated functions after cell sheet harvest [Yang, et. al 2007]. For example, biological soft tissue like brain and adipose are difficult to manipulate. This may cause soft tissue to collapse rather than dislodge or detach. [Olberding, et. al 2006).

Therefore, the creation of blood vessels to facilitate vascularization would not be possible using thermo-responsive culture surfaces due to the characteristic softness of the tissue. Furthermore, it has been noted that the hydrogels are not easily coated with polymers or other ECM proteins [Stampfl, et. al 2008], [Bayramoglu, et. al 2008]. Certain cell types, such as fibroblast requires specific proteins in order to adhere to the surface [Kurihara, et.al 2005]. For these cells we therefore require biocompatible substrates upon which these proteins are readily adsorbed and not pose a significant obstacle to cell sheet formation.

It is also sometimes desirable to grow tissue with different types of cells in a prescribed pattern formation. For example, one may want to place cells which promote angiogenesis amongst cells which promote other types of tissue. This is not possible with the thermo responsive surfaces, since the thermal response can not be concentrated in any specific region and thermal conduction does not allow exposure through a mask. On the other hand, specific patterns can be created on photo-cleavable surfaces using focused beams of light. Hence cells can be selectively removed and others inserted in a controlled manner. We therefore propose a new methodology for cell sheet harvesting and patterning which uses photo cleavable polymers. The major advantage of this technique is the fact that it can be used to pattern cell tissue, simply by exposing to UV light through a mask or writing selectively with a focused beam.

On the other hand, this technique has several major challenges which we were able to overcome; (a) The polymer substrate must be conducive to cell growth and attachment. (b) The energy density and frequency of the radiation must be sufficient to cleave the polymer,

yet low enough as not to cause significant damage to the cells. (c) Cleavage of the polymer must occur without release of residues which are toxic to the cell sheet.

In order to find the optimum polymer within these constraints, we proposed the following photo-cleavable polymers: poly [4-vinylpyridine] (P_4VP); poly [methylmethacrylate] (PMMA); the polymer 1:1 blend, poly [4-vinylpyridine]- poly [methylmethacrylate] (P_4VP-PMMA) and the tri-block copolymer poly [4-vinylpyridine]-poly(phenylvinylketone)- poly [methylmethacrylate] (P_4VP-PVPK-PMMA). We screened these polymers, using various biochemical assays for their influence on cell proliferation and rate of photo cleavage with doses of UVA. The UVA doses should be sufficiently low to have minimal influence on the cell response, and ease of cell detachment and subsequent viability. Even though the UV/VIS absorbance spectra of these commonly used polymers are well established, the absorption peaks tend to be in the UVB or UVC regions, which would also cause severe damage to cells. Here we showed that the peaks were sufficiently broad such that it was possible to achieve a small degree of photo cleavage even when they were irradiated with light in the 300nm region. Since cell attachment occurs on the surface, only a small amount of cleavage was sufficient to lift the cells, which also had the advantage of minimizing any chemicals which may be released after the cleavage. Since the only stimulus necessary for cell sheet harvesting using this methodology is light, no mechanical deformation occurs and it is possible to harvest cell sheets from hard, as well as soft tissues. Furthermore, the polymer we selected to demonstrate this principal, Poly (4-vinylpyridine) is shown to be biocompatible and support cell proliferation to the same extend as the industry standard tissue culture Petri dish plastic. P_4VP also has similar mechanical properties to polystyrene and hence may provide a commercially attractive alternative to TCP.

We propose to use a photo-active substrate, thin film composed of the polymers: poly (4-vinylpyridine) (P_4VP), polymethylmethacrylate (PMMA), the 1:1 blend P_4VP: PMMA and the tri-block copolymer: poly (4-vinylpyridine)-poly (vinylphenylketone)-polymethylmethacrylate (P_4VP-PVPK-PMMA) which can release either a fully or partially confluent layer of cells. The ideal substrate can also be engineered such that it does not leave any residue when the cells are removed, thereby minimizing inflammation. To prevent the inflammatory responses associated with biodegradable scaffolds, we also investigated whether the photo-reactive substance remained on the cell sheets after UV exposure. Without

leaving any residue we proposed a method where non-invasive harvesting of cell sheets is activated by photo-reactivity and the resulting cell sheets are assembled through layer-by-layer deposition to produce heterogeneous and multifunctional tissue. By eliminating limitations posed by traditional tissue engineering methods, we can manipulate non-invasively harvested cell sheets for 3-D tissue regeneration and transplantation.

Finally, we also demonstrated that the polymers could be irradiated through masks which allowed for cell efficient patterning of the tissue. Furthermore, the polymer we selected to demonstrate this principal, Poly (4-vinylpyridine) is shown to be biocompatible and support cell proliferation to the same extend as the industry standard tissue culture Petri dish plastic. P_4VP also has similar mechanical properties to polystyrene and hence may provide a commercially attractive alternative to TCP.

Since UV irradiation is required for removal of the cell sheet I investigated the influence of UV radiation on the cells.

We also investigated the effects of coated TiO_2 particles on cells exposed to UVC. We found that as expected, cells were adversely affected by exposure to UVC and died even after exposure to as little as 3.5 J/cm^2. Addition of 0.4mg/ml TiO2 particles that were uncoated did not provide protection, and the cells died at the same rate. Addition of 4mg/ml of coated TiO_2 on the other hand, did not affect cell viability in the absence of UV light and increased the viability after exposure to UVC radiation. In fact the cells containing the coated particles were indistinguishable for the unexposed control samples even after exposure to as much as $7.1J/cm_2$ of UVC.

1.2 References

[] Langer, R, Vacanti JP, Tissue Engineering. Science, 260, 920-6.1993.

[] Macarthur, B.D., Oreffo, Bridging the gap. R.O.C.Nature, 433, 19, 2005.

[] Badylak, SF. Small intestine sub mucosa (SIS): A biological conducive to smart tissue removed. Tissue engineering: current prospective. Cambridge, MA: Burkhauser Publishers, 1993.

[] McPherson T, Badylak SF. Characterization of fibronectin derived from porcine small intestine sub mucosa. Tissue Engineering 4:75-81, 1998.

[] Sterodimas A, Denair J, Correa WE, Pitaguy I, Tissue engineering in plastic surgery: an up to date review of the current literature, Ann. Plast. Surg. January; 62(1):97-103, 2009.

[] Thomas D. McKnight, Karel Riha, Dorothy E. Shippen, telomeres, telomerase and stability of the plant genome; Plant Molecular biology, vol 48, nr.4, march 2002.

[] Madigan M., Martinko J. (editors) Brosk Biology of Microorganism; 11th edition, Prentice Hall. ISBN 0131443291, 2005.

[] Kanof ME, smith PD, Zola H.; Isolation of whole mononuclear cells from peripheral blood and cord blood; Curr protoc. Immunol. May, chapter 7, unit 7.1, 2001.

[] Celentano DC, Frishman WH.; Matrix metalloproteinase and coronary artery disease: a novel therapeutic target; J.Ciln.Pharmacol. Nov; 37(11):991-1000, 1997.

[] Ito Y, Shinoda M; Influences of proteolytic enzymes on parotin IV. Separation of hydrolyzes in digested parofin by trypsin. (Studies on the physiological chemistry of the salivary glands). Endocr. J., Mar; 8:13-9, 1961.

[] Lorette C. Javois; Methods in Molecular Bilogy: Immunocytochemical Methods and Protocols, Second Edition, vol 115, 257-260, 1999.

[] Hendrick M, Daniels E., The use of stem cells in regenerative medicine; Clinics in Plastic Surgery, vol 30, issue 4, page 499-505, 2003.

[] Griffith, L.G., Naughton, G. "Tissue Engineering – Current Challenges and Expanding Opportunities." *Science.* 295 , 1009-1014, 2002.

[] Kushida, A., Yamato, M., Konno, C., Kikuchi, A., Sakurai, Y., Okano, T. "Temperature-responsive culture dishes allow non-enzymatic harvest of differentiated Madin-Darby canine kidney (MDCK) cell sheets." *J. Biomed. Mater. Res.* 51, 216-223, 2000.

[] Kwon, O.H., Kikuchi, A., Yamato, M., Sakurai, Y., Okano, T. "Rapid cell sheet detachment from Poly (*N*-isoproplyacrylamide)-grafted porous cell culture membranes." *J. Biomed. Mater. Res.* 50, 82-89, 2000.

[] Langer, R., Vacanti, J.P. "Tissue Engineering." *Science.* 260, 920-926. 1993.

[] Ng, K.W., Tham, W., Lim, T.C., Hutmacher, D.W. "Assimilating cell sheets and hybrid scaffolds for dermal tissue engineering." *J. Biomed. Mater. Res.* 75A, 425-438, 2005.

[] Ronneberger, B., Kao, W.J., Anderson, J.M., Kissel, T. "In vivo biocompatibility study of ABA triblock copolymers consisting of poly (L-lactic-co-glycolic acid) A blocks attached to central poly (oxyethylene) B blocks. *J. Biomed. Mater. Res.* 24, 529-545, 1990.

[] Shimizu, T., Yamato, M., Kikuchi, A., Okano, T. "Cell sheet engineering for myocardial tissue engineering." *Biomaterials*. 24 (2003): 2309-2316.

[] Soejima, K., Negishi, N., Nozaki, M., Sasaki, K. "Effect of cultured endothelial cells on angiogenesis in vivo." *Plast. Reconstr. Surg*. 1010, 1552-1560, 1998.

[] Yamato, M., Okano, T. “Cell Sheet Engineering.” *Materials Today*. 7, 42-47, 2004.

[] Yang, J., Yamato, M., Kohno, C., Nishimoto, A., Sekine, H., Fukai, F., Okano, T. “Cell sheet engineering: Recreating tissues without biodegradable scaffolds.” *Biomaterials*. 26 6415-6422, 2005.

[] Yang, J., YaRonneberger, B., Kao, W.J., Anderson, J.M., Kissel, T. “In vivo biocompatibility study of ABA triblock copolymers consisting of poly (L-lactic-co-glycolic acid) a blocks attached to central poly (oxyethylene) B blocks. *J. Biomed. Mater. Res*. 24, 529-545, 1990.

[] Yang, J., Yamato, M., Shimizu, T., Sekine, H., Ohashi, K., Kanzaki, M., Ohki, T., Nishida, K., Okano, T. “Reconstruction of functional tissues with cell sheet engineering.” *Biomaterials.* 28, 5033-5043, 2007.

[] Yamato, M., Shimizu, T., Sekine, H., Ohashi, K., Kanzaki, M., Ohki, T., Nishida, K., Okano, T. “Reconstruction of functional tissues with cell sheet engineering.” *Biomaterials.* 28, 5033-5043, 2007.

[] Masayuki Yamato, Mika Utsumi, Ai Kushida, Chie Konno, Akihiko Kikuchi, Teruo Okano. Tissue Engineering, 7(4): 473-480, 2001.

[] A. Welle, E. Gottwald, K.F. Weibezahn. Biomed Tech (Berlin), 47 Suppl. 1 Pt 1:401-3, 2002.

[] Olberding JE., Suh JKF "A dual optimization for the material parameter identification of a biphasic poroviscoelastic hydrogel: potential application to hypercompliant soft tissue" journal of Biomechanics, 30, 13, 2468-2475, 2006.

Chapter 2

Testing the photo-sensitivity properties of P_4VP, PMMA and P_4VP-PVPK-PMMA

2.1 Introduction

Intelligent polymers are included in the class of polymer systems that exhibit different physical changes in response to small external signaling stimuli [Okano, et.al 1998]. These polymers have been designed to respond to stimuli such as pH [Peppas,et.al 1991], temperature [Yoshida, et.al 1991,Yoshida,et.al 1992,Stayton, et.al 1995],ionic strength [Hosino, et.al 1989], electric field or current[Eisenberg, et.al 1984,Yuk, et.al 1992,Kwon,et.al 1991] and photo irradiation [Irie,et.al 1985,Ito,et al 1999] for application to drug delivery, biomaterials and biotechnology.

Chemical delivery systems that release biological active materials by cleavage of a chemical bond of suitable designed precursor molecules are currently being explored as an alternative to classical encapsulation techniques [Gautschi, et. al 2001]. The release of the active substances from their precursors in the targeted application may be triggered by a variety of reactions conditions such as the action of light [Rochat, 2000], [Plessis, 2001], enzymes or microorganism, hydrolysis, the change of temperature or pH.

Based on the very promising results obtained for the photo-chemical release of aldehydes and ketones from ά-keto esters [Rochat, 2000] [Plessis, 2001], [Kamogawa, 1982], [Enggist, 2001], [Herrmann, 2000], we decided to explore new photochemical delivery system for releasing the cells as a complete layer of a single cell type. Phenyl ketone derivatives are structurally closely related to ά-keto esters and undergo the same Norrish type II photo-fragmentation process.

Phenyl ketones have previously been used in organic synthesis for the preparation of alkenes [Neckers, 1971] or as photo-cleavable surfactants in the isolation and characterization of proteins [Epstein, 1982]. They may also be used for the release of perfumery chemicals in different types of detergents [Levrand, 2002].

We screened different types of polymers like: poly [4-vinylpyridine] (P_4VP), poly [methylmethacrylate] (PMMA), 1:1 blend of these two polymers (P_4VP-PMMA) and the tri-block copolymer: poly [4-vinylpyridine] $_{30}$, poly [vinylphenylketone] $_2$, poly [methylmethacrylate] $_{20}$ (P_4VP-PVPK-PMMA)

The polymers that were created have three basic properties: adhesion to a surface such as a Silicon wafer, activation and control under UV light, and biocompatibility. These three characteristics are essential for the role that this polymer will play in creating a controlled surface for cells to grow on. The chemical structure of photo-sensitive polymers is presented in Figure 2.1.

2.2 Materials and Methods

2.2.1 Materials

Poly (4-vinyl pyridine) and Poly (methylmethacrylate) were purchased from Aldrich from Milwaukee, WI, USA and used without further purification. Poly (vinyl phenyl ketone) is an amorphous solid with the melting point of 74-84°C (Aldrich). Solid and dissolved PVPK are normally used as polymeric photo-sensitizer (Daly, 1987).

The substrate is a silicone wafer coated with photo cleavable polymer. To be a suitable substrate, the photo cleavable polymer must adhere to the silicon wafer, but must otherwise be non-reactive with the polymer under incubation condition. Suitable silicone wafers are available from Wafer World, Inc. from West Palm Beach, Florida.

For this work, poly (4-vinyl pyridine) with molecular weight of 150,000-200,000 and poly (methylmethacrylate) with a molecular weight of 75,000 (Polyscience Corporation) were used.

2.2.2 Preparation of the Silicon Wafer

In order to use Silicon wafers as a surface, they must undergo a process that eliminates any interfering substances, particles, or scratches. The wafers were first cleaved, using tools such as a diamond cutter or a razor. Then they were immersed in trichloroethylene for three minutes in order to remove fingerprints or any heavy residues on wafer surface.

After rinsing the wafers with de-ionized water, they must then be sonicated in methanol for ten minutes to remove residual dust.

Then, in order to remove any organic contamination, the wafers were immersed in a freshly mixed solution of Ammonium Hydroxide (NH_4OH), Hydrogen Peroxide (H_2O_2), and De-ionized water in 1:1:4 ratios for ten minutes at 80°C.

As a post-cleaning check, the wafers were immersed one at a time in a solution of hydrofluoric acid (HF) and De-ionized water in 1:3 ratios for 30 seconds. Then they were rinsed thoroughly with a De-ionized water wash bottle. This step removes the SiO_2 and made the surface hydrophobic.

Next, the surfaces were immersed for ten minutes in a freshly mixed solution of Sulfuric Acid (H_2SO_4), Hydrogen Peroxide (H_2O_2), and De-ionized water at a temperature of 80º C in 1:1:4 ratios. This step removes any ionic or metallic impurities and creates a natural oxide layer (Modified Shirake method) [Shirake, 1986]. After rinsing thoroughly with de-ionized water and dried with Nitrogen gas, the surfaces are hydrophilic and ready to be use.

2.2.3. Spin-Casting and Annealing of the Photosensitive Polymer

Silicon wafers (1:0:0 orientation) were cleaved to achieve ~1×1 cm^2. The solution of the photosensitive polymer P_4VP-PVPK-PMMA was spun cast onto Si wafer at $2{,}5x10^3$ rpm for 30 seconds on a Headway Spin Coater. The coated wafers were transferred to an oil trapped vacuum oven at a pressure of 10^3 Torr for 24 hours at 150°-180°C.This process eliminates excess solvent and removes impurities from the polymer thin film. The oven, as well as any container holding the photosensitive wafers, was covered with aluminum foil to prevent photo-reactivity prior to intentional UV exposure. Annealing is essential for different reasons: to make a stable and uniform polymer layer, and to eliminate any trace of solvent which would be toxic for the cells, at the same time, it is giving a sterile surface.

If the specimen is annealed long enough, it will become homogeneous and the net flow of matter will cease. Given the problem of obtaining a flux equation for this kind of a system, it will take the flux across a given plan to be proportional to the concentration gradient across that plan. The flux can be described by the equation:

$$J = -D\left[\frac{\partial c}{\partial x}\right]$$

Where D=diffusion, ∂c is the concentration and ∂x is the distance.

In order for the diffusion to occur the thin film solution was annealed for 24 h in the vacuum oven. The concentration of solute along the bar is given by the equation (1). This equation can be used to describe the situation where the thin film of tracer is placed on one end or a bar and then allowed to diffuse into the bar. To show that equation (1) is the correct solution two steps are necessary: the differentiation equation and boundary condition.

$$C(x, t) = \frac{bc}{2(\pi Dt)^{1/2}} e^{\left[\frac{-x^2}{4Dt}\right]} \qquad (1)$$

Here x is the distance in either direction normal to the initial solute film. The characteristics of the solution can be seen by plotted the concentration against distance after some diffusion occurred. As more diffusion occurs, the c(x) curve will spread out along the x axis. The aria under the curve remains fixed because the amount of solute is fixed. To understand how the diffusion occur, observe that c(x=0) decreases as $1/t^{1/2}$ while the distance between the plane x=0 and the plane at which c is 1/e xc(x=0) increases as $t^{1/2}$. The distance is given by the equation:

$$x=2\,(Dt)^{1/2}$$

dc/dx versus x is proportional to the flux across any plane at constant x.

If plane x=0, dc/dx=0 so the flux is zero.

d^2c/d^2x versus x is proportional with the rate of accumulation of solute in the region of any plane of constant x.

Equation (1) describes the resulting solute distribution plane where the tracer was placed and is defined as x=0.

To determine the diffusion D, thin sections are removal parallel to the initial interface, after an appropriate anneal. These are sections of constant x, and after the solute concentration of each is measured, a semi-log plot is made of the concentration in each section versus x^2. From equation (1) it is seen that this is a straight line of slope -1/D t so that if time t is know (24 hours) diffusion D can be calculated. [P Shewmon, 1995].

2.2.4 UV Light Irradiation

To demonstrate that the polymer exhibit a precise localized sensitivity to UV light, a photolithography technique may be employed. The wafer was placed in a 35 mm Petri dish. To simulate the culture environment in which cells grow, 3ml of de-ionized water was introduced into the dish.

UV irradiation at 240-280nm (λ=270nm, I=3.98mW/cm^2) was accomplished with a low-pressure mercury lamp (15 Watt rod bulb) placed at a distance of 6.5 cm above the sample surface .The energy of UV light was measured by a radiometer New Port Optical Power Meter, model 840. The films were then masked with a 500 mesh TEM grid and exposed to UV light for various times.

UV irradiation at 320-400nm was produce by UVA bulb F20T12BLB (I=1.44 mW/cm^2) placed at the distance of 20 cm above the sample surface.

Poly (4-vinylpyridine) was dissolved in DMF (dimethylformamide) at a concentration of 7 mg/ml and spun cast onto the freshly cleaned Si wafers at 2.05 x 10^3 rpm. The samples were then annealed in a vacuum oven (P~10^{-3}Torr, T=170˚C) overnight. This process ensures that the solvent used for spinning is removed, leaving a uniform polymer film. The film surfaces were then examined using scanning force microscopy, which indicated that the films were uniform; RMS relative roughness was less than 1nm. The thickness of the P_4VP film was measured using elipsometer and found to be 389±16 nm.

Poly [methylmethacrylate] (PMMA) was dissolved in toluene resulting in homogeneous transparent solution at the concentration of 15mg/ml. The thickness of the film was 79±18nm.

The blend polymer: poly [4-vinylpyridine] - poly [methylmethacrylate] (P_4VP-PMMA) was mixed 1:1 solution, resulting in a spun cast film, 140 ±14 nm thick.

In order to test the lithographic properties of polymers, the silicon wafers were coated with the spun cast annealed polymers films and exposed to UV irradiation for different times.

The tri-block copolymer was solubilized in dimethyl formamide (DMF), a common solvent for polymers. The concentration of the polymer solution used was 10.00 mg/ml.

2.2.5 Poly (4 vinyl pyridine)-P_4VP

Background: The pyridine molecule is well known to undergo photo-cleavage in the pyridine-water solution [Wilzback, 1970] [Nishiyama, 2008]. Under UV-irradiation at 250nm pyridine in the presence of water induced cleavage. The first step is photo-isomerization to Dewar pyridine. The second step is hydrolysis to aldehyde enamine. Aldehyde enamine has an intense absorption band at 366nm with the extinction coefficient of $4x10^{4.}$ The quantum yield of the reaction is low -0.004 [Wilzback, 1970] [Nishiyama, 2008].

The aldehyde enamine is unstable, and in a time scale of the minutes at room temperature reverts to pyridine with water elimination. The formation and rearomatization of the aldehyde enamine is easily observed spectrophotometrically. The Raman spectra confirmed ring opening photoreaction [Vaganova, 2001]. The activation energy of the pyridine cleavage is 3.2Kcal/mol and pyridine closure of system is 0.15Kcal/mol. With increase free pyridine concentration, activation energy of the pyridine ring cleavage lowers to 0.6Kcal/mol. The concentration of water has no significant influence on the activation energy of the pyridine ring cleavage. However, it decreases the activation energy of the closure to 0.05Kcal/mol.

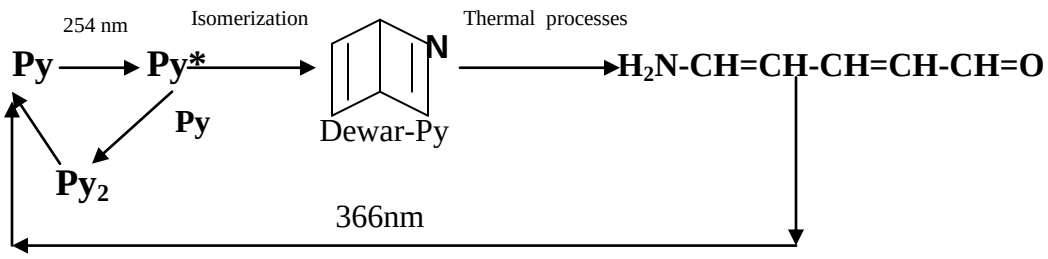

Scheme1. Photoinduced processes of pyridine: Py: Pyridine in the ground state. Py*: Pyridine in the excited state. Another possibility is the Py_2 formation as a product of the bimolecular reaction between Py* and Py.

The origin of the light sensitive system lies with the self-protonated side-chain unit on the backbone of poly (4-vinylpyridine) [Rozenberg, 2000]. Irradiation of the system poly (4-vinylpyridine) with 250 nm wavelength is leading to the protonation of the polymeric pyridine (Py* in the excited state). This process is irreversible [Vaganova, 2000]. The photo induced reaction of pyridine under UV light includes three main stages. The first one is pyridine isomerization, the second one is the cleavage of the free pyridine molecule with aldehyde enamine formation and the third one is the photoproduct interaction with the side chain groups of the polymer. Initially the P_4VP is transforms to Dewar isomer. Then, upon photo hydration, a cleave reaction takes place and Dewar-Py turns to the aldehyde enamine. A main active product of the photoreaction is aldehyde enamine, (5-amino-2, 4-pentadienal), and its derivatives and they have an absorption band at 340 m [Freitag, 1936].

The aldehyde enamine is unstable, and in a time scale of the minutes at room temperature reverts to pyridine. The formation and rearomatization of the aldehyde enamine is observed spectrophotometrically [Wilzback, 1970] [Vaganova, 2007]. Aldehyde enamine has an

intense absorption band at 366nm. Another possibility is Py_2 formation as a product of the bimolecular reaction between Py* and Py.

2.2.6 Poly (methylmethacrylate) – PMMA

Background: PMMA, a thermoplastic polymer, is one of the primary polymeric materials that have been used for fabrication of micro-analytical devices [Soper, 2000], [Boone, 2002], [Becker, 2002].

It has been found that surface carboxylic acid groups are formed upon UV exposure of PMMA surfaces in the atmosphere (surface photochemical modification) [McCarley, 2005].

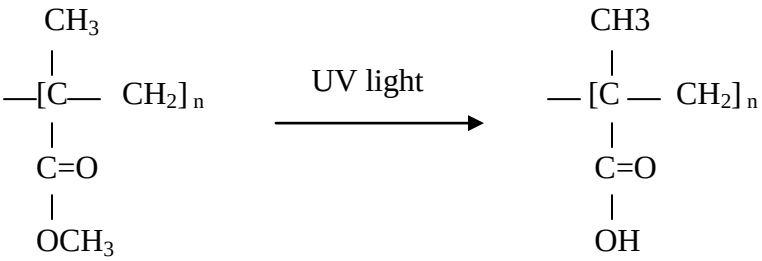

Scheme 2: UV modified PMMA surfaces and formation of carboxylic groups.

Wei and Co.[Wei, 2005] used fluoresceinyl glycine amine to chemically label the carboxylic groups on PMMA surfaces formed during the photolysis process. XPS, a powerful surface analysis technique, provides information on the chemical changes in the very top layer of the PMMA sample where photochemical reactions occur.[Hozumi,2002]. The ration of oxygen/carbon on PMMA surfaces increases when the UV modification time of PMMA

surfaces in air is increases. Also, more carboxylic acid sites are formed with increases modification time [Wei, 2005].

2.2.7 Poly (4-vynilpyridine)-poly (methylmethacrylate)-poly (phenylvinylketone)-P_4VP-PVPK-PMMA: Norrish type II reaction

The photo-cleavable part of tri-block copolymer is characterized by P_4VP and PVPK. In chapter 2.2.4 we discussed about photo-cleavable properties of P_4VP.

In this chapter we will discuss about photo-cleavable properties of PVPK. Figure 2.1 shows the chemical structure of tri-block copolymer.

Photochemistry of carbonyl group, particularly ketones, is very important. Once a molecule is electronically excited by absorption of a photon, it can undergo several competing physical decay reaction like: internal conversion to lower excited states, intersystem crossing between single and triplet states, emission of light and radiationless decay to the ground state and the energy transfer to another chromophore.

The quantum yield of a photoreaction represents the probability that light absorption will produce that reaction. Quantum yield is the only kinetic parameter which can be measured under steady state condition, since photoreactions generally follow zero order kinetics [Zimmerman, 1963].

O^{16}: $1s^2/2s^2 2p^6/3s^2 \mathbf{3p^4}$

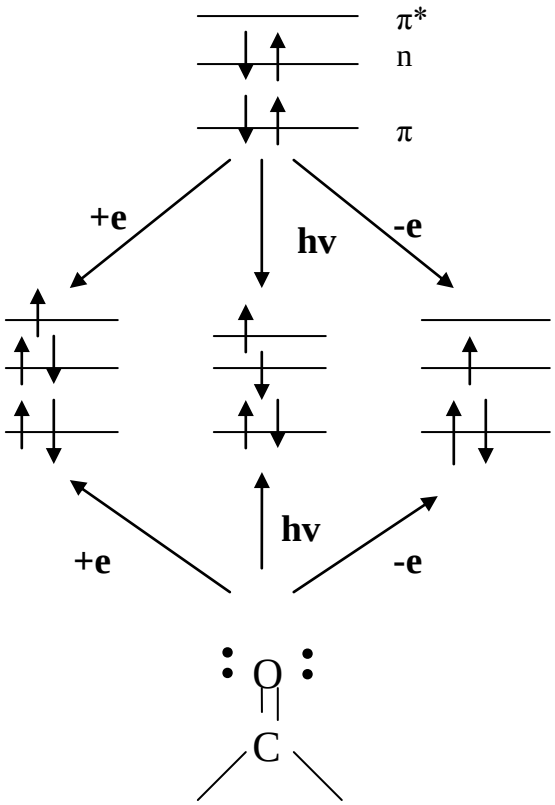

Scheme 3: Chemistry of excited carbonyl group.

There are two distinct types of electronic excitation which occur in the carbonyl compound. First is at λmax=280-300nm and represents an n-π* transition, in which a non bonding electron on oxygen is promoted into a π* orbital. The resulting excited state resembles a diradical with its physical and chemical properties. The second type of electronic excitation is π-π* transition which causes the electron density to move from the benzene ring toward the carbonyl. In the single state all electrons in the molecule are spin paired and in the triple state one set of electronic spins is unpaired. The spin of exited electron can be reversed, leaving the molecule in an excited triplet state: this is called intersystem crossing. The triplet state is a lower electronic energy that the excited singlet state.

There are four primary reaction on n, π* states: £-Cleavage (Norrish type I-the photolysis of ketones into radicals), hydrogen atom absorption, charge transfer complexation, β-cleavage (Norrish type II). It is considered that n-π* excitation is equivalent to oxidizing the n-orbital and reducing the π-system.

Photo cleavable polymer poly [phenyl vinyl ketone] will undergo a Norrish type II photo-elimination reaction [Norrish, et.al 1937].

This will cause a scission in the C-C backbone. As a first step, the Norrish type II fragmentation involves the formation of a 1, 4-biradical (Figure 2.3) by intramolecular γ-hydrogen abstraction by the carbonyl oxygen in its excited (n, π*) triplet state [Scaiano, et. al 1981], followed by C (α)-C (β) bond cleavage.

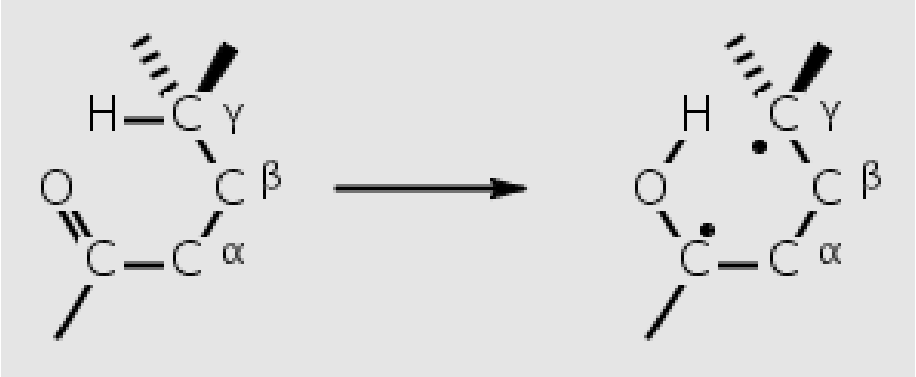

Scheme 4: Norrish type II photoreaction. Norrish type II fragmentation involves the formation of 1, 4-biradical by intramolecular γ-hydrogen abstraction by the Carbonyl oxygen in excited (n, π*) triplet state, followed by C (α)-C (β) bond cleavage.

The reversibility of the intramolecular 1, 5-hydrogen shift and the formation of cyclobutanol are the most important side reactions found in solution [Wagner, et. al 1976]. Cyclobutanol formation was first reported in 1958 by Yang [Yang, et. al 1958]

Carbonyl compounds containing γ C-H bonds undergo, upon electronic excitation, characteristic 1,5-hydrogen shifts to yield both cleavage and cyclization products [Norrish, et. al 1937]

The cleavage reaction is commonly called Norrish type II photo elimination, after its discoverer. With aromatic ketones, both reactions (cleavage and cyclization products) occur only from triplet states [Wagner, et. al 1966].

Phenyl ketones release terminal alkenes together with an enol that easily rearranges to form the corresponding acetophenone derivative.

Norrish type II reaction which controls the triplet life time is an activated process [Grotewold, et. al 1972]. The activation energy for PVPK is 3-3.6 Kcal/mol [Scaiano, et. al 1981].

Due to the fact that the lowest excited (n,π*)[Rochat, et. al 2000] and (π,π*) triplet states of phenyl ketones lie close together, their relative energies are strongly influenced by the polarity of the solvent (such as alcohols) on the one hand and the substituents on the phenyl ring on the other hand.

It is well known that the π, π* triplets of un-substituted phenyl alkyl ketones lie only a few kilocalories above the n, π* triplets [Lamola, et. al 1967]. Electron donating substituents of any kind as well as high solvent polarity invert the order of states.

Increasing the polarity of the solvent increases the relative energy of the (n,π*) state with respect to the (π,π*) [David, et. al 1967], [David, et. al 1969]. In alcohol solvent, products are formed with high efficiency and there is some little racemization observed. Ketone asymmetrically substituted at the γ position undergoes some photo racemization [Schulte-Elte, et. al 1964]. The ability of the solvent to bond hydrogen determines its effectiveness. Thus pyridine is even better than alcohol at enhancing type II quantum yields [Kempainen].

Both electron-donating and electron-withdrawing substituent lower type II quantum yield, but for different reason: the latter affect the biradical, the former affect the triplet state [Wagner, et. al 1969].

The results show that increasing the concentration of PVPK-units involved in the polymer chains raises T_g and enhances the relative value of quantum yields Φ'_{cs}. Thus, it may be assumed that the system undergoes a Norrish type II reaction, which is characteristic for PVPK and PVK copolymers and causes a scission in the C-C backbone, resulting in a decrease in the average molecular weight [Nenkov, et. al 1985]

Main chain scission was previously shown to occur when the polymer is irradiated with ultra-violet light of 366nm [David, et. al 1967] .The absorbance of a solution increases as attenuation of the beam decrease. Absorbance is directly proportional to the path length, b, and the concentration, c, of the absorbing species.

Beer's- Lambert Law states that: $A=\varepsilon bc$, $A=3.3$, where ε is a constant of proportionality called the Absorbtivity. The experimental data show that absorbance for P_4VP-PVPK-PMMA solution is A=3.3.

A quantum yield of 0.3 was obtained for the polymer irradiated in benzene solution [David, et. al1969]. It was found that the quantum yields of main chain scission Φcs values in solution are higher than those in a film at ambient temperature
[Nenkov, et al 1985] because of different mobility of the macromolecules. This was expected because of the lower reactivity of the triplet state of the polymer in the condensed phase. Macromolecules have restricted mobility and the probability of formation of intermediate six-member rings decreased [Amerik, et. al 1971]. Double bonds formed by a Norrish type II reaction can inhibit photo degradation or start polymerization. The quantum yield of the reaction in the polymer film is low, Φ= 0.04. [Wagner, et. al 1974], [Hrdlovic, et. al 1989]).

The average number of scissions of the main chain per molecule (S) is determined by the equation [Kemppainen]:

$$S= \{\eta_o)/ (\eta)\}\ ^{1}/\alpha\text{-}1$$

Where η_o and η are the limiting viscosities before and after irradiation, α is the coefficient in the equation:

$$[\eta] =kM^{\circ}\alpha$$

The photo degradation of poly (vinyl phenyl ketone) leads to the formation of polymer fragments which contain quencher end groups: as a result, the photoreaction shows a self-inhibiting effect, which results from triplet quenching by these unsaturated end groups. The high efficiency of these groups is made possible by the high frequency of triplet energy hopping along the chain. Analysis of the data for polymer samples of different initial chain length leads to the estimation of the critical chain length as 750 units and corresponds to a hopping frequency of 10^{12} s^{-1}[Encinas, et. al 1979].

Triplet life time is measured by Stern-Volmer under steady-state condition. Intramolecular hydrogen abstraction is so rapid that 0.1-100 nsec triplet life time results, too short to be measured by current flash technique [Clark, et. al 1970].

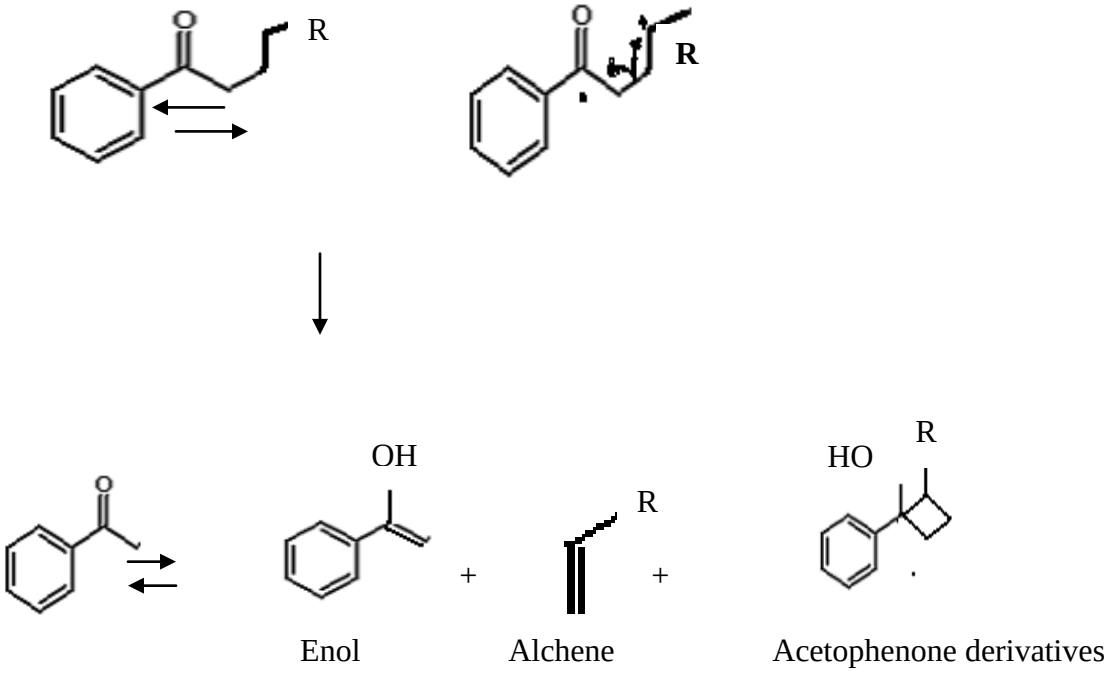

Scheme 5: Norrish type II photo fragmentation of phenyl ketones.

The polymer is solubilized in dimethyl formamide (DMF), a common solvent for polymers. The concentration of the polymer solution used was 10.00 mg/ml.

2.2.8. Floating Polystyrene Films

The polystyrene test was performed **i**n order to determine any traces of PMMA on the cell sheet after UV exposure.

0.3750 g of polystyrene was dissolved in 5mL of laboratory grade (98%) toluene to obtain a 75 mg/ml solution. The PS-toluene solution was then spun-cast upon glass microscope slides at 2500 rpm for 30 seconds to produce a film of approximately 1000 Å of thickness. Four lines, one for each side of the slide, were scored close to the edges of the slide. Using tweezers, the slide was slowly dipped at an angle into a beaker full of deionizer (DI) water to cause the PS film to detach from the slide and float atop the surface of the water. The PS film was attached to silicon wafer coated with the photosensitive polymer thin film.

The resulting double-coated wafer was left covered in aluminum foil in Petri dish to allow the water on the films to evaporate overnight.

The double-coated wafers are exposed to UVC light for one hour in 3 ml DI water. The polystyrene films float onto a surface of DI water, and placed the films atop clean silicon wafers. It was decided that the films be “flipped,” or turned over, to expose the basal side, to observe any traces of PMMA after UV exposure.

The resulting PS film-coated silica wafers were allowed to dry overnight in a half-covered Petri dish for compositional analysis through scanning electron microscopy (SEM).

2.3 Results and discussion

2.3.1 Photolithographic pattern formation: In Figure 2.2a we plot the amount of material removed versus exposure time to UVC for the three types of polymer films tested here. In each case the exposure was performed through a 500 mesh TEM Cu grid and the amount of material removed was determined by measuring the depth of a crater, using atomic force microscopy. From the figure we can see that the etching rate of P_4VP is 40nm/hr, or nearly seven times faster than that of PMMA, which is 6nm/hr. The etch rate of the tri block copolymer is intermediate, 10nm/hr, and that of a 1:1 blend of PMMA and P_4VP is 30nm/hr, or similar to that of the P_4VP homo-polymer.

In order to produce a coating which could be etched during cell culture, it was important to determine whether etching also occurred with light in the UVA frequency band. The results are shown in figure 2.2b, where find that even at this frequency 8nm were removed in 15 minutes from the P_4VP, while nearly no etching occurs in the PMMA film. It is interesting to note though that UVA can etch the polymers as well, albeit at a slower rate. Negligible amounts were removed from the PMMA during the same time, but approximately 2nm was removed from both the polymer blend, as well from the copolymer sample. Since cells only attach to the top layer of the polymer film, this etch rate is shown to be sufficient for lifting off layers of cells which is required for patterning tissue samples. We can also determine if the surface was modified by the UV light through measuring the water contact angle of the surface post irradiation.

In figure 2.2c we plot the water contact angle of P_4VP surfaces versus the exposure time for UVA radiation. From the figure we can see that the water contact angle for the unexposed P_4VP surfaces is 64 degree and decreases to 59 degrees after only five 5 minutes of exposure and 55 degrees after 15 minutes. Further irradiation for 30 minutes decreases the angle to 42 degrees indicating that oxidation of the surface may be occurring.

The tri-block copolymer was covered with water up to 5 hours and showed linear response up to that point. This is represented in Figure 2.2d by the deviation from the theoretical regression curve (pink) versus actual data (black). The cross section shown determines the depth of the square where the polymer was removed after exposure. The photo-sensitive co-polymer was exposed to UVC light for up to 4 hours. This is the maximal time that we could measure the level of polymer removed as the volume of water would be completely

evaporated after this time. After each exposure the removed amount of the films was measured using Atomic Force Microscope. AFM was used in contact mode to give a topographical profile in order to measure the thickness of the polymer.

Figure 2.3 show that 366nm is the pick absorbance where the main chain scission occurs when tri-block copolymer is irradiated with ultra-violet light [David, et. al 1967].

2.3.2 Spin-coating and Annealing of the Photosensitive Polymers

To demonstrate that the photo-sensitive polymer surface is smooth, homogeneous and suitable for the cells to grow on, the polymer was characterized using Scanning Electronic Microscope (SEM). It was shown that the surface indicates that the RMS roughness was less than 1nm. Figure 2.4a presents the spun cast solution of the photosensitive polymer 10 mg/ml onto Si wafer at 2.5 x 10^3 rpm for 30 seconds. SEM shows that spin casting the polymer creates a thin film spinning off the excess polymer. In figure 2.4b SEM shows the uniformity of annealed sample in an ultra high vacuum oven at P~10^3 Torr, T=170 ºC overnight. This experiment prove that annealing process removes the residual solvent; it binds the polymer to the silicon substrate as well as sterilizes the substrate for use in cell culture. It strengthens the bond between the silicone wafer and the photosensitive polymer presenting a homogenous, uniform polymer surface suitable for the cells growth. This process ensures that the solvent used for spinning is removed, leaving a uniform polymer film.

2.3.3 Testing the Photosensitivity of the tri-block copolymer

In order to determine how precisely the photo-sensitive polymer can be removed the polymer films were exposed through 500 mesh Cu mask in 3 ml of D.I. water in Petri dish. Figure 2.5 shows Optical Microscope picture of photo-sensitive part of tri-block copolymer which has been successfully removed after exposure for 4 hours to UVC light in 3 ml DI water. The TEM grid was placed on top of polymer coated Si wafer before UV exposure. The samples were irradiated with a total of 7.5J/cm^2 of 254nm UV light. 500 mesh TEM grid was chosen because of the regular organization and control size of the mesh which is 36µmx36µm. Figures 2.5a and 2.5b show the uniform pattern of the mask transferred onto the polymer-coated silicone surface. This indicates that the polymer was denatured at specific sites, but not generally. High magnification of optical microscope (Figure 2.5a) shows two

different colors: The dark area is area covered by TEM grid and indicates the presence of the polymer on Si wafer. The exposed area is the light area which indicates that the light sensitive part of the block copolymer was removed under UVC exposure. Low magnification of optical microscope shows in Figure 2.5b the uniform patterns of the mask transferred onto the polymer coated silica wafer.

2.3.4 SEM Analysis of UV-Exposed Films

In order to remove the photo-sensitive part of photo-sensitive polymer and to observe the uniform square regions formed at the micron size we image the film using Scanning Electronic Microscope. It was shown that photo-cleavable polymers exhibit a precise localized sensitivity to UV light. Using SEM images we proved that we obtained the shape of TEM grid (36μmx36μm) transfer on the exposed sample. We kept the shape of the square from the TEM grids and also conserved the dimensions 36x36 microns which is indicative of the high-precision of this method.

Figure 2.6 show the SEM pictures of the patterns of TEM grid transferred on the block copolymer exposed to UVC light at different time frame. a) one hour, b) two hours, c) three hours, d) four hours. Also AFM measures the depth of photo-sensitive polymer removed after different time exposure. Using AFM we determined the depth of the square of the polymer removed after four hours exposure to UVC light to be 38nm.

Going further the AFM determines the micron distance of the denatured sites in Figure 2.7b. This distance is 36 μm obtained from a sample exposed to UVC for four hours in 3 ml DI water using 500 mesh grid. Friction mode indicates two types of surfaces proving that the polymer was denatured only at specific sites and no generally. This proves that the light-sensitive part of the polymer was removed only at specific sites when the UV light penetrated through the grid. Also Figure 2.7c shows that AFM cross section determines 38nm of photosensitive polymer was removed after 4 hours UVC light exposure.

2.3.5 Chemical Analysis of UV-Exposed Films through EDAX:

In order to verify that we were able to remove only the exposed parts of photo-sensitive polymer, SEM was performed to determine the EDAX composition of the polymer removed.

The polymer was exposed for 4 hours to UVC light using a 500 mesh grid. We were able to keep the shape of the TEM grid imprinted on the exposed photo-sensitive polymer by 36x36µm. Friction mode indicates two types of surfaces, therefore two types of polymers: area covered by grid (yellow area) shows the presence of photo-sensitive polymer; the UV light exposed area (red area) shows that the light-sensitive part of the polymer was removed. AFM shows the distinctive patterning and the depth of the holes created in the photosensitive polymer by UV light. Figure 2.8 shows the EDAX composition of exposed polymer. Different regions were analyzed by EDAX, imaged by AFM in Figure 2.8b. The picture determined that the shape of TEM grid was very well conserved on the polymer coated Si wafer.

SEM determines the composition of the polymer in three different areas: (2.8b) the exposed aria of the sample (red area) is the area where the light-sensitive part of copolymer was reacting under UVC light because the light was penetrating through TEM grid. This area was analyzed for the oxygen signal through EDAX compositional analysis. The spectrum indicated that a very small carbon peak will be visible at 0.25keV. Also, a very small oxygen peak will be visible at 0.5keV. This means that a trace amount of photo-sensitive polymer is still attacked to the Si wafer.

The aria near the aria covered by TEM grid shows larger carbon peak at 0.25keV and larger oxygen peak at 0.5keV.This means that a larger amount of photo-sensitive polymer remained attached to the Si wafer.TEM grid shows the presence of photo-sensitive polymer. The simulation spectrum for the photosensitive polymer coated silica wafer indicated that a large oxygen peak would be visible at approximately 0.5 keV. This was confirmed by running the spectrum of the P_4VP-PVPK-PMMA coated wafer, which showed a large oxygen peak at 0.5 keV. Since PVPK and PMMA contains a significant amount of oxygen in its chemical composition relative to P_4VP, a significant oxygen spike in the produced spectra would have indicated the presence of photo-cleavable part of the block copolymer.

2.3.6 SEM Analysis of UV-Exposed PS Films

This experiment was designed to determine if PMMA was left on the cells sheet after UV exposure. It is critical for us to obtain pure cell layer without any polymer left, in order to construct the layer by layer tissue where the cells can be in contact with each other. Therefore, no trace of the photosensitive polymer must be present on the basal surface of the harvested

cell sheet. In addition, previous work has shown that almost all biodegradable polymer materials exhibit a strong inflammatory response *in vivo* (Ronneberger, et. al 1990). Therefore, we designed a model that would not leave any trace of polymer.

To confirm this, we floated polystyrene films on the top of the photosensitive polymer-coated wafers and exposed the films to UV light in identical conditions to the cell sheets. Irradiated surfaces of PMMA become hydrophilic and unstable peroxides together with carboxylic groups are formed at the polymer surface producing carbon, hydrogen and oxygen gas [Welle, et. al 2002].

The detached PS sheets were then analyzed for oxygen signals through EDAX compositional analysis. Since PMMA contains a significant amount of oxygen in its chemical composition relative to PS, a significant oxygen spike in the produced spectra would have indicated the presence of PMMA between the layers of the bi-layered tissues. At first, a spectrum was produced for a sample in which the PS film had been "flipped," or oriented so that any PMMA present would be on the immediate surface of the sample.

Figure 2.9 shows the SEM analysis of UV exposed PS films. The simulation spectrum for the PS film on top of photosensitive polymer coated silica wafer indicated that a small oxygen peak would be visible at approximately 0.5 keV (Fig. 2.9b). This was confirmed by running the spectrum of the PVP-PVPK-PMMA-coated wafer, which showed a large oxygen peak at 0.5 keV (Fig. 2.9a). Using these two spectra as references, we produced spectra for the "flipped" and "un-flipped" PS film exposed to UV light. Un-flipped PS film after exposure to UVC light shows no oxygen peak at 0.5keV in Figure 2.9c. Un-flipped PS film means that after exposure to UV light, the PS film was lifted exact as it was and floated onto a clean Si wafer. Figure 2.9d shows that no oxygen peak was found at 0.5 keV after UVC irradiation. Flipped PS film means that after exposure to UV light, the PS film was flipped, so the bottom was facing upwards. These results show that no residue of PMMA was left on the polystyrene film. In all spectra generated, oxygen levels were consistently non-existent; indicating that according to our hypothesis, no residue of PMMA was left on the polystyrene film.

2.4 Conclusion

The photo-cleavable block copolymer: P_4VP-PVPK-PMMA was designed to have three basic properties: adhesion to a surface such as silicon wafer, activation and control under UV light and biocompatibility. To demonstrate that the photo-sensitive polymer surface is smooth, homogeneous and suitable for the cells to grow on, the polymer was characterized using Scanning Electronic Microscope. SEM determined that spin casting and annealing process is necessary to create a thin, homogeneous film. Spin casting the polymer creates a thin film spinning off the excess polymer and the annealing process removes the residual solvent leaving a uniform polymer film.

The localized sensitivity of the polymer was tested by exposing a thin film of photo-sensitive polymer to UV light through a TEM grid. A grid-like pattern directly corresponding to the TEM grid was found to be formed on the surface of the thin film Using TEM grid was determined how precisely the photo-sensitive polymer can be removed under UV light. Using AFM it was determine the depth of the square of the polymer removed after exposure to UVC light for 4 hours in 3 ml DI water irradiated with 7.5 J/cm^2 of 254nm being 38nm. The polymer was removed 10nm/hour of exposure. AFM shows the distinctive patterning and the depth of the holes created in the photosensitive polymer by UV light. EDAX shows the composition analysis through SEM in different arias. AFM was used to measure the thickness of the polymer.

The exposure of polymer surfaces to ultra violet light of short wavelengths emitted by mercury vapor lamps alters the physical behavior and chemical composition of the polymer surfaces. Irradiated surfaces of poly (methylmethacrylate) become hydrophilic and unstable peroxides together with stable carboxylic groups are formed at the polymer surfaces [Welle, 2002].This modification favor strongly the adhesion of hepatocytes, fibroblast and some other cell lines.

UV-exposed PS films determine that no residue of PMMA was left on the polystyrene film. Therefore, no trace of the photosensitive polymer must be present on the basal surface of the harvested cell sheet in order to eliminate the chance of host inflammation.
Also, we have shown that P_4VP polymers and their blends with PMMA can be etched via exposure to UVA radiation.

In summary, it was determined that the polymers exhibit a precise, localized sensitivity to UV light. In addition to culturing whole layers of cells, in the next chapter it will be tested the accuracy of the polymers and manipulate the growth patterns of the cells by pinpointing and denaturing only specific cells. This process could be applicable in the future to the treatment of cancer cells.

2.5 References

[] Okano T, editor. Biorelated polymers and gels-controlled release and application in biomedical engineering. San Diego, CA: Academic Press;1998.

[] Peppas NA, Klier J. Controlled release by using poly (methacryl acid-g-ethylene glycol) hydrogels. J Control Release; 16:203-214, 1991.

[] Yoshida R, Sakai K, Okano T, Sakurai Y, Bae YH, Kim SW. Surface-modulated skin layers of thermal responsive hydrogels as on-off switches: I. Drug release. J Biomater Sci Polym Ed; 3:155-162, 1991.

[] Yoshida R, Sakai K, Okano T, Sakurai Y. Surface modulated skin layers of thermal responsive hydrogels as on-off switches: II. Drug permeation. J Biomater Sci Polym Ed; 3:243-252, 1992.

[] Stayton PS, Shimoboji T, Long C, Chilkoti A, Chen G, Harris JM, Hoffman AS. Control of protein-ligand recognition using stimuli-responsive polymer. Nature; 378:472-474, 1995.

[] Hosino K, Taniguchi M, Marumoto H, Fujii M. Repeated batch conversion of raw starch to ethanol using amylase immobilized on a reversible soluble-autoprecipitating carrier and flocculating yeast cells. Agric Biol Chem; 53:1961-1967, 1998.

[] Eisenberg SR, Grodzinsky AJ. Electrically modulated membrane permeability. J Membr Sci; 19:173-194, 1984.

[] Yuk SH, Cho SH, Lee HB. Electric current-sensitive drug delivery systems using sodium alginate/polyacrylic acid composites. Pharm Res; 9:955-957, 1992.

[] Kwon IC, Bae YM, Kim SW. Electrically erodible polymer gel for controlled release of drugs. Nature; 354:291-293, 1991.

[] Irie M, Iwayanagi T, Taniguchi Y. Photoresponsive polymers reversible solubility change of polystyrene having pendant spinobenzopyran groups and its application to photo resists. Macromolecus; 18:2418-2422, 1985.

[]Ito Y, Sugimura N, Kwon OH, Imanishi Y. Enzyme modification by polymers with solubilities that change in response to photo irradiation in organic media. Nat Biotechnol; 17:73-75, 1999.

[] M. Gautschi, J.A. Bajgrowicz and P. Kraft, Fragrance cheering milestones and perspectives, Chimia, 55,379, 2001.

[] S. Rochat, C. Minardi, J.Y. de Saint Laumer and A. Hermin: Control release of perfumery aldehydes and ketones by Norrishing Type II photo fragmentation of α-keto esters in undegasses solution. Helv. Chim.Acta, 83, 1645, 2000.

[] H. Kamogawa, S.Okabe, M. Nanasawa, Synthesis of polymerizable Acetals, Bull. Chem. Soc. Jpn., 49, 1917, 1976.

[]P. Enggist,S. Rochat, A. Herrmann, Controlled release perfumery alcohols by alkaline hydrolysis of 2-formyl acethylbenzoates and their corresponding phthalides, J. Chem. Perkin trans.2, 438, 2001.

[]A. Herrmann, C. Debonneville, V. Laubscher, Dynamic headspace analysis of the light-induced controlled release of perfumery aldehydes and ketones from L-keto esters in household application, Flavor fragrance J., 15, 41, 2000.

[] D.C. Neckers, R.M. Kellogg, W.L.Prins and B. Schoot. Developmental Photochemistry. The Norrish type II reaction J.Org. Chem., 36, 1838, 1971.

[] W.W. Epstein, D.S. Jones, E. Bruenger and H.C. Rillling, The synthesis of a photo-labile detergent and its use in the isolation characterization of protein, anal. Biochem, 119, 304, 1982.

[] B.Levrand, A. Herrmann, Light induced controlled release of fragrances by Norrish type II photo fragmentation of alkyl phenyl ketones, Firmenich, 2002.

[] R.G.D. Norrish, Trans.Faraday Soc., 33, 1521, 1937

[] Scaiano, J.C. and Selwyn, J. C. Macromolecules 14, 1723, 1981.

[] P.J.Wagner, Type II photo elimination and photocyclization of ketones, Acc. Chem.Res. 4, 168, 1976.

[ ] P.J.Wagner, Chemistry of excited triplet organic carb. Compounds, Top. Curr, Chem., 66, 1, 1976.

[] N.C.Yang and D.H. Yang, J. Amer. Chem. Soc., 80, 2913, 1958.

[] P.J.Wagner and G.S. Hammond, J. Amer. Chem., Soc., 88, 1245, 1966.

[] Grotewold, J.,Soria, D, Previtali, C.M, Scaiano, J. C.J.Photochemistry 1, 471, 1972/1973.

[] A.A.Lamola, J.Chem. Phys., 47, 4810, 1967.

[] David, C., Demarteau, W. Geuskens, G. Polymer Lond. 8, 497,1967.

[] C. David, W. Dermateau. F. Derom, and G. Geuskens, Notes and communication, Service de Chimie Générale II, Université Libre de Bruxelles, Brussels, Belgium, August, 15, 1969.

[] K.H.Schulte-Elte and G.Ohloff, Tetrahedron Lett. 1143,1964.

[] A. E. Kemppainen, unpublished results.

[] P.J.Wagner and G. Capen, Mol. Photochem., 1, 173, 1969.

[] G.Nenkov, T. Bogdantsaliev, T.Georgieva and V. Kabaivanov; Polymer Photochemistry (6) (1985) Elsevier Applied science Publishers Ltd.England, 1985.

[] G. Nenkov, T. Bogdantsaliev, T. Georgieva and V. Kabaivanov: Scientific Ind. Centrum for Special Polymers, 11576, Sofia, Polymer Photochemistry (6), 475-482, 1985.

[] Amerik, Y. and Guillet, J.E., Macromolecules, 4, 375-9,1971.

[] P.J.Wagner, Type II photo elimination and photocyclization of ketones, Acc ChemRes., 4,168, 1974.

[] Hrdlovic, P., Lucas, I. International Conference on advance in stabilization and Controlled degradation of polymers: Patsis, A.V.E, Technomic, Lancaster, PA, Vol2, pp66-78, 1989.

[] Dan, E. and Guillet, J.E.: Macromolecules, 6, 230-5, 1973.

[] M.V. Encinas, K. Funabashi, and J.C. Scaiano Triplet energy migration in polymer photochemistry. A model for the photo degradation of Poly (phenyl vinyl ketone) in solution. American Chemical Soc., vol12, no 6, 1979.

[] W.D.K.Clark, A.D.Litt and C.Steel, J. Amer. Chem. Soc.,91, 5413 (1969); G. Porter and M.R.Topp, Proc. Roy. Soc., Ser. A.315, 163,1970.

[] A.Ishizaka, Y. Shiraki, J. Electroche. Soc., Low temperature surface cleaning of silicon and its application to silicon MBE, 133, 4:666-671, 1986.

[] Ronneberger, B., Kao, W.J., Anderson, J.M., Kissel, T. "In vivo biocompatibility study of ABA triblock copolymers consisting of poly (L-lactic-co-glycolic acid) A blocks attached to central poly (oxyethylene) B blocks. *J. Biomed. Mater. Res*. 24, 529-545, 1990.

[] A. Welle, E. Gottwald, K.F. Weibezahn. Biomed Tech (Berlin), 47 Suppl. 1 Pt 1:401-3, 2002.

[12] Wilzback K.E. and Rausch D.J: J. Am. Chem. Soc. 92:7, 2178-2179, 1970.

[13] Nishiyama S, Tajima M, Yoshida Y.: Photo-irradiation effects on poly (vinyl pyridines): Colloids and Surfaces A: Physicochem.Eng.Aspects 313-314, 479-483, 2008.

[14] Rozenberg M, Vaganova E., Yitzchaik S., FTIR study of self-protonation and gel formation in pyridinic solution of poly (4-vynilpyridine), NJC 24, pp.109-112, 2000.

[15] Vaganova E., Meshulam G., Kotler Z., Rozenberg M. and Yitzchair S., Photoinduced structural changes in Poly (4-Vinyl Pyridine): A luminescence study, Jor. Fluorescence, vol10, no.2, 2000.

[16] Freitag H., Chem. Ber. 69B, 32-35, 1936.

[17] Vaganova E., Damm C., Israel G., Yitzchaik S.: Photoinduced Pyridine Cleavage-Closure in Viscous Polymer Solution: Journal of Fluorescence, Vol.12, No. 2, 2007.

[19] Wei S., Vaidya B., Patel A., Soper S., McCarley R.: Photochemical Patterned Poly (methyl methacrylate) Surfaces Used in the Fabrication of Micro analytical devices, J.Phys. Chem., 109, 16988-16996, 2005.

[]Soper, S.A,; Ford,S.M.;Qi, S.;McCarley, R.L.; Kelly,K.; Murphy, M.C.; Anal Chem. 72,642A-651A, 2000.

[] Boone, T.D.; Fan, Z. H.; Hopper H.H.; Ricco, A. J.;Tan, H.; Williams, S.J. Anal Chem.,74,78A-86A, 2002.

[] Becker, H.; Locascio,L.e. Talanta , 56, 267-287, 2002.

[] McCarley, R.L.; Vaidya,B.; Wei S.; Smith A.F.;Patel,A.B.; Feng,J.;Murphy, M.C.;Soper, S.A. J.Am. Chem.Soc., 127, 842-843, 2005.

2.6 Figure Caption

Figure 2.1: Chemical composition of tri-block copolymer, photo-sensitive polymer P_4VP-PVPK-PMMA.

Figure 2.2:. Photo-sensitive polymers removed after (a) UVC exposure ; (b) UVA exposure. In each case the exposure was performed through a 500 mesh TEM Cu grid and the amount of material removed was determined by measuring the depth of a crater, using atomic force microscopy;(c) contact angle of P_4VP surfaces exposed to different UVA doses; (d) The polymer was covered with water up to 5 hours and showed linear response up to that point. This can be seen by the deviation from the theoretical regression curve (pink) vs. actual data (black).

Figure 2.3 Absorbance spectrum of photo sensitive polymer P_4VP-PVPK-PMMA.

Figure 2.4: Photo-resist spinner**:** The solution of the photosensitive polymer was spun cast onto Si wafer at 2.5 x 10^3 rpm for 30 seconds spinning off the excess solvent.(a) SEM of a sample with spun polymer.(b) SEM shows the uniformity of annealed sample in an ultra high vacuum oven at P~10^3 Torr, T=170 C overnight. Annealing is essential for different reasons: to make a stable and uniform polymer layer, and to eliminate any trace of solvent which would be toxic for the cells, at the same time, it is giving a sterile surface.

Figure 2.5: Photo-pattered triblock co-polymer surfaces.
The polymer was exposed to UVC light for 4 hours using 500 mesh TEM grids. Optical microscope image (2.6a): Dark area indicates the presence of photo-sensitive polymer on Si wafer. The light area indicates that the light sensitive part of the polymer was removed under UVC exposure. This means that the polymer was denatured at specific sites and no generally. (b) Image of photo patterned tri-block copolymer; here a 500 mesh Cu grid was used as a mask (36 micron square), exposure time is 4 hours.

Figure2.6: SEM shows the patterns of TEM grid transferred on the block copolymer exposed to UVC light at different time frame. a) one hour, b) two hours, c) three hours, d) four hours. Also AFM measures the depth of photo-sensitive polymer removed after different time exposure.

Figure2.7: Characterization of photo-sensitive polymer exposed to UVC light for 4 hours using 500 mesh grids. a) SEM shows the distinctive patterns obtains by

exposing the sample through TEM grid to UV light. b) AFM determines the distance of the denatured sites to be 36 µm. Friction mode indicates two types of surfaces proving that the polymer was denatured only at specific sites and no generally. c) AFM cross section determines the depth of the square of the photosensitive polymer removed by UV light. After 4 hours exposure the polymer removed was 38nm.

Figure2.8: EDAX composition of tri-block copolymer:
(a) AFM shows the uniform patterns of the mask transferred onto the polymer coated silica wafer.
(b) Different regions analyzed by EDAX, imaged by AFM.
(1, 2, 3) SEM determines the composition of the polymer in three different areas:
1) In the exposed aria where the polymer was reacting under UVC light, the spectrum indicates very low carbon and oxygen peak.
2) The aria near the aria covered by TEM grid shows small carbon, oxygen peak.
3) The aria covered by TEM grid shows the presence of photo-sensitive polymer. The spectrum indicates large carbon and oxygen peak comparable with the unexposed sample as references.

Figure2.9: SEM Analysis of UV-Exposed PS Films **a**) unexposed photosensitive polymer coated silica wafer shows a large oxygen peak at 0,5keV.This is the control data. b) The PS film on top of photosensitive polymer coated silica wafer indicates that a small oxygen peak is visible at 0.5keV. c) Un-flipped PS film after exposure to UVC light shows no oxygen peak at 0.5keV. Un-flipped PS film means that after exposure to UV light, the PS film was lifted exact as it was and floated onto a clean Si wafer.d) Flipped PS film after exposure to UVC light shows no oxygen peak at 0.5keV. Flipped PS film means that after exposure to UV light, the PS film was flipped, so the bottom was facing upwards. These results show that no residue of PMMA was left on the polystyrene film.

2.7 Figures

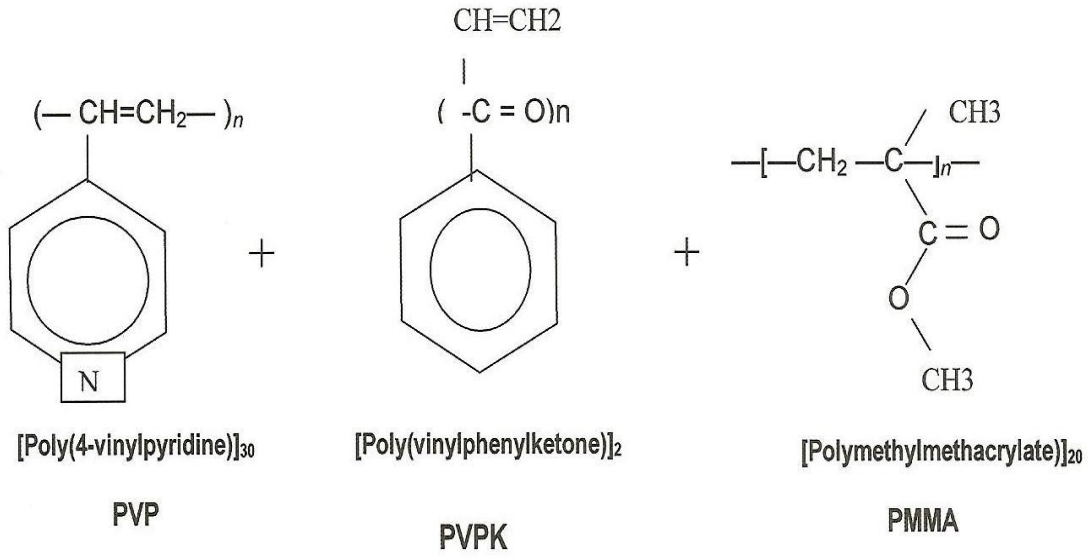

Figure 2.1

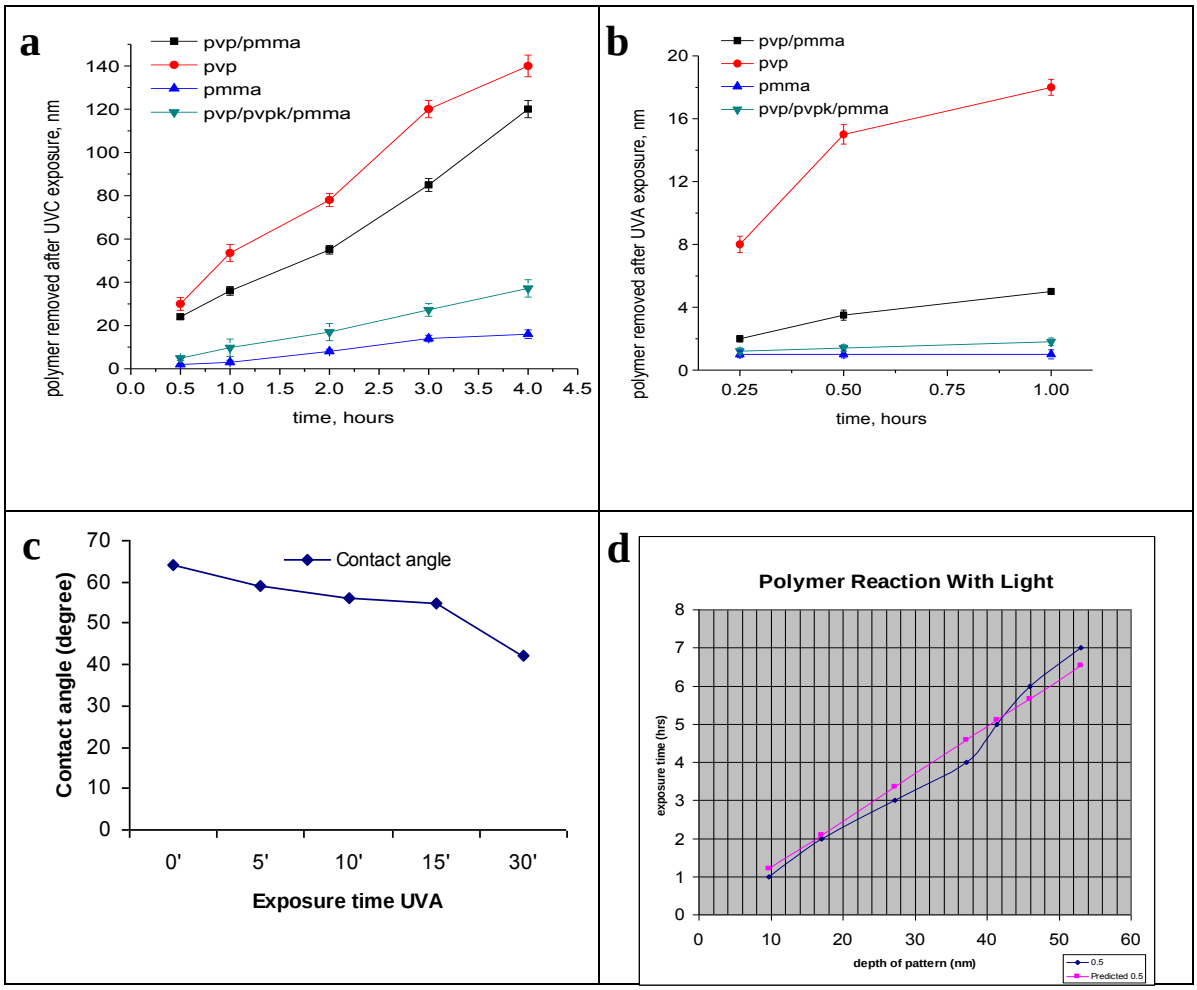
a
pvp/pmma
pvp
pmma
pvp/pvpk/pmma
polymer removed after UVC exposure, nm
time, hours
b
pvp/pmma
pvp
pmma
pvp/pvpk/pmma
polymer removed after UVA exposure, nm
time, hours
c
Contact angle
Contact angle (degree)
Exposure time UVA
0'
5'
10'
15'
30'
d
Polymer Reaction With Light
exposure time (hrs)
depth of pattern (nm)
0.5
Predicted 0.5

Figure 2.2

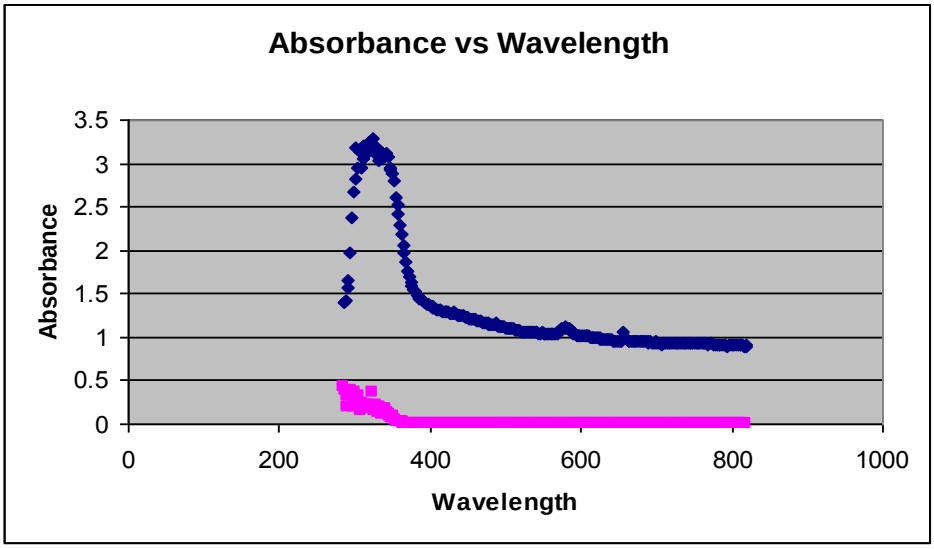
Absorbance vs Wavelength
Absorbance
3.5
3
2.5
2
1.5
1
0.5
0
0
200
400
600
800
1000
Wavelength

Figure 2.3

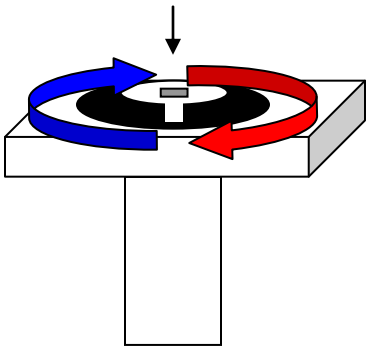

SPINNER

Spin cast polymer

Annealed polymer

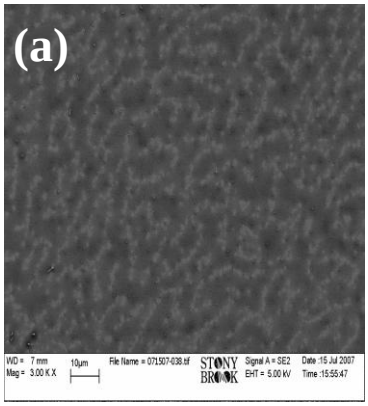

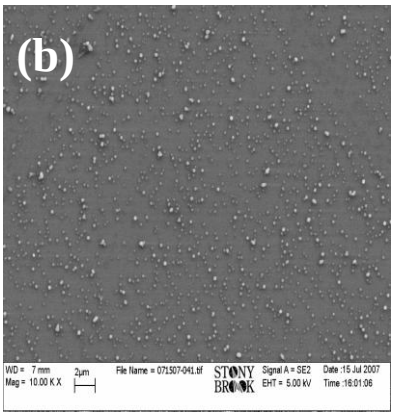

Figure 2.4

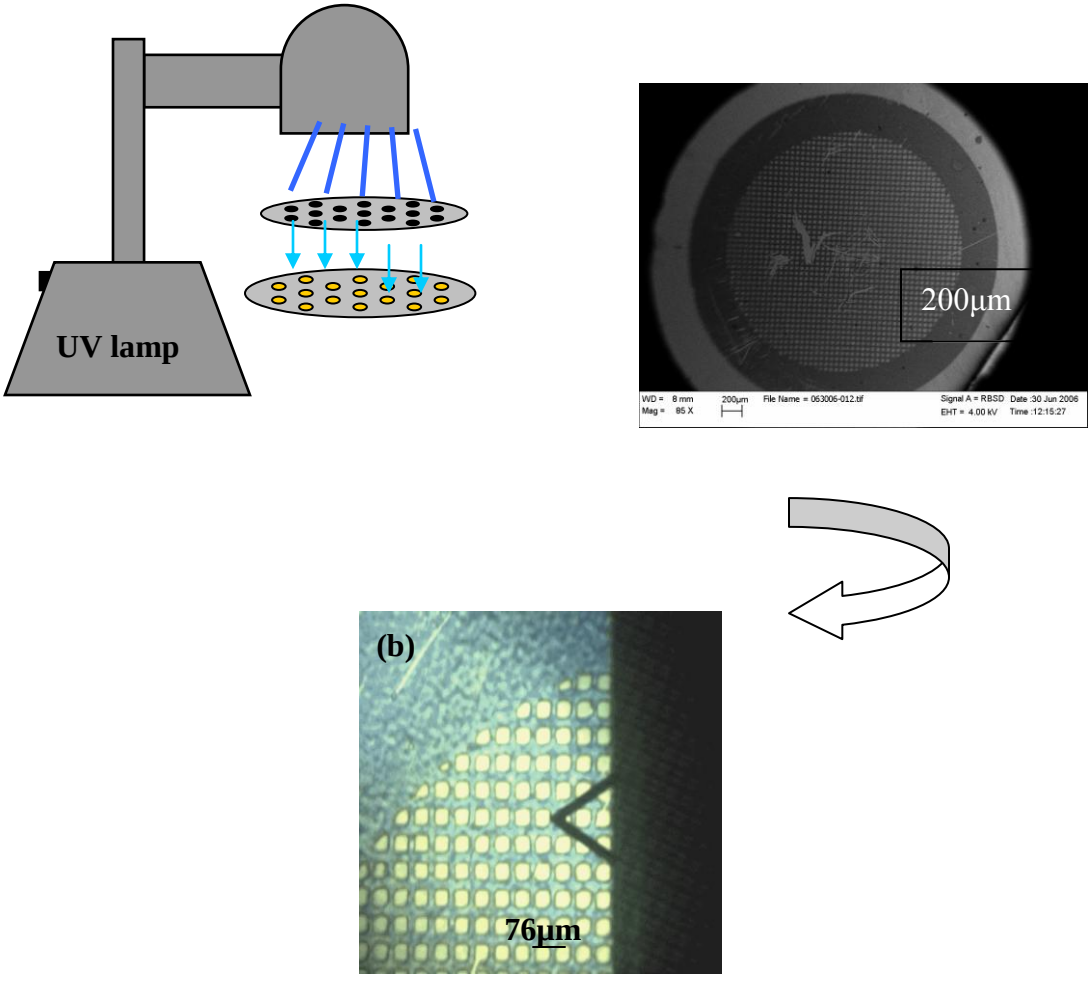
UV lamp
200µm
WD = 8 mm
Mag = 85 X
200µm
File Name = 063006-012.tif
Signal A = RBSD Date :30 Jun 2006
EHT = 4.00 kV Time :12:15:27
(b)
76µm

Figure 2.5

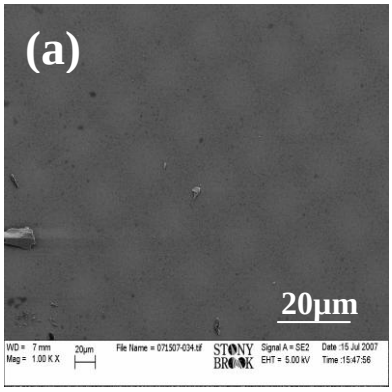

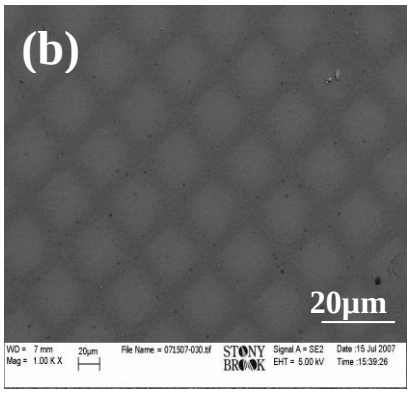

4.85nm removed after 30'exposure

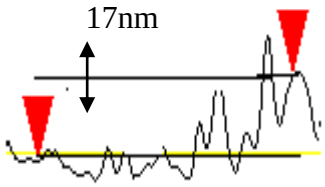

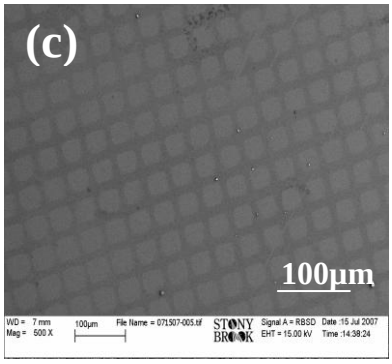

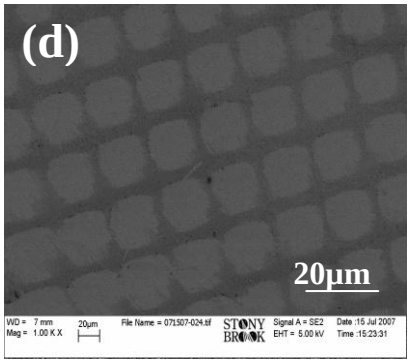

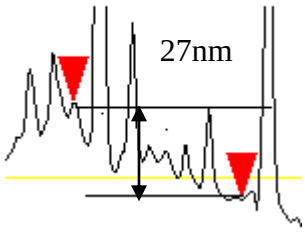

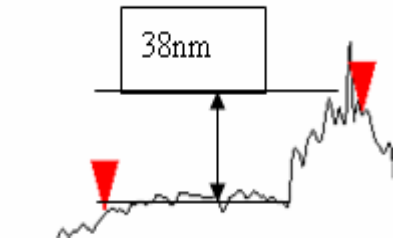

Figure 2.6

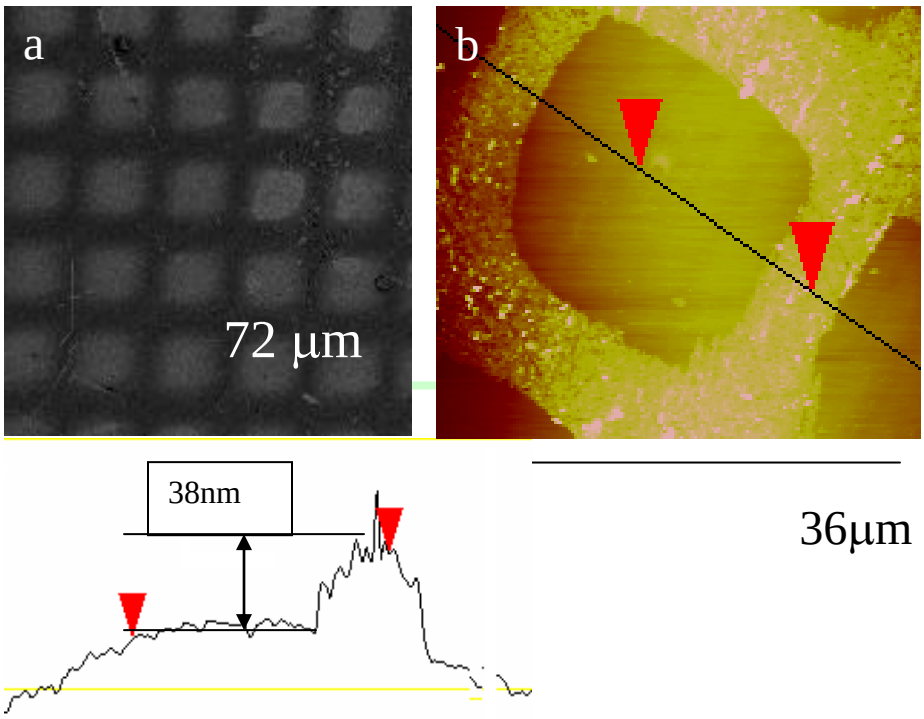

Figure 2.7

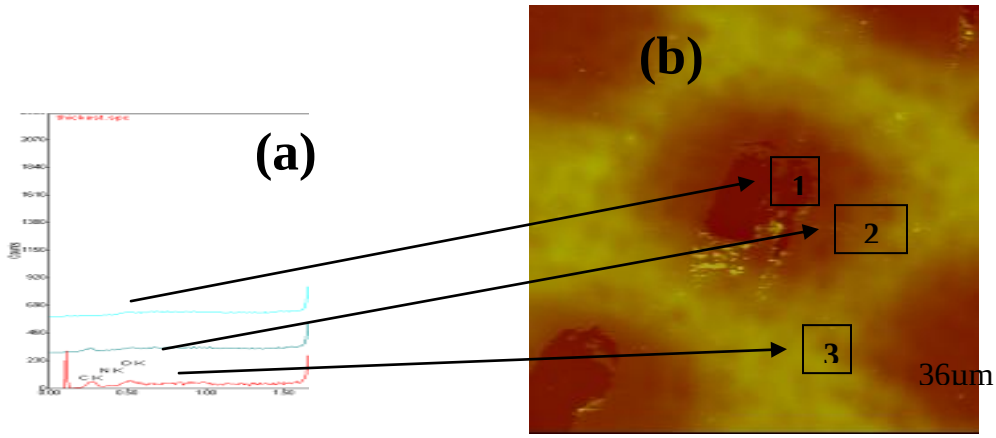

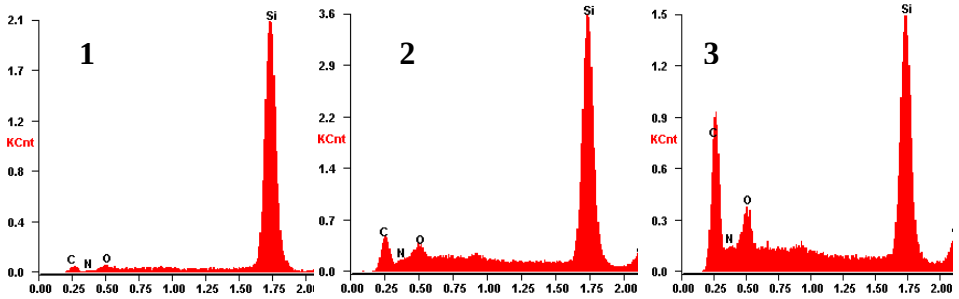

EDAX of the center of hole	EDAX near center of hole	EDAX covered area

Figure2.8

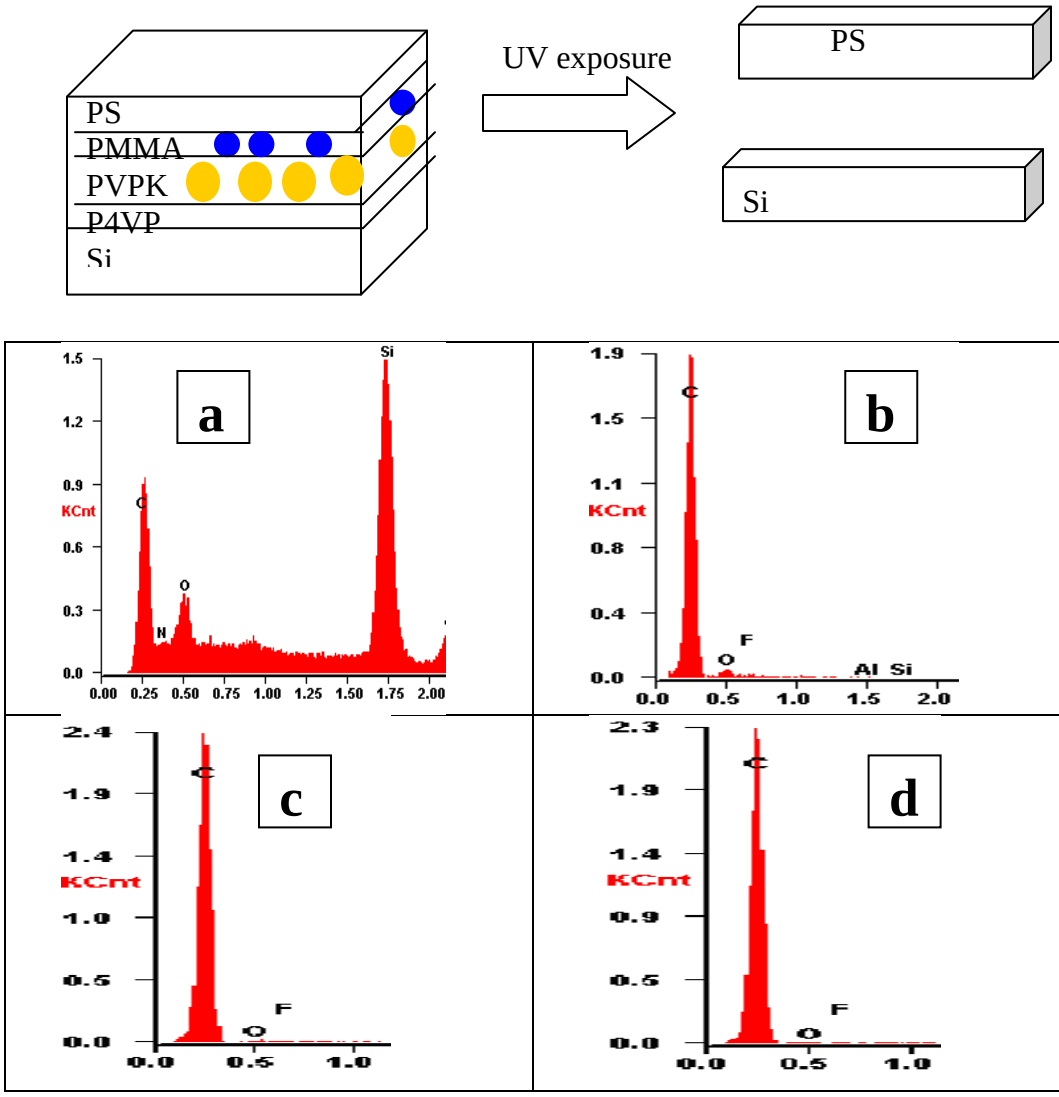

Figure 2.9

Chapter 3

Cells compatibility with photosensitive polymers

3.1 Introduction

In vitro tissue models are growing very fast in order to get closer to the in vivo situation. Comparative cell cultures using monolayer, multicellular sheroids [Wu, 1999] and co-cultures [Bhatia,1998] confirmed that the in vivo performance of an organ is related to the extracelullar matrix surrounding of cell, homologous and heterologous intercellular communication and a precisely determined super cellular architecture. Structured co-culture of hepatocytes and fibroblast on micro-patterned surfaces was leading to the concept of tissue engineering [Ingber, 1997], [Bhatia, 1999]. Using silane or thiol micro-contact printing or other techniques are not well suited for polymeric cell culture substrates. The presented masked UV irradiation of polymeric cell culture substrates opens a simple, fast, and economical route to obtain chemically patterned substrates [Welle, 2002].

It was presented on chapter 2 that the exposure of polymer surfaces to ultra violet light of short wavelength emitted by mercury lamps alters the physical behavior and chemical composition of the polymer surface. These modifications favor strongly the adhesion of fibroblasts and some other cell lines.

The sun irradiates more energy in the ultraviolet spectral region (100-400nm) than in that of visible light (400-700nm). It is well recognized that UV light in the range 280-400 is responsible for the majority of photo damage to the skin. The shortest of these wavelengths (UVC, 100-280nm) are absorbed completely by atmospheric oxygen (O_2) and the ozone layer (O_3). UVC is the most energetic and hence can cause the highest amount of damage. A wavelength in the UVB range (280-320nm) are absorbed efficiently, though incomplete, by ozone; UVB is mostly stopped within the epidermis and causes the inflammation known as “sunburn”; while UVA (320-400nm) is absorbed only weakly and is therefore more easily transmitted to the earth’s surface. UVA is the longest wavelength component and can penetrate into the dermis where melanoma originates.[Hidaka,1997] [Matsumara,2004].

Mammalian cells react to irradiation with UV light with a number of biochemical changes including the expression of distinct genes, called the UV response. The UV response is regulated by transcription factors and involves genes related to signal transduction, antioxidant defense, and cell cycle control [Scharffetter,2000], [Holbrook, 1996], [Shaulian, 2000], [Karin,1998], [Shackelford,1999] .

UVA irradiation induces collagenase in human dermal fibroblast [Scharffetter,1991].

UVB-inducible genes comprise several proteinases, among them matrix metalloproteinases (MMP's) [Scharffetter, 2000], [Brenneisen, 1996], [Fisher 1996].

Brenneisen and Co [Brenneisen,2002] demonstrated an imbalance after irradiation of human dermal fibroblast in vitro at wavelengths in UVB range. A significant increase in MMP-1 and MMP-3 mRNA and protein level was detected 24 hours subsequent to irradiation. In vivo experiments using human volunteers showed that induction of metalloproteinase and activities occurred at UVB doses well below those that cause skin reddening [Fisher 1996].

There are identified two signaling pathway for the mammalian UV response. The first pathway originates in the cell nucleus with indirect (oxidative) [Halliwell, 1991] or direct DNA damage as the primary signal [Herlich,1992][Mount, 1996]. There was evidence that the induction of inflammatory cytokines as well as of delayed UV-responsive genes requires UVC-damage DNA as primary chromophore [Blattner, 1998].

The second pathway consists of UV irradiation is the generation of reactive oxygen species (ROS) near or within the cell membrane. Reactive oxygen species can be sub-classified into free radicals-superoxide(anion)($O_2^{\cdot -}$), which appears to play a central role as other reactive intermediates are formed from it, hydroxyl radical (HO), and peroxyl radical (ROO.); or nonradical compounds such as singlet oxygen (O2), organic peroxides (ROOH)and hydrogen peroxide (H2O2) [Nordberg,2001], [Hancock,2001]. In addition, UVA [Wlaschek, 1995] and UVB [Masaki, 1995], [Jurkiewicz, 1994] were demonstrated as further sources of reactive oxygen species in human keratinocytes and fibroblast culture.

The exposure to UVC must come from artificial sources. Preliminary human studies have shown that exposure to UVC significantly decreases the time to healing of superficial pressure ulcers [Wills,1983][Nussbaum,1994]. The mechanism of action of UVC to promote healing are epidermal hyperplasia with enhanced re-epithelialization or desquamation of the leading edge keratinocytes at the periphery of the wound, stimulation of granulation tissue formation,

a bactericidal effect, and sloughing of necrotic tissues[Kloth,1995]. Additionally, potential mechanisms are proposed from in vitro studies of the effect of 254nm UVC on cells which have shown an increase in both transforming growth factor alpha (TGF-alpha) production and the number of epidermal growth factor receptors (EGFR) [Ellem,1988] [Ley,1992] [Sachsenmaier,1994] [Huang,1996].

The majority of UVC rays are absorbed by the epidermis in intact skin; with wounds and denuded surfaces the total energy is absorbed by dermal components. Fibroblasts are the major functional cell of the dermis and are responsible for production of major dermal structural components including collagen and fibronectin. When incorporated into fibroblast populated collagen lattices (CFLs), they cause a contraction of the lattice which is similar to wound contraction[Bell,1979]. Fibronectin is a factor necessary for lattice contraction; lattice constructed without fibronection do not contract [Gillery,1996].It has been shown that CFLs constructed with dermal fibroblast from skin chronically exposed to ultraviolet (UVA and UVB) light contract at a faster rate than CFLs constructed with UV-protected cells, but the magnitude of the difference in rate is dependent on age of the donor[Marks,1990].

It is known that in vitro aging of fibroblast results in alterations of cytoskeletal and extracellular matrix molecules (specifically fibronection) of human dermal fibroblast [Pieraggi,1984].

Morykwas and Co. shows the effects of UVC on naïve dermal fibroblast, focusing on released and cell-bound fibronectin (FN) and contraction of fibroblast-populated collagen lattice. Fibroblast cultures were irradiated by 187.5mJoules/cm2 of 254 nm UV light and resulted in an increase in the amount of fibronection released into the medium. Exposure of fibroblast to UVC light caused a decrease in the amount of fibronection bound to the cells surfaces and an increases in the amount of fibronection released into the medium [Morykwas, 1998]

A novel methodology was proposed for the non-invasive harvesting of cells as well as the tissue reconstruction layer-by-layer using a photo-sensitive thin film composed of the poly (4-vinylpyridine); polymethylmethacrylate, 1:1 blend of these polymers and triblock co-polymer (P_4VP-PVPK-PMMA) .These polymers possesses three characteristics essential to its role in this study: it adheres easily to surfaces, it is photo-responsive, and it is biocompatible. The first two advantages were proved in chapter 2. Another advantage is that after UV exposure to release the cell layer, the photo-sensitive polymers are spontaneously removed leaving the

cell layer free of any polymers. This gives us the opportunity to construct cell layers in contact with each other without getting any inflammation.

Also, since the only stimulus necessary for cell sheet harvesting using this methodology is UV light, it is possible to harvest cell sheets of hard tissues, as well as soft tissues such as nerve tissue and blood vessel tissue. Layer-by-layer deposition of these cell sheets can then be utilized to create multilayered, multifunctional tissue constructs for almost any organ. In addition, previous work has shown that almost all biodegradable polymer materials exhibit a strong inflammatory response *in vivo* (Ronneberger, et. al 1990). We screened these polymers presented in chapter 2, using various biochemical assays for their influence on cell proliferation and rate of photo cleavage with doses of UVA. The UVA doses should be sufficiently low to have minimal influence on the cell response, and ease of cell detachment and subsequent viability. Even though the UV/VIS absorbance spectra of these commonly used polymers are well established, the absorption peaks tend to be in the UVB or UVC regions, which would also cause severe damage to cells. Here we showed that the peaks were sufficiently broad such that it was possible to achieve a small degree of photo cleavage even when they were irradiated with light in the 300nm region. Since cell attachment occurs on the surface, only a small amount of cleavage was sufficient to lift the cells, which also had the advantage of minimizing any chemicals which may be released after the cleavage. Since the only stimulus necessary for cell sheet harvesting using this methodology is light, no mechanical deformation occurs and it is possible to harvest cell sheets from hard, as well as soft tissues.

3.2 Material and methods/Experimental procedure

3.2.1. Cell culture

Neonatal dermal fibroblast was provided by Coriell Institute for Medical Research. Human dermal fibroblast CF-29 (Caucasian female 29 years old) and CF-24 was purchased from Cascade Biologics. The cells were routinely cultured in the Dulbecco's Modified Eagle Medium (DMEM) with 10% Fetal Bovine Serum (FBS) and 1% Penicillin-Streptomycin (PS) (full-DMEM).Human keratinocytes were provided by Cascade Biologics, and also culture in the full-DMEM. Mouse osteoblasts (MC-3T3) were cultured in Alpha Minimum Essential Medium (GIBCO) mixed with 10% Fetal Bovine Serum and 1% Penicillin-Streptomycin.

These types of cells were plated separately on the photosensitive polymer coated Si wafers at a cell density of 3000 or 10^5 cells/cm², depending on the experiment purpose. All the cells were incubation in a Napco 5430 Incubator at 37 C with 4.9% CO2 and 100% humidity.

After incubated for pre-determined time, the cells were fixed, permeabilized, then stained with Alexa Flour 488 phallodium (Invirogen, Carlsbad, California) and Propidium Iodide (HPLC, Sigma Chemical Co., St. Louis, MO) for actin cytoskeleton and nucleus, respectively. The morphology of the cells was visualized with a Leica TCS SP2 laser scanning confocal microscopy (Leica Micro-system Inc., Bannockburn IL). Images were also obtained by using the Hg lamp, which has an excitation filter of 450-490 nm and an emission filter of long pass (LP) at 515 nm.

To test the cell on the patterned polymer film, the photosensitive copolymer was spin casting on 1cm²x1cm² glass microscope slide and annealed the film for 12 hours at 170˚C in a vacuum of 10^3 Torr. Dermal fibroblast (neonatal and adult) was plated on the thin film with density of 3,000cells/cm² to 10^5cells/cm² and cultured in the full-DMEM. After 3 days incubation, the samples attached with cells were exposed to UV for different amount of time.

Dermal fibroblasts were plated onto the polymer surface following several steps: Remove all the culture medium from the flask; add 4 ml Trypsin/EDTA solution to the flask. Rock the flask to ensure that the entire surface is covered. (Trypsin is an enzyme what denatured the cells membrane, so cells can detach from flask [Ito,et.al 1961]. Trypsine cleaves peptide bonds of lysine and arginine residues); Incubate the flask at 1-4 minutes, because 37°C is the optimum enzymatic reaction temperature. The cells have to detached from flask and floating in the liquid; When the cells have become partially detached and rounded, rap the flask gently to dislodge the cells from the surface of the flask; Add 5-6 ml of DMEM 1X with 10% BCS. DMEM is Dulbecco's Modification of Eagle's Media (standard media for fibroblast culture) containing 4.5gr/l glucose and L-glutamine without Sodium Pyruvate. This media is used to neutralize the enzymatic reaction of trypsine; BCS, Iron supplemented serum is Bovine Calf Serum used for cellular proliferation (increase the population), cellular growth and protein production. Meets specification of <=10EU/ml of endotoxin and <=10mg/dl of hemoglobin. Iron supplemented serum is filtered through triple 100nm pore-size filtration system. Bovine calf serum supplemented with chemically defined components including vitamins, amino acids, trace metals and other small molecules to stimulate cell growth and proliferation.

3.2.2 Alamar Blue: Cell viability activity was evaluated with AlamarBlue reagent (Invitrogen). Cells were platted in a 96-well plate at six different densities (100,000 cells to 3,250 cells) in 100ul of media. After 24 hour in the incubator the samples are exposed to UVA for 15, 30 and 60 minutes. 10% of AlamarBlue reagent was added directly to each well; the plates were incubated at 37°C for 1-4 hours allowing cells to convert resazurin to resorufin. The absorbance signal is measured on a plate reader of spectrophotometer DAL1025 Micro plate reader at 560 nm excitation and 590 nm absorbance. Calibration curve was used to calculate the cells number on day1, day3 and day6 after 1.3J/cm^2, 2.6J/cm^2 and 5.2J/cm^2 of UVA light.

3.2.3 MTS*:* Cell mitochondrial activity was evaluated with Cell Titer 96 Aqueous One Solution Cell Proliferation Assay (Promega). Cells were plated in a 96-well plate at six different cells densities from (100,000 cells to 3,250 cells) in 100µl of media. After 24 hours incubation the samples were exposed to UVA for 15, 30 and 60 minutes. 20% of the MTS solution was added to each well; the samples were incubated for 1 hour at 37° C. The absorbance was read at 490nm by the automated micro plate reader ELX800.

3.2.4 ROS determination*:* Reactive Oxygen Species were determined using 5-(and-6)-chloromethyl-2', 7'-dichlorodihydrofluorescein diacetate, acetyl ester (CM-H_2DCFDA) (Invitrogen) where 50,000 cells were placed in each well of 96-well cell tissue culture dish in 50ml media. After that, 100 µl of a working solution of CM-H_2DCFDA was added to each well and incubated at 37^{o}C for 20 minutes. An additional 100 µl of 25 mM NaN_3 solution was added to each well and placed to the incubator for 2 hours. Fluorescence was determined with a BIO-TEK EL800 Micro plate reader at 490 nm excitation and 580 nm emission.

3.2.5 FITC Annexin V Apoptosis Detection Kit II: The apoptotic program is characterized by certain morphologic features, including loss of plasma membrane asymmetry and attachment, condensation of the cytoplasm and nucleus, and internucleosomal cleavage of DNA. Loss of plasma membrane is one of the earliest features. In apoptotic cells, the membrane phospholipids phosphatidylserine (PS) is translocated from the inner to the outer leaflet of the plasma membrane, thereby exposing PS to the external cellular environment. Annexin V is a 35-36 KDa Ca^{2+} dependent phospholipids-binding protein that has a high

affinity for PS, and binds to cells with exposed PS. Annexin V may be conjugated to fluorochromes including FITC. Since externalization of PS occurs in the early states of apoptosis, FITC Annexin V staining can identify apoptosis at an earlier stage than assays based on nuclear changes such as DNA fragmentation.

3.2.6 Change of Medium to Reduce Refraction

Initially, it was thought to expose the samples to UV light while having the plated silicone wafers immersed in the 10% DMEM solution, to sustain the fibroblast cells. However, it was realized that the amount of refraction of the UV light by the solution posed a problem. Refracted light would make it more difficult to denature specific portions of the photosensitive polymer. If a tissue having a specific pattern of cells is to be achieved, refraction would pose a problem. For this reason, the plated silicone wafers were immersed in a phosphate buffer solution (PBS) which is able to sustain the cells for the duration of the experiment and which causes no appreciable refraction of UVC light. The ions from the phosphate buffer solution are providing sustenance and maintain a suitable pH for the dermal fibroblast cells. In principle, any solution that can sustain the cells for a sufficient duration and that limits the refraction of UVC light to acceptable levels, may be suitable for use during the UV exposure procedure.

3.2.7 Film Patterning: In chapter two we discussed about the lithographic properties of photo-sensitive polymers. Prior to UV irradiation, the cells were washed twice with phosphate buffered saline (PBS). UV irradiation at 240-280nm (λ=270nm, I=3.98mW/cm^2) was accomplished with a low-pressure mercury lamp (15 Watt rod bulb) placed at a distance of 6.5 cm above the sample surface .The energy of UV light was measured by a radiometer New Port Optical Power Meter, model 840. The films were then masked with a 500 mesh TEM grid and exposed to UV light for various times.

UV irradiation at 320-400nm was produce by UVA bulb F20T12BLB (I=1.44 mW/cm^2) placed at the distance of 20 cm above the sample surface. Twenty samples were prepared for each type of fibroblast: 10 with control fibroblast and 10 with UVC-irradiated cells.

In order to determine the localized sensitivity of neonatal dermal fibroblast plated on photo-sensitive polymer coated Si wafer the samples were exposed to UV light using an oval

TEM grid. The concentration of photo-sensitive polymer is 8.35 mg/ml and the thickness of a polymer film is 160nm. A grid-like pattern directly corresponding to the TEM grid was found to be formed on the surface of the sample. Low density neonatal dermal fibroblast, 3000 cells/ cm^2, were plated on the photo-sensitive polymeric film. The samples were cultured in the full-DMEM for 3 days in Napco 5430 Incubator at 37 C with 4.9% CO2 and 100% humidity. After 3 days in the incubator the samples were exposed to UV light.

3.2.8 Compatibility of the photosensitive polymer with neonatal dermal fibroblast cells:

In order to assess the compatibility of the photosensitive polymers, neonatal dermal fibroblasts were plated directly on the silicon wafers coated with spun cast films of the photosensitive polymers and placed in $35mm^2$ Petri dishes containing 3 milliliters of media. Cells were counted on days 1, 3 and 6. Some of the samples were fixed and the actin filaments were stained with Alexaflor, while the nuclei were stained with Propidium iodide.

3.3 Results and Discussion

3.3.1 Biocompatibility of Neonatal Dermal Fibroblasts with the Photosensitive Polymers

In order to evaluate biocompatibility of the coated substrates for cell culture, we first compared the doubling times of the neonatal dermal fibroblasts cells on each type of substrate relative to a TCP control. We plated 3,000 cells on each substrate, allowed them to adhere for 24 hours, and then counted at day 1, 3 and 6. The counts are plotted as a function of incubation time in figure 2.a. We found that the doubling times on the P_4VP homo-polymer or P_4VP blend polymer coated substrate were indistinguishable from that measured on the TCP, or 36(1), 37(1) 35(1) hours respectively. On the other hand, Figure 2b shows that the doubling times measured on the PMMA coated substrate was 60 (2) hours, or significantly longer (p=.0001).

In order to determine the ratio of living/dead cells for P_4VP, P_4VP/PMMA substrate 10µl of Tryphan blue was added at 10µl of cells media. The percentage of cell viability is 98% and 96% on the P_4VP and the P4VP/PMMA substrates versus 93% control TCP and 90% on PIPAAm-grafted TCP surfaces (4).

In order to determine whether the cell morphology was consistent with the cell count data, we also stained the samples for actin with Alexaflour and PI, and they imaged them the samples with confocal microscopy. The cell counts on each sample are shown in figure 2a together with the confocal microscopy images taken on day 3. From the figure 3a, 3b, 3c we can see that the results are comparable to the TCP control (Figure 3d) for all polymers except for the PMMA film surface, where a significant decrease in counts is observed.

3.3.2 Effects of UV Exposure on Neonatal Dermal Fibroblasts

In order to gauge the effect of UV exposure on the cells in the frequency band and energy density where ablation occurs, we plated neonatal dermal fibroblast cells at a density of 100,000 cells /cm^2 on the P_4VP coated substrates. The cells were incubated for 24 hours and then exposed to UVA radiation for 15 minutes, 30 minutes, and 1 hour for a total UVA dose of 1.3J/cm^2, 2.6 J/ cm^2 and 5.2J/ cm^2 respectively. The cells were counted immediately after exposure, and then after one and three days of incubation following irradiation. The results are shown in figure 4a. From the figure we can see that immediately after irradiation there is no significant decrease in cell count for the dosages used. After 24 hours, we observe no change for the samples exposed for 15 minutes, and a decrease of 11% and 19% for those exposed for 30 and 60 minutes, respectively. On day three we find that the samples exposed for 15 and 30 minutes, had completely recovered, and the count rate for those exposed for one hour was 23% percent less than the control.

3.3.2a Cell Sheet Detachment

Cell sheets detached and floated off from the P_4VP substrates were transferred to another P_4VP substrate for further testing. Here we determined that a minimum of 5 min irradiation, which corresponded to 432mJ/cm^2 was required in order to remove an intact layer of cells. An optical image of the cell sheets removed after irradiation with 432mJ/cm^2 and 2.6J/cm^2 are shown in figure 4b and 4c respectively. The area of the cells plated was 1 cm^2 and approximately 0.8 cm^2 was removed from the center of each sample. The latter sheet was also fixed and stained and the cells imaged with confocal microscopy. From the image shown in figure 4d, we can see that even at the higher irradiation dose, the cells in the sheet were confluent and well spread.

In order to further probe the condition of the cells, the cells were re-plated, cultured for various times and tested with different biological assays. The experimental sequence is illustrated in figure 5.

3.3.3 Investigation of the effects of low dose UVA irradiation

As shown in figure 5, we first plated neonatal dermal fibroblasts cells at high density (100,000/cm^2) on a P_4VP substrate, incubated for 24 hours and irradiated them with 1.44mW/cm^2 for 5, 10, 15, 30, and 60 min. In each case we observed that the cell sheet could be lifted from the substrate immediately following irradiation without trypsin or other agents, which confirmed our hypothesis that release of the upper layer, even if it was only 8nm thick, would be sufficient to remove the area upon which the cells were adhered. The cell sheet were collected in a flask, diluted in DMEM, and re-plated on multiple sets of P_4VP coated substrates at a lower density (12,500cells/cm^2) where a more detailed series of assays were performed as shown in figure 5.

3.3.3 a Cell Viability: Cell viability was first determined before plating by staining a group of cells with tryphan blue and comparing the viability with a control group which was cultured on TCP and lifted by enzymatic digestion with trypsin. The viability of cells harvested after UV irradiation was measured to be 94% which compared very favorable with the value of 93% measured for the control sample harvested by enzymatic digestion. Another method for determining viability is testing for apoptosis, where viability is assayed by flow cytometry after annexin V-FITC/propidium iodide staining. FITC Annexin V staining precedes the loss of membrane integrity which accompanies the later stages of cells death resulting from either apoptotic or necrotic processes. Staining with FITC Anexin V is typically used in conjunction with a vital dye such as propidium iodide (PI) to investigate early apoptotic cells (PI negative, FITC Annexin V positive). The cells that are considered viable are FITC Annexin V and PI negative. The results are shown in figure 6 where the viability of the control sample was found to be 96% versus 95% of the cells exposed to 1.3J/cm2 and 88% for the cells exposed to 2.6 J/cm2.

Cell Proliferation: In order to show the differences in proliferation, between cells irradiated for 30min and un-irradiated cells, the cells were counted with a hemocytometer on days 0, 3,

and 6 after plating on P_4VP coated substrates, and the results plotted in figure 7a. From the data we were able to obtain a doubling time of 37(2) hours for the irradiated samples, in good agreement with 36(1) obtained from the un-irradiated control sample.

We also imaged the cells with confocal microscopy, on days 0, and 6. From the figures 7b, 7c we can see that immediately after irradiation the appearance of the cells is not changed from that of the non-irradiated control sample figures 7d and 7e. From the figures we see that the cells remain well extended and continue to show highly organized actin fibers and intact nuclear membranes. Hence, no discernable damage in morphology is observed when the exposed cells are *lifted* and *replated* following irradiation.

3.3.3b Alamar Blue Cell Viability Reagent: Figure 8a, b, c presents cell viability results on day 1, day 3 and day 6 after UVA exposure. Cell viability and proliferation is indicated through the conversion of resazurin to resorufin. Resazurin, a non-fluorescent indicator dye, is converted to highly red fluorescent resorufin via reduction reactions of metabolically active cells. The amount of fluorescence produced is proportional to the number of living cells, and hence the florescence could be calibrated as discussed previously. From the figure 8a we can see that the difference in florescence intensity between the irradiated samples and the control at day1 is between 12% and 27% based on the UV irradiation of 1.3J/cm^2, 2.6J/cm^2 and 5.2 J/cm^2. On day 3 the difference is between 7% and 12% and on day 6 the difference is between 6% and 9% based on UV dose. This result shows that the cells had a minimal damage after 15 minutes exposure to UVA. Similarly, the doubling time, as calculated from this technique is 39(1) for the non-irradiated control and 40(1) hour for the irradiated samples, regardless of exposure time.

3.3.3c MTS Cell Mitochondrial Activity: Mitochondrial activity is another measure of cell activity, which can be assessed by using MTS staining. In Figure 9 we plot the mitochondrial activity, normalized to the un-irradiated control samples on days 1 and 6 following UVA irradiation. Figure 9a shows that after 24 hours there is a decrease in activity of 1.5%, 5%,13%, 15%, and 20% , respectively for the samples irradiated for 5,10, 15,30, and 60 minutes. On day 6 though, the difference decreases to 9% for the samples irradiated for 15, 30, and 60 minutes, indicating that the cells are recovering.

3.3.3d ROS Assay: Another way to gauge the damage to the cells is via determination of the ROS production resulting from irradiation, since it is well established that even a small amount of UV exposure results in the production of ROS. We therefore measured the amount of ROS products in the cells following UVA irradiation for different times. The results are plotted in figure 10, where we can see that on day 1 following irradiation the amount of ROS products produced in the samples following 5 and 10 minutes of exposure was not significantly different from the control, un-irradiated sample. The amount of ROS products formed seems to increase abruptly following 15 minutes of irradiation and did not increase further following 30 and 60 minutes of irradiation. After three days, the difference in ROS production for the samples irradiated for 15 minutes or longer decreased relative to the control, but the differences between the different irradiation times becomes apparent only on day 6. Hence from these assays we can conclude that the minimum irradiation dose which is capable of ablating the surface polymer layer and removing an intact layer of cells, the amount of additional ROS produced due to the irradiation is negligible.

3.3.4 Cell tissue patterning using light sensitive polymers

In order to demonstrate that we can use the techniques described here to produce a patterned cell layer, the part of the cell layer with a specific geometry was removed from the polymer surface after UVA exposure through a mask and then replaced with cells of a different type. Figure 11a shows a schematic of the patterning experiment. Neonatal dermal fibroblasts were plated at a density of 100,000 cells/cm^2 on the polymer surface and incubated for 24 hours. The cells were then exposed to the UVA for 30 minutes through a mask, as shown in the figure, and removed from an oval area, 0.2mm in diameter, from the center of the layer. In figure 11b we show the border between the exposed and unexposed regions, where we can clearly see that all cells were removed from the exposed section, while the cells in the unexposed section are confluent and well spread. Fibronectin was then added to the media and Keratinocytes were then plated in the area where the neonatal dermal fibroblast were removed following exposure and incubated for 24 hours. The border between the two types of cells is imaged with confocal microscopy and shown in figure 11c, where we can see the keratinocytes adhere to the polymer surface. In figure 11d we show high magnification image of the same region, where we can see that the two types of cell layers have begun to inter diffuse.

3.4 Conclusion: We have shown that P_4VP polymers and their blends with PMMA can be etched via exposure to UVA radiation. Furthermore, we also showed that these polymers could be used as a cell culture substrate, upon which the proliferation rates and cells viability of neonatal cells was comparable to that on tissue culture Petri dish. Based on these findings we also demonstrated that irradiation with UVA could be used to pattern and lift off cell sheets cultured from P_4VP substrate. The cell sheets that were removed were then re-plated at a low density and counted at one, three and six days after irradiation. We show that only a small amount of degradation occurred and the doubling time was close to the control, indicating that the cells have recovered from the radiation. The minimum exposure time when the cells were able to be removed was 0.432 J/cm^2. At this dose no discernable effect was observed after 5 minutes in the production of ROS and metabolism, as measured by MTS assays.

3.5 References

[] F.J.Wu, et al.: Enhanced cytochrome P450 IA1 activity of self-assembled rat hepatocytes spheroids, Cell Transplantation, vol.8, pp.233-246, 1999.

[] S.N.Bhatia et al., Probing heterotypic cell interaction: Hepatocyte function in micro fabricated co-cultures, J.Biomater. Sci. Polym. Edn. Vol. 9, pp.1137-1160, 1998.

[] D.E.Ingber, Engineering cell shape and function through control of substrate adhesion, in Polymer Surfaces and Interfaces: Characterization, Modification and Application, K.L.Mittaland K.W. Lee, Editors, VSP: Utrecht, The Netherlands, p.413-424, 1997.

[] S.N.Bhatia and C.S.Chen, tissue engineering at the Micro-scale, Biomedical Micro devices, vol.2, pp 131-144, 1999.

[] A. Welle and E. Gottwald, UV-based patterning of polymer substrates for cell culture application, Biomed. Microdev. Vol.4, pp.33-41, 2002.

[] Hidaka H., Horikoshi S., Serpone N., and Knowland J., J. Photochem. Photobiol. A, 111,205-213, 1997.

[] Matsumara Y. and Ananthaswamy H., Toxicol. Appl. Pharmacol., 195, 298-308,2004.

[] Scharffetter-Kochanek K, Brenneisen P, Wenk J. et al. Photoaging of the skin from phenotype to mechanism. Exp.Gerontol.35: 307-316, 2000.

[] Holbrook, N.J, Liu Y, Fornace A.J Signaling events controlling the molecular response to genotoxic stress, EXS 77:273-288, 1996.

[] Shaulian, E, Schreiber M, Piu F, The mammalian UV response: c-Jun induction is required for exit from p53-imposed growth arrest. Cell 103: 897-907, 2000.

[] Karin, M, Mitogen activated protein kinase cascades as regulators of stress responses. Ann.N.Y.Acad. Sci.851:139-146, 1998.

[] Shackelford R.E, Kaufmann W.K, Paules R.S Cell cycle control, check-point mechanism, and genotoxic stress. Environ. Health Perspect.107 (suppl.1): 5-24, 1999.

[] Brenneisen P, Oh J, Wlaschen M, Ultraviolet B wavelength dependence for the regulation of two major matrix-metalloproteinases and their inhibitor TIMP-1 in human dermal fibroblast. Photochem. Photobiol. 64:877-885, 1996.

[] Fisher G.T, Datta S.C, Talwar H.S, Molecular basis of sun-induced premature skin aging and retinoid antagonism. Nature 379: 335-339, 1996.

[] Halliwell, B. and Aruoma O.I. DNA damage by oxygen-derived species. Its mechanism and measurement in mammalian systems. FEBS Lett. 281:9-19, 1991.

[] Mount D.W. DNA repair. Reprogramming transcription. Nature 383:763-764,1996.

[] Blattner C., Bender K., Herrlich P., Pahmsdorf H.J. Photoproducts in transcriptionally active DNA induce signal transduction to the delayed ultraviolet-responsive genes for collagenase and matallothionein. Oncogene 16: 2827-2834., 1998.

[] Nordberg J., and Arner E.S. Reactive oxygen species, antioxidants, and the mammalian thioredoxin system. Free Radical. Biol. Med. 31: 1287-1312, 2001.

[] Hancock J.T., Desikan R. and Neill S.J. 2001. Role of reactive oxygen species in cell signaling pathways. Biochem. Soc. Trans. 29: 345-350, 2001.

[] Wlaschek M., Briviba G.P., Stricklin G.P. Singlet oxygen may mediate the ultraviolet A-induced synthesis of interstitial collagenase.J. Invest. Dermatol. 104 , 194-198, 1995.
[] Masaki H., Atsumi T., Sakurai. Detection of hydrogen peroxide and hydroxyl radicals in murine skin fibroblast under UVB irradiation. Biochem. Biophys. Res. Commun. 206 , 474-479, 1995.

[] Jurkiewicz B.A., Buettner G.R. Ultraviolet light-induced free radical formation in skin : an electron paramagnetic resonance study. Photochem. Photobiog.59, 1-4, 1994.

[] Wills EE, AndersonTW, Beattie BL, et al. Randomized placebo-controlled trial of ultraviolet light in the treatment of superficial pressure sores. J.Amer. Geriatr. Soc 31, 131-3, 1983.

[] Naussbaum RL, Biemann I, Mustard B. Comparison of ultrasound/ultraviolet-C and laser for treatment of pressure ulcers in patients with spinal cord injury. Phys Ther 74 :812-25, 1994.

[] Kloth LC. Physical modalities in wound management : UVC, therapeutic healing and electrical stimulation. Ost. Wound. Manag 41, 18-27, 1995.

[] Ellem KAO, Culliman M, Baumann KC, et al. UVR induction of TGFa : a possible autocrine mechanism for the epidermal melanocytic response and for promotion of epidermal carcinogenes. Carcinogenesis 5 :797-801, 1988.

[] Ley KD, Ellem KAO. UVC modulation of epidermal growth factor receptor number in HeLaS3 cells. Carcinogenesis 13 :183-7, 1992.

[] Sachsenmaier C, Radler-Pohl A, Zinck R, et al. Involvement of growth factor receptors in the mammalian UVC response. Cell 78 :963-72, 1994.

[] Huang R, Wu J, et all. UV activatesgrowth factor receptors via reactive oxygen intermediates. J Cell Biol 133 :211-20, 1996.

[] Bell E, Ivarsson B, Merrill C. Production of a tissue-like structure by contraction of collagen lattices by human fibroblast of different proliferative potential in vitro. Proc Nat Acad. Science USA 76 :1274-8, 1979.

[] Gillery P, Maquart FX, Borel JP. Fibronectin dependence of the contraction of collagen lattices by human dermal fibroblasts. Exp Cell Res 167, 29-37, 1986.

[] Marks MW, Morykwas MJ, Wheatley MJ. Fibroblast mediated contraction in actinally exposed and actinically protected aging skin. Plast Reconstr Surg 86, 255-9, 1990.

[] Pieraggi MT, Julian M, Bouissou H. Fibroblast changes in cutaneous aging. Virchows Arch A pathol Anat Histolpathol 402, 275-87, 1984.

[] Morykwas m, Malcolm M, Effects of ultraviolet light on fibroblast fibronectin production and lattice contraction. Wounds, 10(4), 111-117, 1998.

3.6 Figure Captions

Figure 3.1: Etching rate of PMMA, P_4VP, and P_4VP/PMMA polymers exposed to the following radiation: (a) 3.98mW/cm2 of UVC, (b) 1.44 mW/cm2 of UVA and (c) contact angle of P_4VP surfaces exposed to different UVA doses.

Figure 3.2: Neonatal dermal fibroblast were plated with an initial density of 3000 cells/cm^2 on P_4VP, PMMA, P_4VP/PMMA substrates and the control sample was plated on tissue culture Petri dish plastic. (a) The growth curves obtained on the different substrates and (b) the doubling time calculated from the data in (a).

Figure 3.3: Confocal microscope images of the neonatal dermal fibroblast obtained on day three after platting 3000 cell/cm^2. The actin fibers were stained with Alexaflour Phalloidin 488 and the nuclei are stained with Propidium Iodide. The cells were plated on different substrates (a) PMMA, (b) P_4VP, (c) P_4VP/PMMA and (d) Tissue Culture Petri Dish.

Figure 3.4: (a) Proliferation of neonatal dermal fibroblasts plated on P_4VP at a density of 10^5cells/cm2 and irradiated with 1.44mW/cm2 of UVA for 15 minutes (1.3J/cm2), 30 minutes (2.6J/cm2) and 60 minutes (5.2J/cm2). The control sample was not irradiated. Confocal microscopy images of the cells, stained with Alexaflour Phalloidin 488 and Propidium iodide. Phase-contrast (top view) microscopy image of the sheet of neonatal dermal fibroblasts detached after (b) 5 minutes of UVA exposure and (c) 30 minutes of UVA exposure. (d) Confocal microscope picture of the cell sheet removed after 30 minutes UVA exposure.

Figure 3.5: Schematic of the experimental sequence designed to measure the effects of 30 minutes exposure to UVA radiation (2.6 J/cm2) on cell proliferation, cells viability, mitochondrial function, ROS production and apoptosis.

Figure 3.6: Apoptosis detection assay of the cells according to schematic in figure 5 after incubation of day1 (a) unexposed sample, (b) sample exposed to 1.3J/cm^2 and (c) sample exposed to 2.6 J/cm^2. Cells viability was assayed by flow cytometry after annexinV-FITC/propidium iodide staining. Numbers indicated express viable cells (lower left quadrant) as a percentage of total cells.

Figure 3.7: Neonatal dermal fibroblasts plated on a P_4VP surface, lifted following exposure and then replated at a density of 12,500 cells/cm2, according to the schematic shown in fig 5. (a) Growth curve of the control (un-exposed sample) versus the samples exposed to UV irradiation. Confocal microscopy images of the cells stained with Alexaflour Phalloidin 488 and Propidium iodide and imaged on day 0 and day 6 following exposure; (b ,c) Unexposed control and (d, e) exposed for 30 minutes.

Figure 3.8: Alamar blue viability assays of the neonatal dermal fibroblast cells, removed from the P4VP surface via UVA exposure, re-plated according to fig 5 , measured on days (a) one (b) three and (c) six. The corresponding proliferation curve (d) and the doubling time (e).

Figure 3.9: Mitochondrial activity assays of the cells according to the schematic in figure 5 after incubation of (a) day 1 and (b) day 6.

Figure 3.10: Assay of ROS product formation of the cells according to schematic in figure 5 measured after (a) day 1 (b) day 2 and (c) day 6.

Figure 3.11: (a) Schematic of the experimental protocol used to produce tissue with adjacent areas composed of two distinct cell populations. Confocal images of a patterned tissue containing a central area of keratinocytes surrounded by dermal fibroblasts. (b) The dermal fibroblast area imaged immediately after removal of the circular central area, as shown in part a. (c) The central portion of the tissue imaged 24 hours after plating keratinocytes. Interfacial region between the two types of tissue is showing attachment of the keratinocytes to the dermal fibroblast layer. (d) High magnification image (63X) of figure (11c) presenting the keratinocytes plated on the UVA exposed area.

3.7 Figures

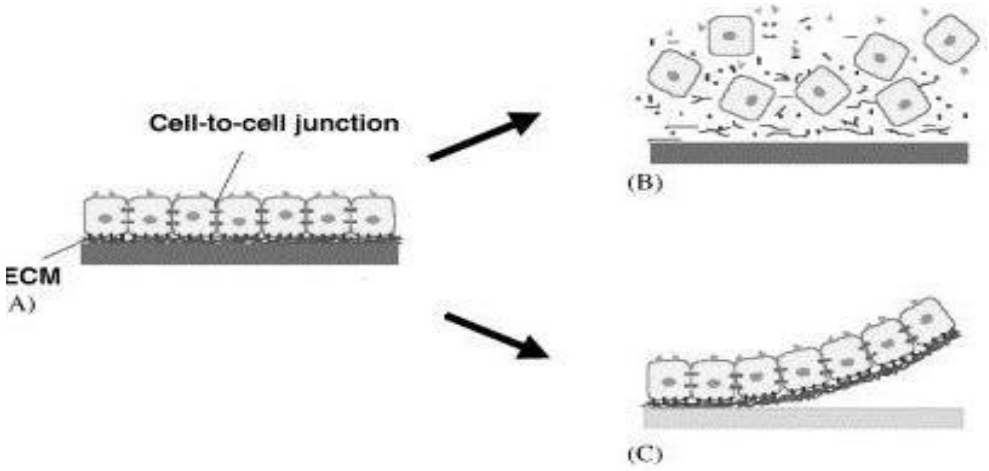

Figure 3.1

a

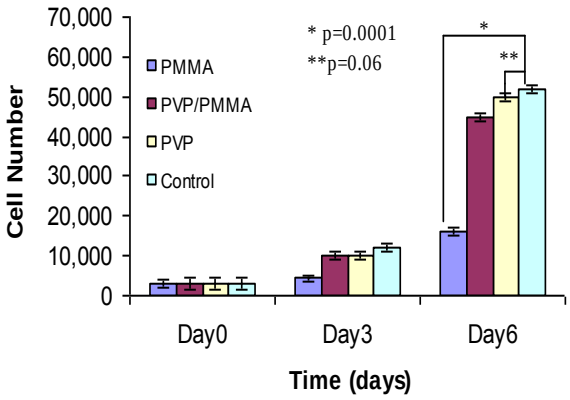
70,000
60,000
50,000
40,000
30,000
20,000
10,000
0
Cell Number
PMMA
PVP/PMMA
PVP
Control
* p=0.0001
**p=0.06
*
**
Day0
Day3
Day6
Time (days)

b

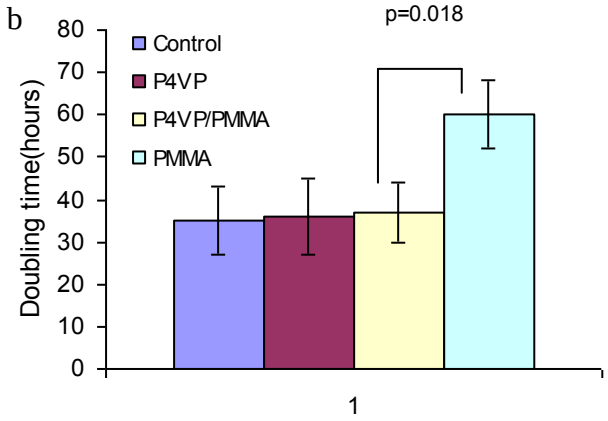
p=0.018
80
70
60
50
40
30
20
10
0
Doubling time(hours)
Control
P4VP
P4VP/PMMA
PMMA
1

Figure 3.2

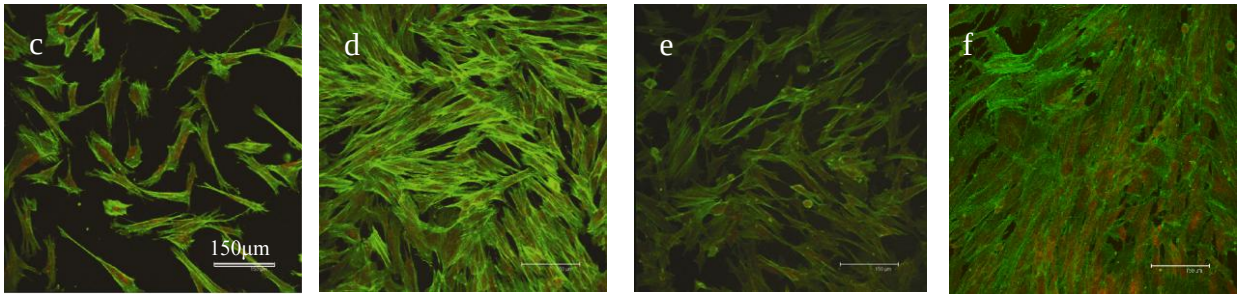

Figure 3.3

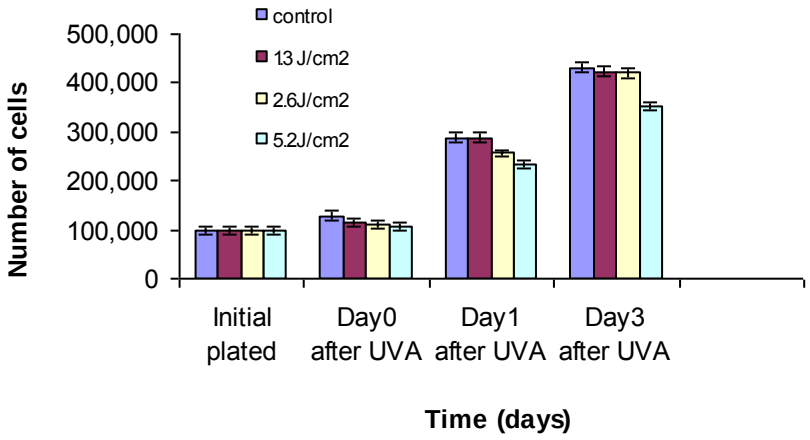
control
1.3 J/cm2
2.6J/cm2
5.2J/cm2
500,000
400,000
300,000
200,000
100,000
0
Number of cells
Initial plated
Day0 after UVA
Day1 after UVA
Day3 after UVA
Time (days)

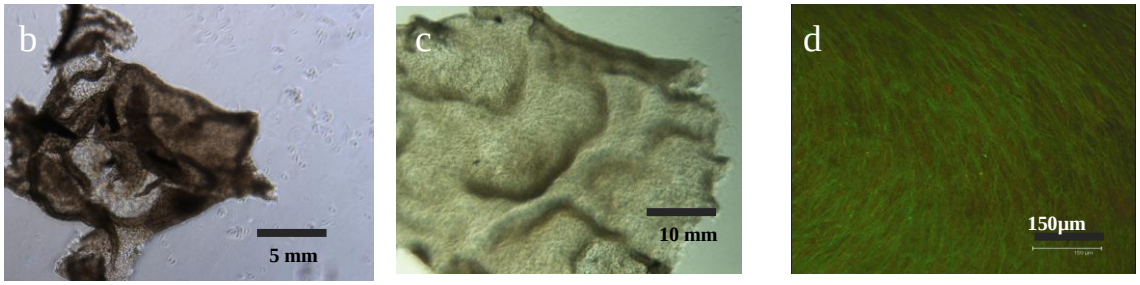
b
5 mm
c
10 mm
d
150µm

Figure 3.4.

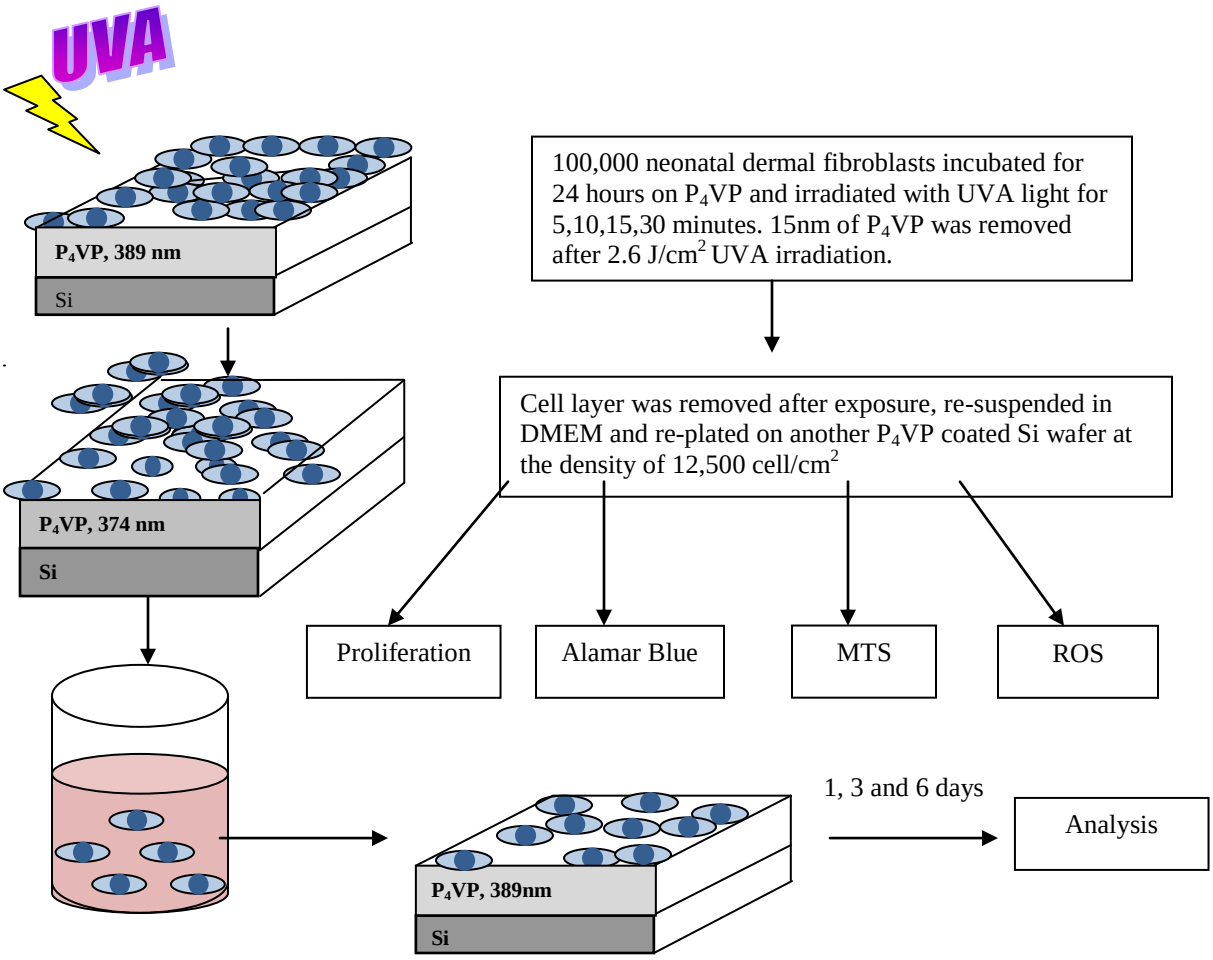
UVA
P4VP, 389 nm
Si
100,000 neonatal dermal fibroblasts incubated for 24 hours on P4VP and irradiated with UVA light for 5,10,15,30 minutes. 15nm of P4VP was removed after 2.6 J/cm2 UVA irradiation.
P4VP, 374 nm
Si
Cell layer was removed after exposure, re-suspended in DMEM and re-plated on another P4VP coated Si wafer at the density of 12,500 cell/cm2
Proliferation
Alamar Blue
MTS
ROS
1, 3 and 6 days
Analysis
P4VP, 389nm
Si

Figure 3.5.

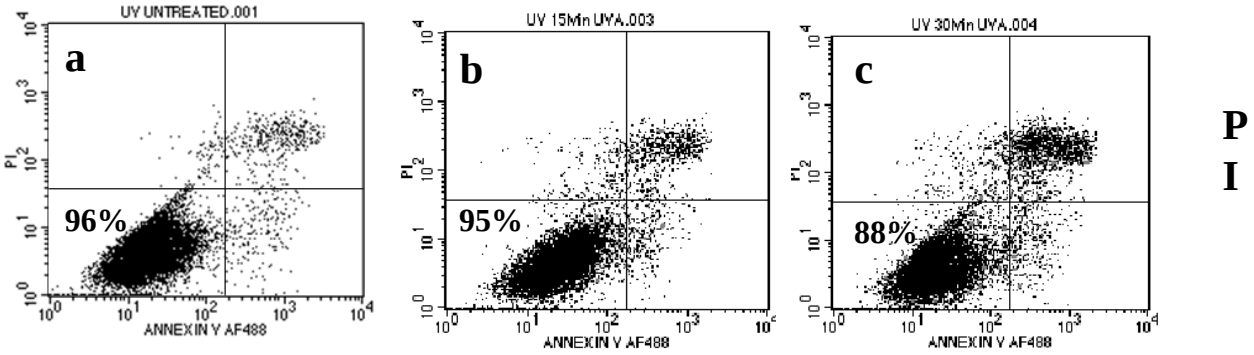

Annexin V-AF488

Figure 3.6

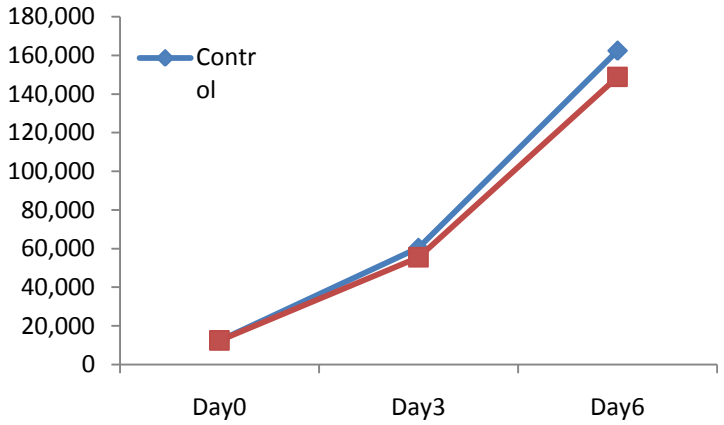
180,000
160,000
140,000
120,000
100,000
80,000
60,000
40,000
20,000
0
Control
Day0
Day3
Day6

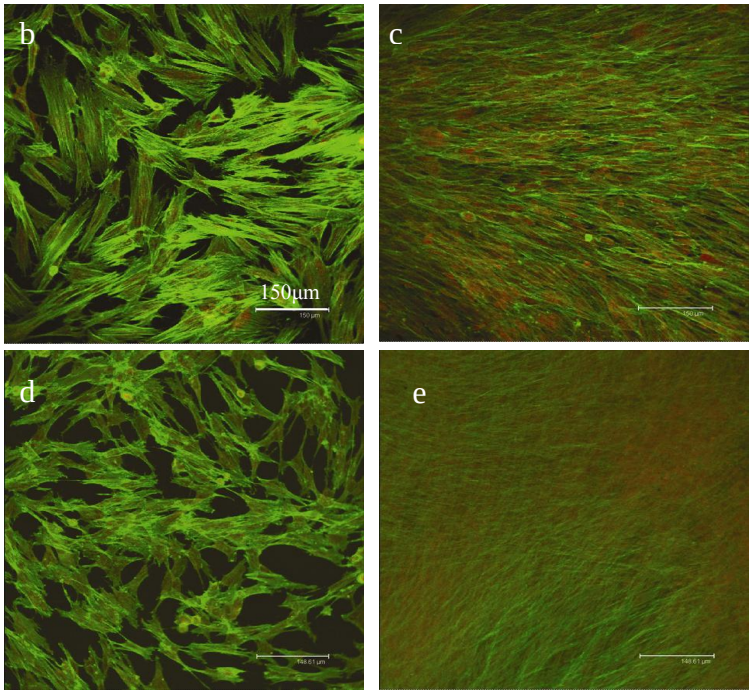
b
150µm
c
d
e

Figure3.7

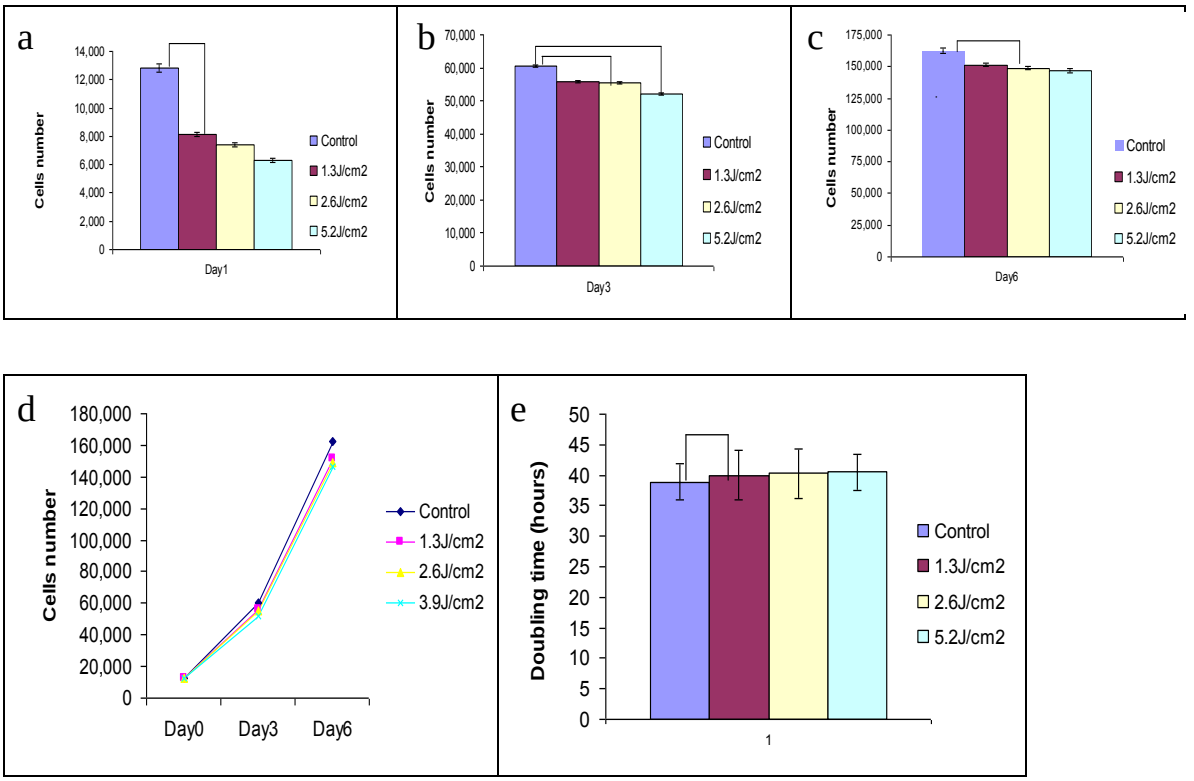
a
Cells number
14,000
12,000
10,000
8,000
6,000
4,000
2,000
0
Day1
Control
1.3J/cm2
2.6J/cm2
5.2J/cm2
b
Cells number
70,000
60,000
50,000
40,000
30,000
20,000
10,000
0
Day3
Control
1.3J/cm2
2.6J/cm2
5.2J/cm2
c
Cells number
175,000
150,000
125,000
100,000
75,000
50,000
25,000
0
Day6
Control
1.3J/cm2
2.6J/cm2
5.2J/cm2
d
Cells number
180,000
160,000
140,000
120,000
100,000
80,000
60,000
40,000
20,000
0
Day0
Day3
Day6
Control
1.3J/cm2
2.6J/cm2
3.9J/cm2
e
Doubling time (hours)
50
45
40
35
30
25
20
15
10
5
0
1
Control
1.3J/cm2
2.6J/cm2
5.2J/cm2

Figure 3.8

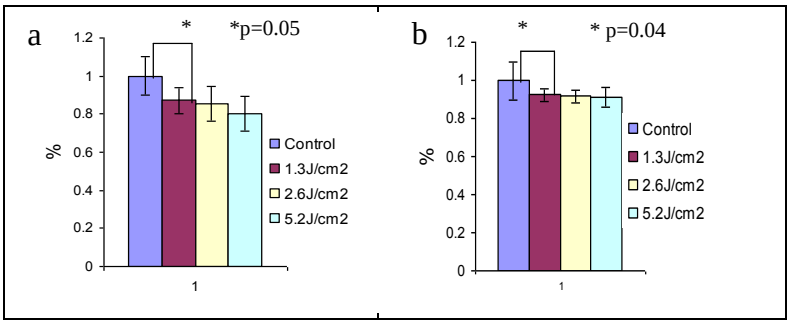
a
*
*p=0.05
1.2
1
0.8
0.6
0.4
0.2
0
%
Control
1.3J/cm2
2.6J/cm2
5.2J/cm2
1
b
*
* p=0.04
1.2
1
0.8
0.6
0.4
0.2
0
%
Control
1.3J/cm2
2.6J/cm2
5.2J/cm2
1

Figure 3.9

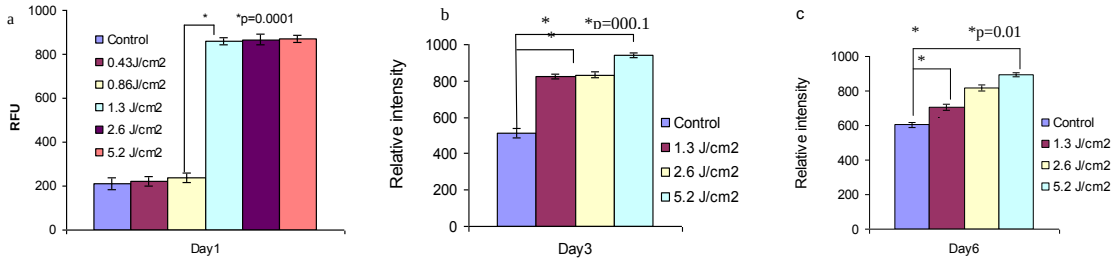
a
1000
800
600
400
200
0
RFU
*
*p=0.0001
Control
0.43J/cm2
0.86J/cm2
1.3 J/cm2
2.6 J/cm2
5.2 J/cm2
Day1
b
*
*
*p=000.1
Relative intensity
Control
1.3 J/cm2
2.6 J/cm2
5.2 J/cm2
Day3
c
*
*
*p=0.01
Relative intensity
Control
1.3 J/cm2
2.6 J/cm2
5.2 J/cm2
Day6

Figure 3.10

a

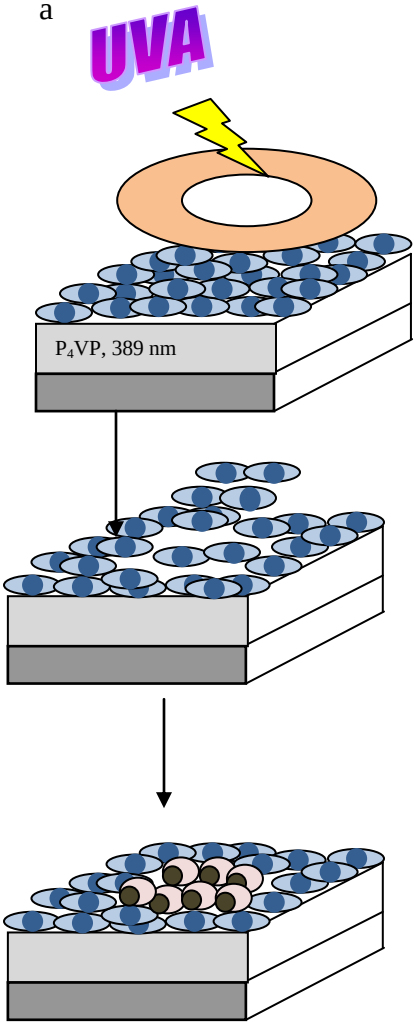

100,000 neonatal dermal fibroblasts incubated for 24 hours on P_4VP and irradiated with UVA light for 30 minutes through an oval grid.

Only the cells exposed to UVA were removed.

Keratinocytes were plated in the exposed area.

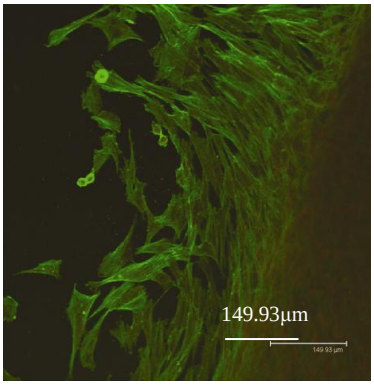

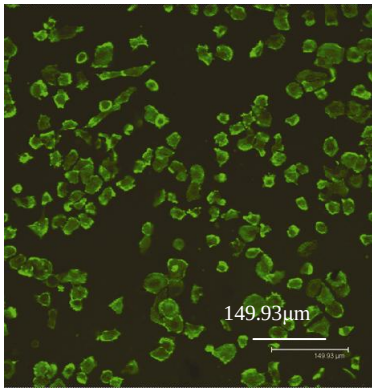

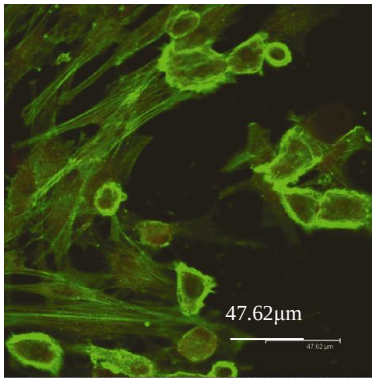

Figure 3.11

Chapter 4

Coated TiO2 particles which afford complete protection for cells to UVC exposure

4.1 Introduction

The sun irradiates more energy in the ultraviolet spectral region (100-400nm) than in that of visible light (400-700nm). It is well recognized that UV light in the range 280-400 is responsible for the majority of photo damage to the skin. The shortest of these wavelengths (UVC, 100-280nm) are absorbed completely by atmospheric oxygen (O_2) and the ozone layer (O_3). UVC is the most energetic and hence can cause the highest amount of damage in the cells. A wavelength in the UVB range (280-320nm) are absorbed efficiently, though incomplete, by ozone; UVB is mostly stopped within the epidermis and causes the inflammation known as “sunburn”; while UVA (320-400nm) is absorbed only weakly and is therefore more easily transmitted to the earth’s surface. UVA is the longest wavelength component and can penetrate into the dermis where melanoma originates.[Hidaka,1997] [Matsumara,2004].

The exposure to UVC must come from artificial sources. The majority of UVC rays are absorbed by the epidermis in intact skin; with wounds and denuded surfaces the total energy is absorbed by dermal components. UVC damages the cells preventing proliferation, induces ROS and DNA damage.

TiO_2 is known to be biologically inert and non-toxic at the micro-scale in humans and animals [Bernard, 1990], [Chen, 1988], [Hart, 1998].TiO_2 is used in cosmetics where its high absorbance for UV radiation is used to increase the SPF factors of sunscreens. However, once it absorbs UV light, TiO_2 catalyses the generation of ROS. Dunford et al. (19) showed that TiO2 can be a potential hazardous material since ROS products cause genetic damage and other unfavorable effects in living tissue [Long, 2007]. TiO_2 is known to photocatalize the production of ROS when the particle are on nanoscale dimention because it is increasing the surface area and the electron flux. The particle smaller then 20nm can cause inflammatory raction in animals and humans [Ophus, 1979] [Oberdorster, 1994].Cells culture decrease in the growth rate in the presence of 0.1mg/ml nanoparticles TiO2 [Sayers, 2006]. Many reports

linked the cytotoxicity of TiO2 nanoparticles to induce oxidative damage [Gurr, 2005]. Lee et al [Lee,2007] showed that grafting a dense polymer coating onto the TiO_2 particles can trap the photoelectron and suppress ROS production. Zhi Pan et al [Zhi Pan, 2009] showed that TiO2 added to the cells and cultures do not penetrate the cells. Particles coated with a dense grafted polymer brush are shown to prevent the adherence to the cell membrane and hence the penetration of cells, which decreases reactive oxygen species (ROS) formation and protect cells. We therefore performed a study in order to determine how these particles can protect the cells exposed to UVC.

4.2 Material and methods:

4.2.1 TiO2 particle characterization

SEM was used to estimate the particle size, shape and suspended status of dry TiO_2 powder. In order to image each particle clearly, the powder was dispersed in ethanol and spread on a carbon coated TEM grid.

4.2.2 Cell culture and function studies

Neonatal Human Dermal fibroblasts were purchased from Skin Bank Cascade Biologics (Portland, Oregon). Fibroblasts growth media was comprised of Dulbecco's Modified Eagle Medium (DMEM) supplemented with 10% Fetal Bovine Serum (FBS) and 1% Penicillin-Streptomycin (PS). Cells were maintained using a NAPCO 5430 Incubator at 37° C with 5.0% CO_2 and 100% humidity. Cell numbers were quantities using a Coulter Particle Counter (Beckman Coulter).

In the classic experiment cells were grown in the 35 mm^2 Petri dish. After that, cells were trypsinized, the enzyme reaction was stopped with media and the aliquot of 100 ml cell solution was placed in each well of the 96-wells dish for further experiments. Following the different incubation periods, cells were fixed, permeabilized, then stained with Alexa Flour 488 phaloidin (Invitrogen, Carlsbad, CA) and Propidium Iodide (HPLC, Sigma Chemical Co., St. Louis, MO) to visualize the actin cytoskeleton and nucleus. The morphology of the cells

was visualized with a Leica TCS SP2 laser scanning confocal microscope (Leica Micro-system Inc., Bannockburn).

TiO2 media was prepared by dispersing the nanoparticles in the same full-DMEM at different concentrations, followed by 30 minutes sonications and 5 minutes stirring to get an homogenous distribution. The experimental samples were prepared by culturing cells in these TiO2 media at different concentrations. Media was changed every 2-3 days.

Immunofluorescence images of cells were taken with a 40X oil lens on a Leica TCP SP2 laser scanning confocal microscope (Leica Microsystem) after the cells were stained by alexa flour 488 phalloidin for actin and propidium iodide for nuclei. With MetaMorph software (Universal Imaging) the cells area in these confocal images can be measured.

Counting the cells, we seeded 3000 cells/well in 24-well dish in full-DMEM or TiO2 media for 2-3 days. After that the cells were rinsed 3 times with PBS to remove any suspended particles and dead cells. At the end the cells were detached with trypsin and counted with a hemacytometer. Each experimental group had 3 replicates to get the average cell number under each condition.

4.2.3 TEM

TEM was used to monitor how TiO2 nanoparticles penetrate the cells and where it stays in the cells. The fresh samples were rinsed 3 times with PBS and plated 15x 10^4 on plastic film in six well plates. The samples were then incubated for 24 hours in the incubator and exposed to 3.5 J/cm2 UVA. After exposure the cells were incubated for another 24 hours and fixed with a solution of 10%xxxxx. After washing the cells with distilled water, TEM samples were dried and imaged with Joel (model 1200EX) transmission electronic microscopy. We analyzed the images by characterizing the penetration and distribution of TiO2 nanoparticles.

4.2.4 TiO_2 Particle coating

Rutile TiO2 nanoparticles were coated by chemically grafting a antioxidant/anionic and hydrophobic polymer molecules directly onto the surface (26). Antioxidant from grape seed (Oligomeric Proanthocyanidis) and anionic polymer (Poly-methylvinylether/maleic acid)

were mixed at 1:1 ratio and dissolved in a 22:1 water/denatured ethanol solution using a light mixing at 25°C, When the solution was uniform, a new mixture was prepared of 30% (w/w)of antioxidant/anionic polymer solution, 22% (w/w) DI water, 43% (w/w) titanium dioxide and 5% hydrophobic polymer (Trietoxysilylethyl Polydimethylsiloxyethanyl dimethicone form Shin-Etu Chemical Co.,Ltd). The resulting slurry was sonicated for 30 minutes at 25°C with an Ultrasonic probe (Sonicor Instrument Co.) at 20 KHz and then centrifuge for 15 minutes at 9000 rpm. The product was washed with DI water three times to ensure that the unattached materials have been removed. The product was dried at 110°C under vacuum for 16-20 hours. Lee et al. (26) have shown that it was possible to chemically graft a dense charged polymer onto the TiO2 particle using sonochemical methods. This layer was able to trap electrons emitted by the particles and form a dense polymer brush with a grafting density on one chain per 0.6nm. It is known that the stretched brushes do not adhere to surfaces, because entropic hindrance prevents further distortion of the brush, resulting in hard core repulsion. Zhi Pan at al. (27-zhi pan article) shows that this effect prevents the coated particle from adhering to the cell surface membrane.

4.2.5 UV light exposure

UV irradiation at 240-280nm (λ=270nm, I=3.98mW/cm^2) was accomplished with a low-pressure mercury lamp (15 Watt rod bulb) placed at a distance of 6.5 cm above the sample surface .The energy of UV light was measured by a radiometer New Port Optical Power Meter, model 840.

4.2.6 Alamar blue

Cell viability activity was evaluated with AlamarBlue reagent (Invitrogen). Cells were platted in a 96-well plate at six different densities (100,000 cells to 3,250 cells) in 100ul of media. After 24 hour in the incubator the samples are exposed to UVA for 15, 30 and 60 minutes. 10% of AlamarBlue reagent was added directly to each well; the plates were incubated at 37°C for 1-4 hours allowing cells to convert resazurin to resorufin. The absorbance signal is measured on a plate reader of spectrophotometer DAL1025 Micro plate

reader at 560 nm excitation and 590 nm absorbance. Calibration curve was used to calculate the cells number on day1, day3 and day6 after 1.3J/cm^2, 2.6J/cm^2 and 5.2J/cm^2 of UVA light.

4.2.7 MTS

Cell mitochondrial activity was evaluated with Cell Titer 96 Aqueous One Solution Cell Proliferation Assay (Promega). Cells were plated in a 96-well plate at six different cells densities from (100,000 cells to 3,250 cells) in 100µl of media. After 24 hours incubation the samples were exposed to UVA for 15, 30 and 60 minutes. 20% of the MTS solution (which one) was added to each well; the samples were incubated for 1 hour at 37° C. The absorbance was read at 490nm by the automated micro plate reader ELX800.

4.3 Results and discussions

4.3.1 Coated TiO_2 nanoparticle characterization

In figure 4.1a we show SEM micrographs of the TiO_2 particles used. In order to image the particle directly, the spheres were dispersed in ethanol and then spread a droplet of solution on a carbon coated TEM grid. The average width of the particles is 15.0+/-3.5nm.

4.3.2 Proliferation of neonatal dermal fibroblast coated with TiO_2 nanoparticles

Figure 4.2 show confocal microscope pictures of neonatal dermal fibroblast coated with polymeric TiO_2 at the concentration of (a) 0.4mg/ml, (b) 0.8mg/ml, (c) 4 mg/ml, (d) 10mg/ml, (e) 40mg/ml and (f) 80mg/ml after 7 days of incubations. Based on these pictures we found out that polymeric coated TiO2 does not harm the cells.

We first compared the doubling times of the neonatal dermal fibroblasts incubated with coated particles relative to control. We plated 3,000 cells in full- DMEM and DMEM with 4mg/ml coated TiO2 particles, allowed them to adhere for 24 hours, and then counted at day 3 and 6. The counts are plotted as a function of incubation time in figure 4.2g. We found that the doubling time of cells incubated with 0.4mg/ml coated particle are almost indistinguishable from the control sample or 35(1), 36(1) hours respectively.

4.3.3 Effects of UV Exposure on Neonatal Dermal Fibroblasts

In order to gauge the effect of UV exposure on the cells we plated neonatal dermal fibroblast cells at a density of 10^6 cells /cm^2 on the P_4VP-PKPV-PMMA coated substrates. The cells were incubated for 24 hours and then exposed to UVC radiation for 15 minutes, 30 minutes, and 1 hour for a total UVC dose 14.3 J/cm2.

Figure 4.3a shows the unexposed neonatal dermal fibroblast. From the figure 4.3b we can see that samples exposed to 3.5J/cm^2 irradiation show a significant decreased (65%) in cell count compared with the control –unexposed samples.

It is well known that exposure to UVC can produce other more subtle damage to cells. In order to protect the cells against UVC damage the cells were incubated with TiO_2 coated particles.

Figure 4.4 show the neonatal dermal fibroblast incubated for 24 hours with polymeric TiO_2 at concentration of (a) 0.4mg/ml, (b) 0.8mg/ml, (c) 4mg/ml, (d) 10mg/ml, (e) 40mg/m, (f) 80mg/ml exposed to 3.5J/cm2 irradiation. We observed that at lower concentration of polymeric TiO_2 (0.4mg/ml and 0.8mg/ml) the cells were not protected against UV irradiation. Based on this experiment the best concentration of polymeric TiO_2 is 4mg/ml and 10mg/ml. At a higher concentration we observe that the cells show sigh of deterioration.

Figure 4.4g shows the un-exposed neonatal dermal fibroblast coated with 4mg/ml. Confocal microscope pictures show that samples incubated with 4mg/ml TiO_2 nanoparticles and exposed to 3.5 J/cm2 UV light were comparable with the unexposed sample.

We tried different concentration of coated nanoparticles but 4 mg/ml polymeric TiO_2 seems to be the best concentration in order to protect the cells against UV light exposure.In order to prove that the exposed cells are not affected by the dose of UVC light we used two biological assays: Alamar blue and MTS.

4.3.4 Alamar Blue Cell Viability Reagent

Figure 4.5 a, b, c presents cells viability results on day1, day4 and day7 after UVA exposure for the samples coated with 0.8mg/ml regular TiO_2 and 4mg/ml polymeric coated TiO_2. Cells viability and proliferation is indicated through the conversion of resazurin to resorufin. Resazurin, a non-fluorescent indicator dye, is converted to highly red fluorescent resorufin via

reduction reactions of metabolically active cells. The amount of fluorescence produced is proportional to the number of living cells, and hence the florescence was calibrated as discussed previously.

The cells were then counted one, four, and seven days after exposure. The results are plotted in figure 4.5, where we can see that after 24 hours of radiation, there was a decrease of 75% to 92% for the uncoated cells, 21% to 27% for the regular TiO_2 and 2.1% to 2.2% for the cells coated with 4mg/ml polymeric TiO_2. After seven days, the decrease was 99% for the uncoated cells, 63% to 72% for the cells coated with regular TiO_2 and 2% for the cells coated with polymeric TiO_2. Hence the amount of initial damage is proportional to the dose and type of coating. On the other hand the ability of the remaining cells to recover depends on changes in the doubling time.

Figure 4.6 show the cells viability for the samples coated with 10mg/ml polymeric TiO_2 at the concentration of 50,000; 25,000; 12,500; 6,125 and 3125 cells. High density cells exposed to UVC light for 30 minutes shows similar results like the unexposed cells. Based on this data for the cell coated with 10mg/ml polymeric TiO_2 the exposure distance to UV lamp is not significant. We got similar results for the cells exposed to 30 minutes UVC at distance of 50cm versus the 6.5cm (higher UV irradiation dose than 50cm).

Figure 4.7 show the cells viability of the samples coated with 0.4mg/ml polymeric TiO_2 at the concentration of 50,000; 25,000; 12,500; 6,125 and 3125 cells. Based on this data we observe that the concentration of polymeric TiO_2 (0.4mg/ml) is not enough to protect the neonatal against UVC irradiation dose.

Also, figure 4.8 show the cells viability of the samples coated with 0.8mg/ml polymeric TiO_2. We observed that exposed cells to UVC irradiation died at lower and higher dose.

From this data we conclude that two concentration of polymeric TiO2 were effective against UVC irradiation: 4mg/ml and 10mg/ml.

4.3.5 MTS Cell Mitochondrial Activity:

Figure 4.9 a, b, c show the mitochondrial activity on day 1, day 4 and day 7 after UVC irradiation for the uncoated neonatal dermal fibroblast and the 4mg/ml coated polymeric TiO_2. Figure 4.9a shows day1 after the UVC exposure at 2.8J/cm^2 and 3.5J/cm^2 irradiation. We can

see a decreased of 99% of cells energy for the uncoated samples. The coated samples with 4mg/ml polymeric TiO2 shows the same energy level like the un-irradiated control sample. The results are consisted for day4 and day7 where we observed that the un-coated neonatal dermal fibroblast died at the UV irradiation of 2.8 and 3.5J/cm^2.

Figure 4.10 shows the neonatal dermal fibroblast coated with 10mg/ml of 50,000; 25,000; 12,500; 6,250 and 3125 cells. We observed that the high density cells and low density were protected by 10 mg/ml polymeric TiO2. The exposed samples have the same energy level like the un-exposed control samples. Seven days in the incubator after UV irradiation show that the cells were protected against UVC light.

4.4 Conclusion:

In this study, we showed that rutile TiO2 nanoparticles impair cell function and protection against UVC exposure. Particles that were coated with a polymer brush did not adhere to the cells membrane and protect the cells to the exposure of 3.5J/cm2 UV irradiation. Coated TiO2 particles provide good protection for cells against UVA, B and C radiation. We proved that relatively high concentrations of polymeric TiO_2 work best at 4mg/ml and10mg/ml.

We observed that higher concentrations of polymeric TiO_2 block gas and nutrient flow to the neonatal dermal fibroblast.

In order to determine if UVC irradiation does not affect the cells another type of biological assay will be performed in the future work. We proposed the ROS and Apoptosis test to characterize the exposed neonatal dermal fibroblast.

4.5. References

[] Hidaka H., Horikoshi S., Serpone N., and Knowland J., J. Photochem. Photobiol. A, 111,205-213, 1997.

[] Matsumara Y. and Ananthaswamy H., Toxicol. Appl. Pharmacol., 195, 298-308, 2004.

[] Bernard, B.K., Osheroff, M.R.., Mennear, J.H. Toxicology and Carcinogenesis Studies of Dietary Titanium Dioxide-Coated Mica in Male and Female, Fisher 344 Rats. J. Toxicol. Environ.Health 29 : 417-429, 1990.

[] Chen, J.L., Fayerweather, W.E., Epidemiologic Study of Workers Exposed to Titanium Dioxide. J.Occup.Environ. Med. 30, 937-942, 1988.

[] Hart, G.A., Hesterberg, T.W. In vitro toxicity of respirable size particules of diatomaceous earth and crystalline silica compared with asbestos and titanium dioxide. J. Occup.Environ. Med. 40 :29-42, 1998.

[] Oberdorsen, G., Ferin, J., Lehnert, B.E. Correlation between particle size, in vitro particle persistance and lung injury. Environ. Health Perspect. 102, 173-179, 1994.

[] Sayes, C.M., Wahi, R., Kurian, P.A., Liu, Y.P., West, J.L., Ausman, K.D., Warheit, D.B., Colvin, V.L. Correlating nanoscale titanium structure with toxicity : A cytotoxicity and inflamatory response study with human dermal fibroblasts and human lung epithelial cells. Toxicol.Sci.92 :174-185, 2006.

[] Gurr, J.R., Wang A.S.S., Chen, C.H., Jan, K.Y., Ultrafine titanium dioxide particles in the absence of photoactivation can induce oxidative damage to human bronchial epithelial cells. Toxicology 213 :66-73, 2005.

[] Lee, W.A., Pernodet N., Li, B.Q., Lin, C.H., Hatchwell, E., Rafailovich, M.H., Multicomponent polymer coating to block photocatalytic activity of TiO2 nanoparticule. Chem.Commun. 4815-4817, 2007.

[] Pan, Z., Lee, W.A., Slutsky, L., Clark, R.A.F., Pernodet, N., Rafailovich M.H., Adverse effects of titanium dioxide nanoparticle on human dermal fibroblasts and how to protect cells. Small 5 no.4, 511-520, 2009.

4.6. Figure legends:

Figure4.1 SEM images of rutile TiO2 nanoparticles.

Figure4.2. Confocal Microscope pictures of neonatal dermal fibroblast coated with (a) 0.4mg/ml, (b) 0.8 mg/ml, (c) 4mg/ml, (d) 10mg/ml, (e) 40mg/ml and (f) 80mg/ml. (g) Proliferation of neonatal dermal fibroblast incubated with 4mg/ml rutile TiO2 nanoparticle versus un-coated control sample.

Figure 4.3 Confocal images of neonatal dermal fibroblast plated at the density of 100,000 cells/sample and incubated for 24 hours: a) control, unexposed sample versus b) exposed sample to 3.5J/cm2UV light.

Figure 4.4 Neonatal dermal fibroblast incubated for 24 hours with different concentrations of polymeric coated TiO2 a) 0.4mg/ml b) 0.8mg/ml, c) 4mg/ml, d) 10mg/ml,e) 40mg/ml, f) 80mg/ml exposed to 3.5J/cm2 UV light. (g) Unexposed sample at 4 mg/ml. The best concentration of polymeric TiO_2 is 4mg/ml.

Figure 4.5 Alamar blue of neonatal dermal fibroblast on (a) day1, (b) day4, and (c) day7 after UV light exposure. The samples were coated with 0.8mg/ml regular TiO_2 and 4mg/ml polymeric TiO_2. High concentration of polymeric coated particles protects the cells in the culture from UVC irradiation.

Figure 4.6 Alamar Blue of different concentration of neonatal dermal fibroblast coated with 10mg/ml polymeric TiO2 and irradiated with 30’ UVC irradiation at 50cm and 6.5cm away from lamp. (a) day1, (b) day4 and (c) day7 after irradiation.

Figure 4.7 Alamar Blue of different concentration of neonatal dermal fibroblast coated with 0.4mg/ml polymeric TiO2 and irradiated with 30’ UVC irradiation at 50cm and 6.5cm away from lamp. (a) day1, (b) day4 and (c) day7 after irradiation.

Figure 4.8 Alamar Blue of different concentration of neonatal dermal fibroblast coated with 0.8mg/ml polymeric TiO2 and irradiated with 30’ UVC irradiation at 50cm and 6.5cm away from lamp. (a) day1, (b) day4 and (c) day7 after irradiation.

Figure 4.9 MTS assay for the cells coated with 4mg/ml polymeric TiO2 versus the uncoated neonatal dermal fibroblast.

Figure 4.10 MTS assay for neonatal coated with 10mg/ml polymeric TiO2 at different cells concentration.

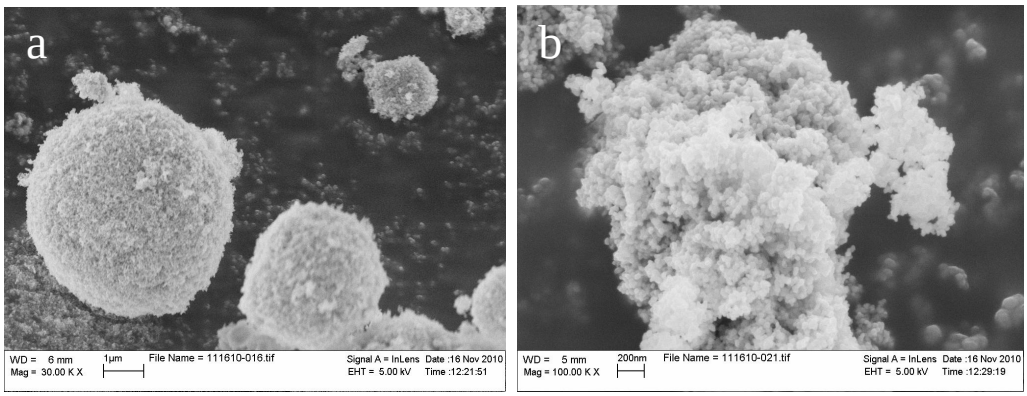
a
WD = 6 mm
Mag = 30.00 K X
1µm
File Name = 111610-016.tif
Signal A = InLens Date :16 Nov 2010
EHT = 5.00 kV Time :12:21:51
b
WD = 5 mm
Mag = 100.00 K X
200nm
File Name = 111610-021.tif
Signal A = InLens Date :16 Nov 2010
EHT = 5.00 kV Time :12:29:19

Figure 4.1

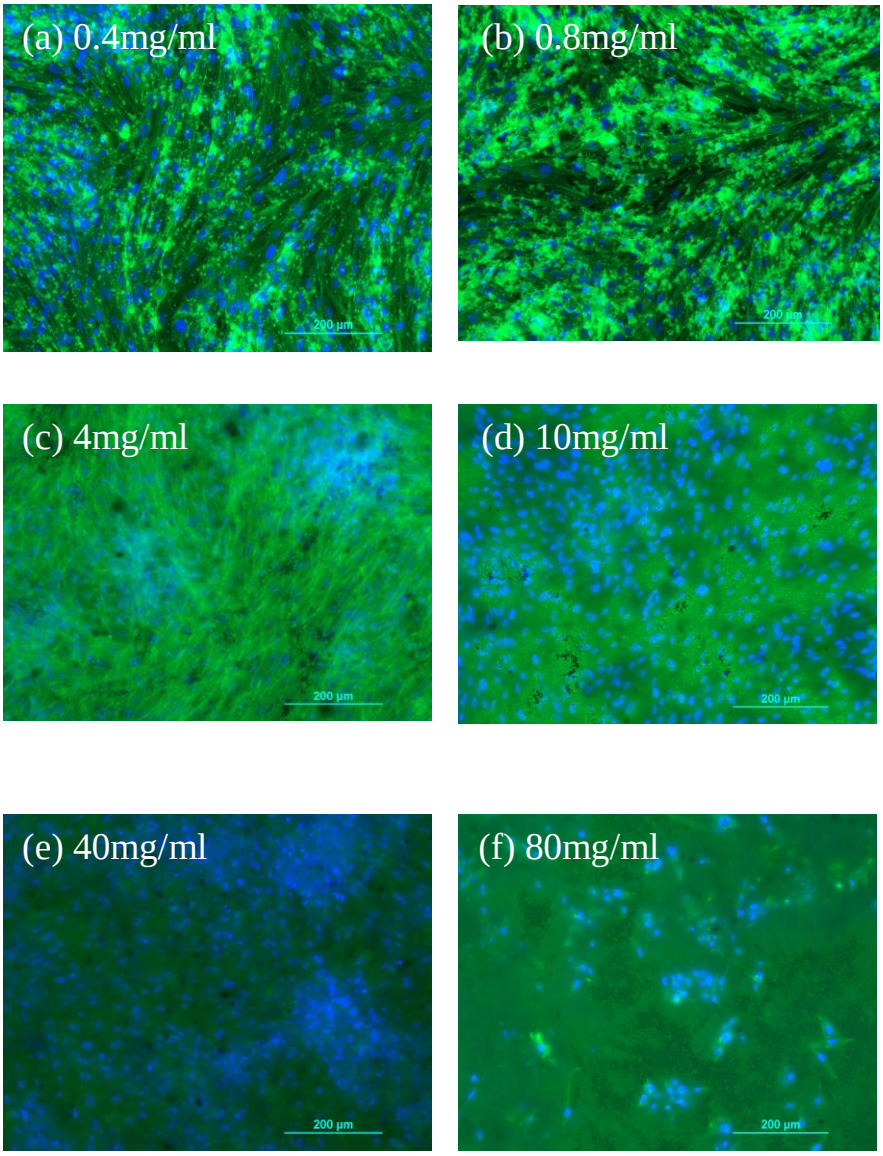
(a) 0.4mg/ml
(b) 0.8mg/ml
(c) 4mg/ml
(d) 10mg/ml
(e) 40mg/ml
(f) 80mg/ml
200 µm

(g)

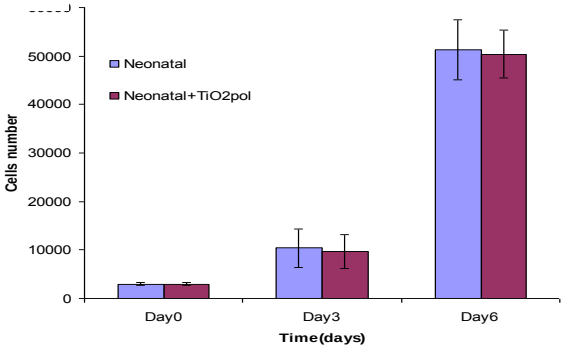
Neonatal
Neonatal+TiO2pol
Cells number
50000
40000
30000
20000
10000
0
Day0
Day3
Day6
Time(days)

Figure 4.2.

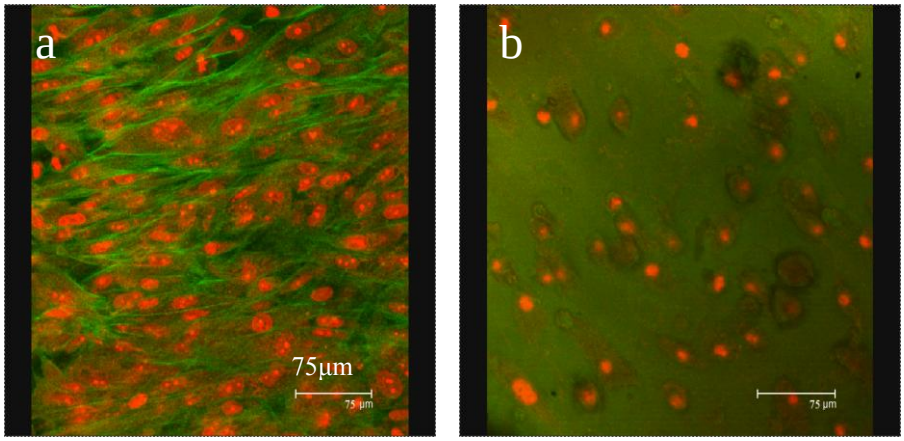

Figure 4.3.

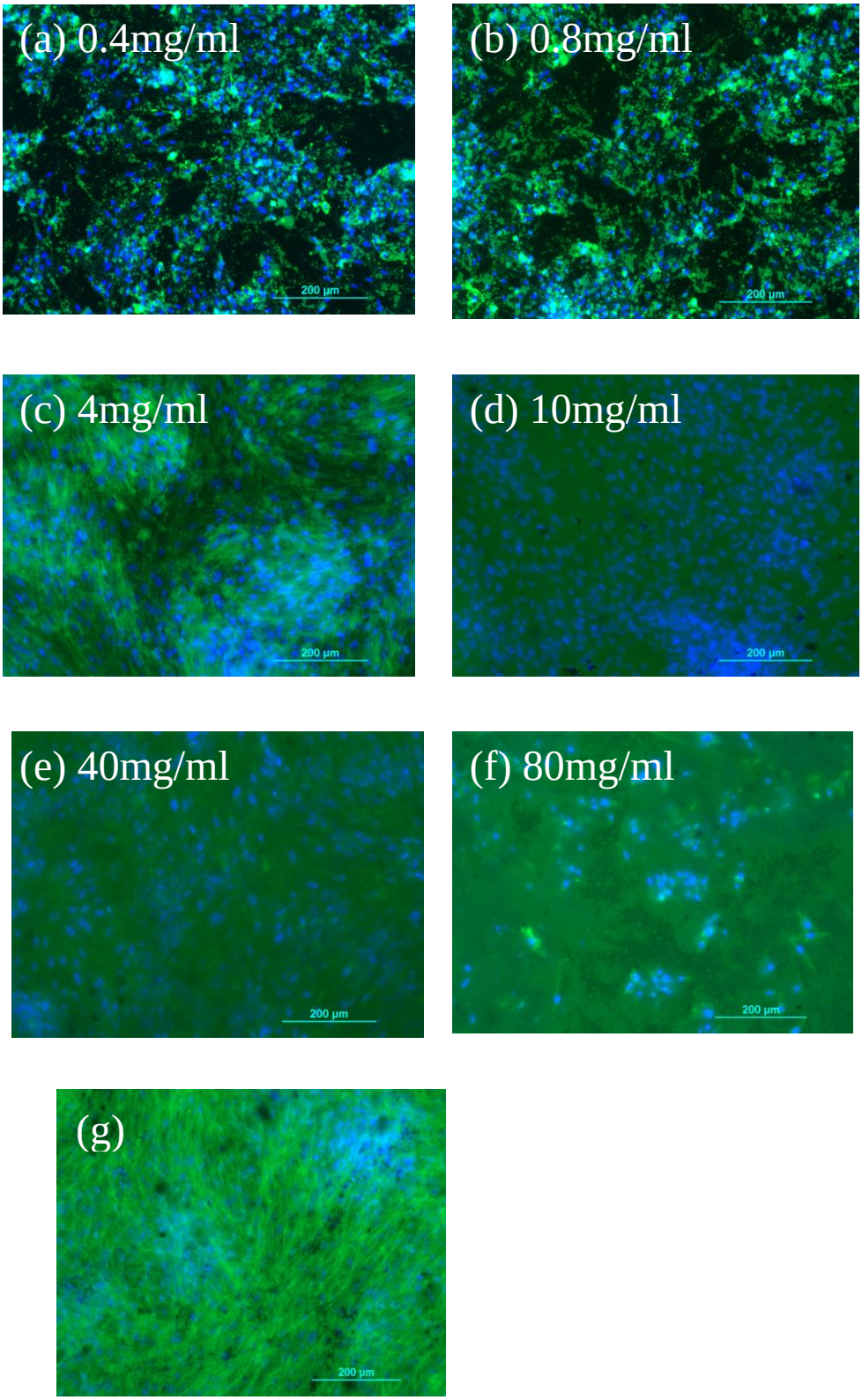
(a) 0.4mg/ml
200 µm
(b) 0.8mg/ml
200 µm
(c) 4mg/ml
200 µm
(d) 10mg/ml
200 µm
(e) 40mg/ml
200 µm
(f) 80mg/ml
200 µm
(g)
200 µm

Figure 4.4

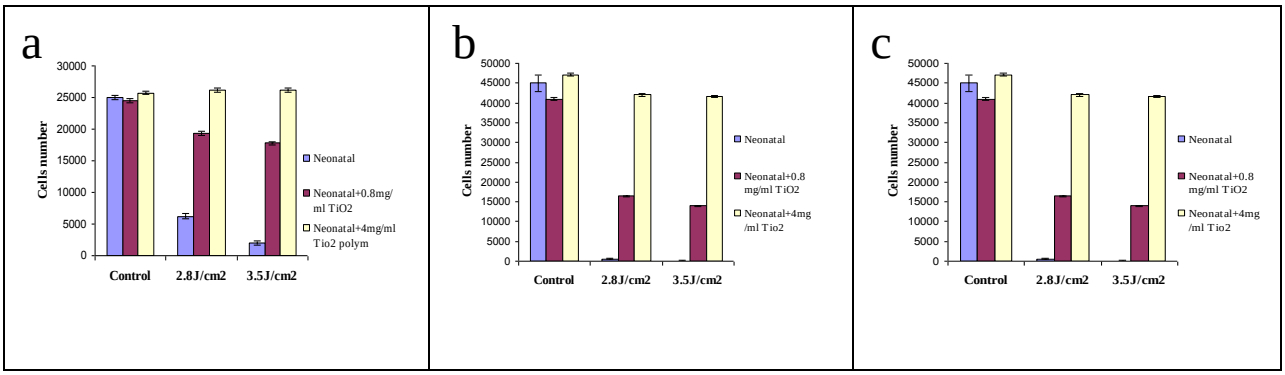
a
Cells number
30000
25000
20000
15000
10000
5000
0
Control
2.8J/cm2
3.5J/cm2
Neonatal
Neonatal+0.8mg/ ml TiO2
Neonatal+4mg/ml Tio2 polym
b
Cells number
50000
45000
40000
35000
30000
25000
20000
15000
10000
5000
0
Control
2.8J/cm2
3.5J/cm2
Neonatal
Neonatal+0.8 mg/ml TiO2
Neonatal+4mg /ml Tio2
c
Cells number
50000
45000
40000
35000
30000
25000
20000
15000
10000
5000
0
Control
2.8J/cm2
3.5J/cm2
Neonatal
Neonatal+0.8 mg/ml TiO2
Neonatal+4mg /ml Tio2

Figure 4.5

a

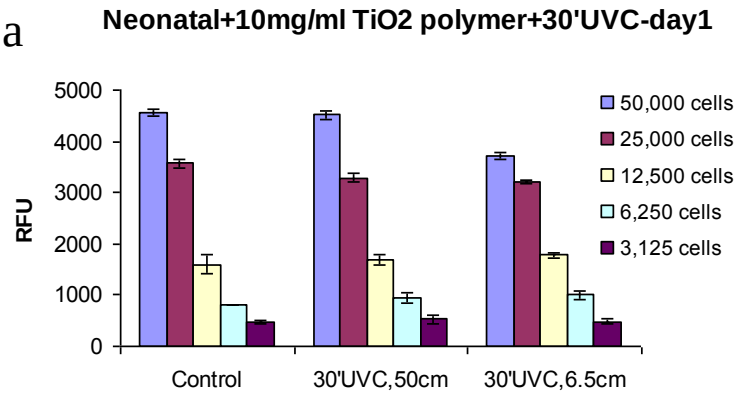
Neonatal+10mg/ml TiO2 polymer+30'UVC-day1
RFU
5000
4000
3000
2000
1000
0
Control
30'UVC,50cm
30'UVC,6.5cm
50,000 cells
25,000 cells
12,500 cells
6,250 cells
3,125 cells

b

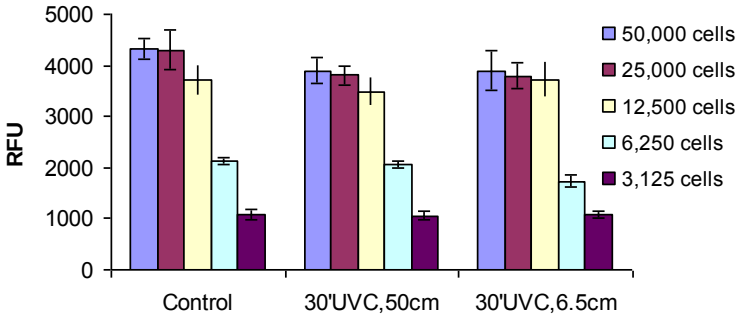
Neonatal+10mg/ml TiO2+30'UVC-day4
RFU
5000
4000
3000
2000
1000
0
Control
30'UVC,50cm
30'UVC,6.5cm
50,000 cells
25,000 cells
12,500 cells
6,250 cells
3,125 cells

c

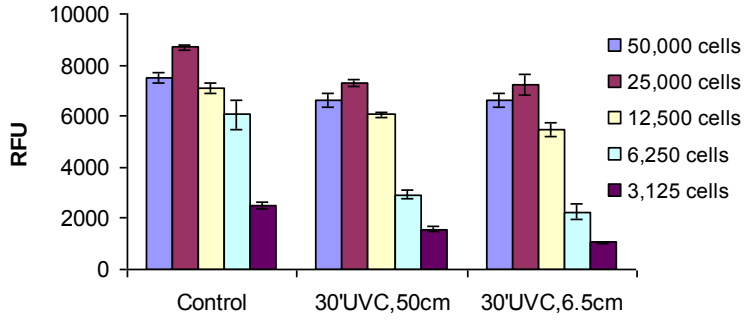
Neonatal+10mg/mlTiO2polymer+30'UVC-day7
RFU
10000
8000
6000
4000
2000
0
Control
30'UVC,50cm
30'UVC,6.5cm
50,000 cells
25,000 cells
12,500 cells
6,250 cells
3,125 cells

Figure 4.6.

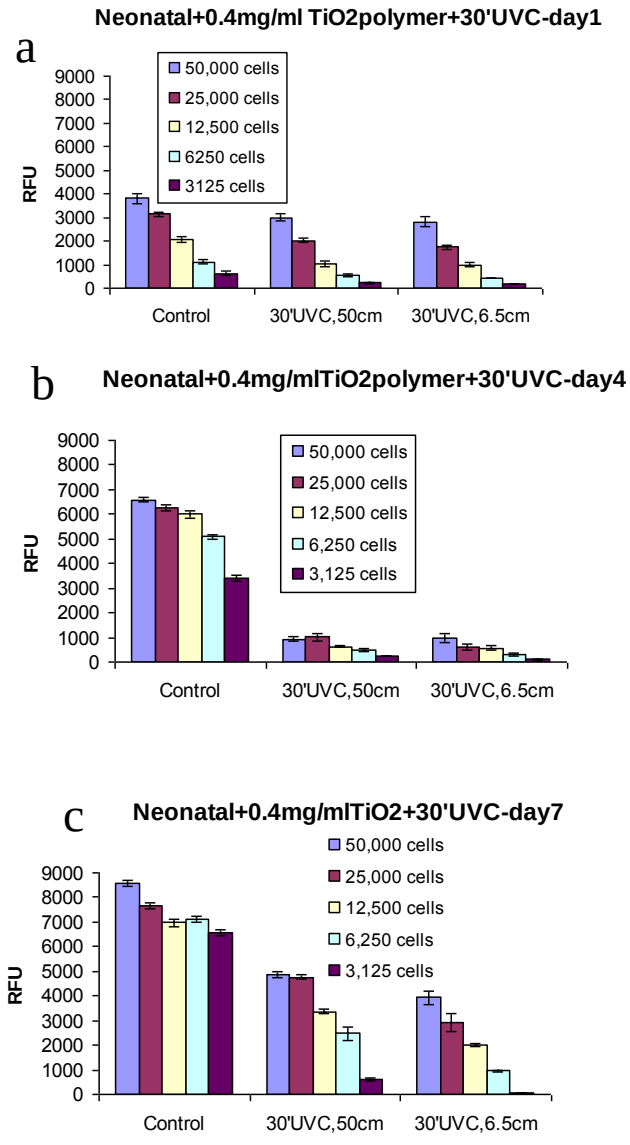

Figure 4.7.

a

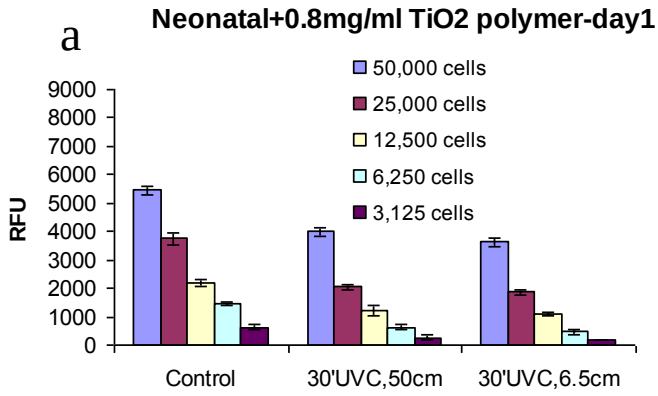
Neonatal+0.8mg/ml TiO2 polymer-day1
50,000 cells
25,000 cells
12,500 cells
6,250 cells
3,125 cells
RFU
9000
8000
7000
6000
5000
4000
3000
2000
1000
0
Control
30'UVC,50cm
30'UVC,6.5cm

b

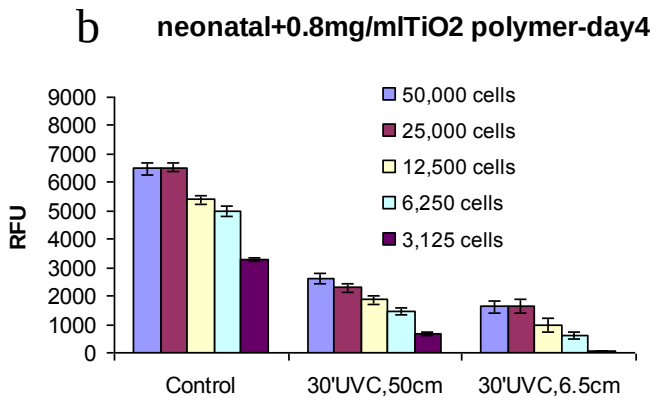
neonatal+0.8mg/mlTiO2 polymer-day4
50,000 cells
25,000 cells
12,500 cells
6,250 cells
3,125 cells
RFU
9000
8000
7000
6000
5000
4000
3000
2000
1000
0
Control
30'UVC,50cm
30'UVC,6.5cm

c

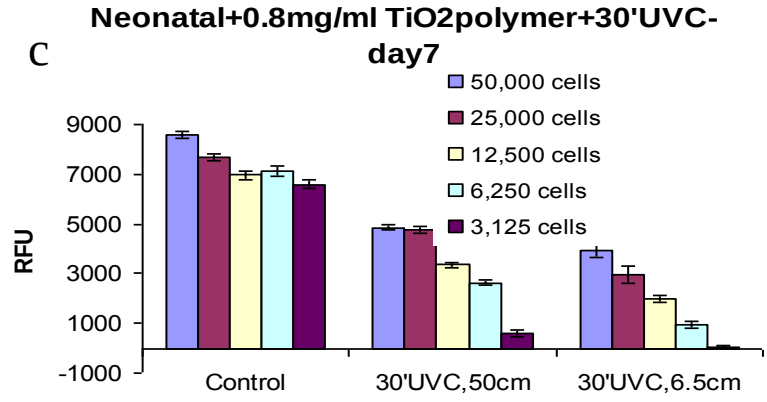
Neonatal+0.8mg/ml TiO2polymer+30'UVC-day7
50,000 cells
25,000 cells
12,500 cells
6,250 cells
3,125 cells
RFU
9000
7000
5000
3000
1000
-1000
Control
30'UVC,50cm
30'UVC,6.5cm

Figure 4.8

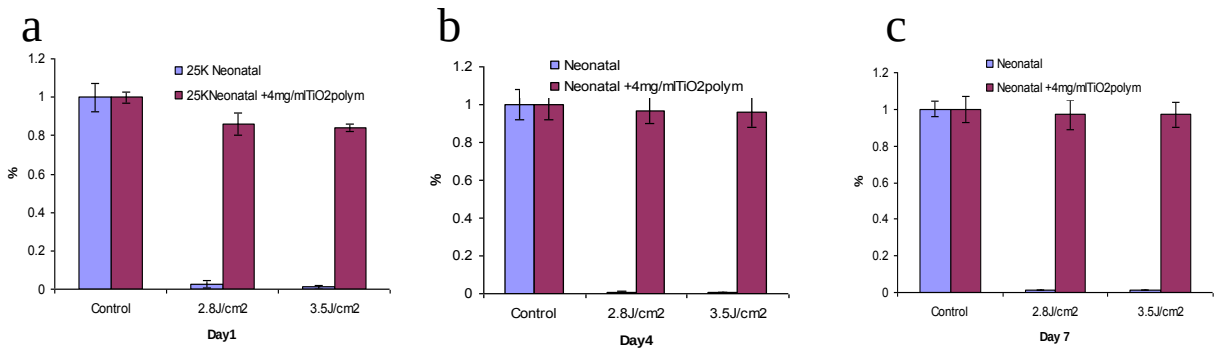

Figure 4.9.

a

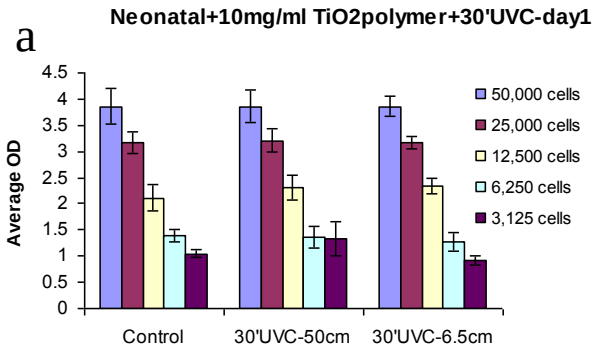

b

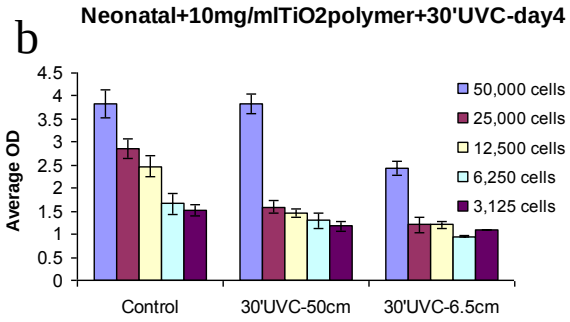

c

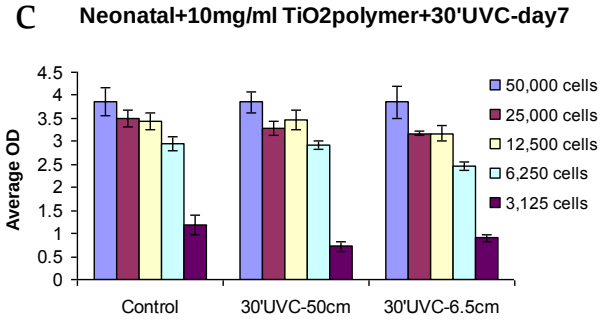

Figure 4.10

References:

[] Langer, R, Vacanti JP, Tissue Engineering. Science, 260, 920-6.1993.

[] Macarthur, B.D., Oreffo, Bridging the gap. R.O.C.Nature, 433, 19, 2005.

[] Badylak, SF. Small intestine sub mucosa (SIS): A biological conducive to smart tissue removed. Tissue engineering: current prospective. Cambridge, MA: Burkhauser Publishers, 1993.

[] McPherson T, Badylak SF. Characterization of fibronectin derived from porcine small intestine sub mucosa. Tissue Engineering 4:75-81, 1998.

[] Sterodimas A, Denair J, Correa WE, Pitaguy I, Tissue engineering in plastic surgery: an up to date review of the current literature, Ann. Plast. Surg. January; 62(1):97-103, 2009.

[] Thomas D. McKnight, Karel Riha, Dorothy E. Shippen, telomeres, telomerase and stability of the plant genome; Plant Molecular biology, vol 48, nr.4, march 2002.

[] Madigan M., Martinko J. (editors) Brosk Biology of Microorganism; 11th edition, Prentice Hall. ISBN 0131443291, 2005.

[] Kanof ME, smith PD, Zola H.; Isolation of whole mononuclear cells from peripheral blood and cord blood; Curr protoc. Immunol. May, chapter 7, unit 7.1, 2001.

[] Celentano DC, Frishman WH.; Matrix metalloproteinase and coronary artery disease: a novel therapeutic target; J.Ciln.Pharmacol. Nov; 37(11):991-1000, 1997.

[] Ito Y, Shinoda M; Influences of proteolytic enzymes on parotin IV. Separation of hydrolyzes in digested parofin by trypsin. (Studies on the physiological chemistry of the salivary glands). Endocr. J., Mar; 8:13-9, 1961.

[] Lorette C. Javois; Methods in Molecular Bilogy: Immunocytochemical Methods and Protocols, Second Edition, vol 115, 257-260, 1999.

[] Hendrick M, Daniels E., The use of stem cells in regenerative medicine; Clinics in Plastic Surgery, vol 30, issue 4, page 499-505, 2003.

[] Griffith, L.G., Naughton, G. "Tissue Engineering – Current Challenges and Expanding Opportunities." *Science*. 295 , 1009-1014, 2002.

[] Kushida, A., Yamato, M., Konno, C., Kikuchi, A., Sakurai, Y., Okano, T. "Temperature-responsive culture dishes allow non-enzymatic harvest of differentiated Madin-Darby canine kidney (MDCK) cell sheets." *J. Biomed. Mater. Res.* 51, 216-223, 2000.

[] Kwon, O.H., Kikuchi, A., Yamato, M., Sakurai, Y., Okano, T. "Rapid cell sheet detachment from Poly (*N*-isoproplyacrylamide)-grafted porous cell culture membranes." *J. Biomed. Mater. Res.* 50, 82-89, 2000.

[] Langer, R., Vacanti, J.P. "Tissue Engineering." *Science.* 260, 920-926. 1993.

[] Ng, K.W., Tham, W., Lim, T.C., Hutmacher, D.W. "Assimilating cell sheets and hybrid scaffolds for dermal tissue engineering." *J. Biomed. Mater. Res.* 75A, 425-438, 2005.

[] Ronneberger, B., Kao, W.J., Anderson, J.M., Kissel, T. "In vivo biocompatibility study of ABA triblock copolymers consisting of poly (L-lactic-co-glycolic acid) A blocks attached to central poly (oxyethylene) B blocks. *J. Biomed. Mater. Res*. 24, 529-545, 1990.

[] Shimizu, T., Yamato, M., Kikuchi, A., Okano, T. “Cell sheet engineering for myocardial tissue engineering.” *Biomaterials*. 24 (2003): 2309-2316.
[] Soejima, K., Negishi, N., Nozaki, M., Sasaki, K. “Effect of cultured endothelial cells on angiogenesis in vivo.” *Plast. Reconstr. Surg*. 1010, 1552-1560, 1998.

[] Yamato, M., Okano, T. “Cell Sheet Engineering.” *Materials Today*. 7, 42-47, 2004.

[] Yang, J., Yamato, M., Kohno, C., Nishimoto, A., Sekine, H., Fukai, F., Okano, T. “Cell sheet engineering: Recreating tissues without biodegradable scaffolds.” *Biomaterials*. 26 6415-6422, 2005.

[] Yang, J., YaRonneberger, B., Kao, W.J., Anderson, J.M., Kissel, T. “In vivo biocompatibility study of ABA triblock copolymers consisting of poly (L-lactic-co-glycolic acid) a blocks attached to central poly (oxyethylene) B blocks. *J. Biomed. Mater. Res*. 24, 529-545, 1990.

[] Yang, J., Yamato, M., Shimizu, T., Sekine, H., Ohashi, K., Kanzaki, M., Ohki, T., Nishida, K., Okano, T. “Reconstruction of functional tissues with cell sheet engineering.” *Biomaterials.* 28, 5033-5043, 2007.

[] Yamato, M., Shimizu, T., Sekine, H., Ohashi, K., Kanzaki, M., Ohki, T., Nishida, K., Okano, T. “Reconstruction of functional tissues with cell sheet engineering.” *Biomaterials.* 28, 5033-5043, 2007.

[] Masayuki Yamato, Mika Utsumi, Ai Kushida, Chie Konno, Akihiko Kikuchi, Teruo Okano. Tissue Engineering, 7(4): 473-480, 2001.

[] A. Welle, E. Gottwald, K.F. Weibezahn. Biomed Tech (Berlin), 47 Suppl. 1 Pt 1:401-3, 2002.

[] Olberding JE., Suh JKF "A dual optimization for the material parameter identification of a biphasic poroviscoelastic hydrogel: potential application to hypercompliant soft tissue" journal of Biomechanics, 30, 13, 2468-2475, 2006.

[] Okano T, editor. Biorelated polymers and gels-controlled release and application in biomedical engineering. San Diego, CA: Academic Press, 1998.

[] Peppas NA, Klier J. Controlled release by using poly (methacryl acid-g-ethylene glycol) hydrogels. J Control Release; 16:203-214, 1991.

[] Yoshida R, Sakai K, Okano T, Sakurai Y, Bae YH, Kim SW. Surface-modulated skin layers of thermal responsive hydrogels as on-off switches: I. Drug release. J Biomater Sci Polym Ed; 3:155-162, 1991.

[] Yoshida R, Sakai K, Okano T, Sakurai Y. Surface modulated skin layers of thermal responsive hydrogels as on-off switches: II. Drug permeation. J Biomater Sci Polym Ed; 3:243-252, 1992.

[] Stayton PS, Shimoboji T, Long C, Chilkoti A, Chen G, Harris JM, Hoffman AS. Control of protein-ligand recognition using stimuli-responsive polymer. Nature; 378:472-474, 1995.

[] Hosino K, Taniguchi M, Marumoto H, Fujii M. Repeated batch conversion of raw starch to ethanol using amylase immobilized on a reversible soluble-autoprecipitating carrier and flocculating yeast cells. Agric Biol Chem; 53:1961-1967, 1998.

[] Eisenberg SR, Grodzinsky AJ. Electrically modulated membrane permeability. J Membr Sci; 19:173-194, 1984.

[] Yuk SH, Cho SH, Lee HB. Electric current-sensitive drug delivery systems using sodium alginate/polyacrylic acid composites. Pharm Res; 9:955-957, 1992.

[] Kwon IC, Bae YM, Kim SW. Electrically erodible polymer gel for controlled release of drugs. Nature; 354:291-293, 1991.

[] Irie M, Iwayanagi T, Taniguchi Y. Photoresponsive polymers reversible solubility change of polystyrene having pendant spinobenzopyran groups and its application to photo resists. Macromolecus; 18:2418-2422, 1985.

[]Ito Y, Sugimura N, Kwon OH, Imanishi Y. Enzyme modification by polymers with solubilities that change in response to photo irradiation in organic media. Nat Biotechnol; 17:73-75, 1999.

[] M. Gautschi, J.A. Bajgrowicz and P. Kraft, Fragrance cheering milestones and perspectives, Chimia, 55,379, 2001.

[] S. Rochat, C. Minardi, J.Y. de Saint Laumer and A. Hermin: Control release of perfumery aldehydes and ketones by Norrishing Type II photo fragmentation of α-keto esters in undegasses solution. Helv. Chim.Acta, 83, 1645, 2000.

[] H. Kamogawa, S.Okabe, M. Nanasawa, Synthesis of polymerizable Acetals, Bull. Chem. Soc. Jpn., 49, 1917, 1976.

[]P. Enggist,S. Rochat, A. Herrmann, Controlled release perfumery alcohols by alkaline hydrolysis of 2-formyl acethylbenzoates and their corresponding phthalides, J. Chem. Perkin trans.2, 438, 2001.

[]A. Herrmann, C. Debonneville, V. Laubscher, Dynamic headspace analysis of the light-induced controlled release of perfumery aldehydes and ketones from L-keto esters in household application, Flavor fragrance J., 15, 41, 2000.

[] D.C. Neckers, R.M. Kellogg, W.L.Prins and B. Schoot. Developmental Photochemistry. The Norrish type II reaction J.Org. Chem., 36, 1838, 1971.

[] W.W. Epstein, D.S. Jones, E. Bruenger and H.C. Rillling, The synthesis of a photo-labile detergent and its use in the isolation characterization of protein, anal. Biochem, 119, 304, 1982.

[] B.Levrand, A. Herrmann, Light induced controlled release of fragrances by Norrish type II photo fragmentation of alkyl phenyl ketones, Firmenich, 2002.

[] R.G.D. Norrish, Trans.Faraday Soc., 33, 1521, 1937

[] Scaiano, J.C. and Selwyn, J. C. Macromolecules 14, 1723, 1981.

[] P.J.Wagner, Type II photo elimination and photocyclization of ketones, Acc. Chem.Res. 4, 168, 1976.

[ ] P.J.Wagner, Chemistry of excited triplet organic carb. Compounds, Top. Curr, Chem., 66, 1, 1976.

[] N.C.Yang and D.H. Yang, J. Amer. Chem. Soc., 80, 2913, 1958.

[] P.J.Wagner and G.S. Hammond, J. Amer. Chem., Soc., 88, 1245, 1966.

[] Grotewold, J.,Soria, D, Previtali, C.M, Scaiano, J. C.J.Photochemistry 1, 471, 1972/1973.

[] A.A.Lamola, J.Chem. Phys., 47, 4810, 1967.

[] David, C., Demarteau, W. Geuskens, G. Polymer Lond. 8, 497,1967.

[] C. David, W. Dermateau. F. Derom, and G. Geuskens, Notes and communication, Service de Chimie Générale II, Université Libre de Bruxelles, Brussels, Belgium, August, 15, 1969.

[] K.H.Schulte-Elte and G.Ohloff, Tetrahedron Lett. 1143,1964.

[] A. E. Kemppainen, unpublished results.

[] P.J.Wagner and G. Capen, Mol. Photochem., 1, 173, 1969.

[] G.Nenkov, T. Bogdantsaliev, T.Georgieva and V. Kabaivanov; Polymer Photochemistry (6) (1985) Elsevier Applied science Publishers Ltd.England, 1985.

[] G. Nenkov, T. Bogdantsaliev, T. Georgieva and V. Kabaivanov: Scientific Ind. Centrum for Special Polymers, 11576, Sofia, Polymer Photochemistry (6), 475-482, 1985.

[] Amerik, Y. and Guillet, J.E., Macromolecules, 4, 375-9,1971.

[] P.J.Wagner, Type II photo elimination and photocyclization of ketones, Acc ChemRes., 4,168, 1974.

[] Hrdlovic, P., Lucas, I. International Conference on advance in stabilization and Controlled degradation of polymers: Patsis, A.V.E, Technomic, Lancaster, PA, Vol2, pp66-78, 1989.

[] Dan, E. and Guillet, J.E.: Macromolecules, 6, 230-5, 1973.

[] M.V. Encinas, K. Funabashi, and J.C. Scaiano Triplet energy migration in polymer photochemistry. A model for the photo degradation of Poly (phenyl vinyl ketone) in solution. American Chemical Soc., vol12, no 6, 1979.

[] W.D.K.Clark, A.D.Litt and C.Steel, J. Amer. Chem. Soc.,91, 5413 (1969); G. Porter and M.R.Topp, Proc. Roy. Soc., Ser. A.315, 163,1970.

[] A.Ishizaka, Y. Shiraki, J. Electroche. Soc., Low temperature surface cleaning of silicon and its application to silicon MBE, 133, 4:666-671, 1986.

[] Ronneberger, B., Kao, W.J., Anderson, J.M., Kissel, T. "In vivo biocompatibility study of ABA triblock copolymers consisting of poly (L-lactic-co-glycolic acid) A blocks attached to central poly (oxyethylene) B blocks. *J. Biomed. Mater. Res*. 24, 529-545, 1990.

[] A. Welle, E. Gottwald, K.F. Weibezahn. Biomed Tech (Berlin), 47 Suppl. 1 Pt 1:401-3, 2002.

[12] Wilzback K.E. and Rausch D.J: J. Am. Chem. Soc. 92:7, 2178-2179, 1970.

[13] Nishiyama S, Tajima M, Yoshida Y.: Photo-irradiation effects on poly (vinyl pyridines): Colloids and Surfaces A: Physicochem.Eng.Aspects 313-314, 479-483, 2008.

[14] Rozenberg M, Vaganova E., Yitzchaik S., FTIR study of self-protonation and gel formation in pyridinic solution of poly (4-vynilpyridine), NJC 24, pp.109-112, 2000.

[15] Vaganova E., Meshulam G., Kotler Z., Rozenberg M. and Yitzchair S., Photoinduced structural changes in Poly (4-Vinyl Pyridine): A luminescence study, Jor. Fluorescence, vol10, no.2, 2000.

[16] Freitag H., Chem. Ber. 69B, 32-35, 1936.

[17] Vaganova E., Damm C., Israel G., Yitzchaik S.: Photoinduced Pyridine Cleavage-Closure in Viscous Polymer Solution: Journal of Fluorescence, Vol.12, No. 2, 2007.
[19] Wei S., Vaidya B., Patel A., Soper S., McCarley R.: Photochemical Patterned Poly (methyl methacrylate) Surfaces Used in the Fabrication of Micro analytical devices, J.Phys. Chem., 109, 16988-16996, 2005.

[]Soper, S.A,; Ford,S.M.;Qi, S.;McCarley, R.L.; Kelly,K.; Murphy, M.C.; Anal Chem. 72,642A-651A, 2000.

[] Boone, T.D.; Fan, Z. H.; Hopper H.H.; Ricco, A. J.;Tan, H.; Williams, S.J. Anal Chem.,74,78A-86A, 2002.

[] Becker, H.; Locascio,L.e. Talanta , 56, 267-287, 2002.

[] McCarley, R.L.; Vaidya,B.; Wei S.; Smith A.F.;Patel,A.B.; Feng,J.; Murphy, M.C.;Soper, S.A. J.Am. Chem.Soc., 127, 842-843, 2005.

[] F.J.Wu, et al.: Enhanced cytochrome P450 IA1 activity of self-assembled rat hepatocytes spheroids, Cell Transplantation, vol.8, pp.233-246, 1999.

[] S.N.Bhatia et al., Probing heterotypic cell interaction: Hepatocyte function in micro fabricated co-cultures, J.Biomater. Sci. Polym. Edn. Vol. 9, pp.1137-1160, 1998.

[] D.E.Ingber, Engineering cell shape and function through control of substrate adhesion, in Polymer Surfaces and Interfaces: Characterization, Modification and Application, K.L.Mittaland K.W. Lee, Editors, VSP: Utrecht, The Netherlands, p.413-424, 1997.

[] S.N.Bhatia and C.S.Chen, tissue engineering at the Micro-scale, Biomedical Micro devices, vol.2, pp 131-144, 1999.

[] A. Welle and E. Gottwald, UV-based patterning of polymer substrates for cell culture application, Biomed. Microdev. Vol.4, pp.33-41, 2002.

[] Hidaka H., Horikoshi S., Serpone N., and Knowland J., J. Photochem. Photobiol. A, 111,205-213, 1997.

[] Matsumara Y. and Ananthaswamy H., Toxicol. Appl. Pharmacol., 195, 298-308,2004.

[] Scharffetter-Kochanek K, Brenneisen P, Wenk J. et al. Photoaging of the skin from phenotype to mechanism. Exp.Gerontol.35: 307-316, 2000.

[] Holbrook, N.J, Liu Y, Fornace A.J Signaling events controlling the molecular response to genotoxic stress, EXS 77:273-288, 1996.

[] Shaulian, E, Schreiber M, Piu F, The mammalian UV response: c-Jun induction is required for exit from p53-imposed growth arrest. Cell 103: 897-907, 2000.

[] Karin, M, Mitogen activated protein kinase cascades as regulators of stress responses. Ann.N.Y.Acad. Sci.851:139-146, 1998.

[] Shackelford R.E, Kaufmann W.K, Paules R.S Cell cycle control, check-point mechanism, and genotoxic stress. Environ. Health Perspect.107 (suppl.1): 5-24, 1999.

[] Brenneisen P, Oh J, Wlaschen M, Ultraviolet B wavelength dependence for the regulation of two major matrix-metalloproteinases and their inhibitor TIMP-1 in human dermal fibroblast. Photochem. Photobiol. 64:877-885, 1996.

[] Fisher G.T, Datta S.C, Talwar H.S, Molecular basis of sun-induced premature skin aging and retinoid antagonism. Nature 379: 335-339, 1996.

[] Halliwell, B. and Aruoma O.I. DNA damage by oxygen-derived species. Its mechanism and measurement in mammalian systems. FEBS Lett. 281:9-19, 1991.

[] Mount D.W. DNA repair. Reprogramming transcription. Nature 383:763-764,1996.

[] Blattner C., Bender K., Herrlich P., Pahmsdorf H.J. Photoproducts in transcriptionally active DNA induce signal transduction to the delayed ultraviolet-responsive genes for collagenase and matallothionein. Oncogene 16: 2827-2834., 1998.

[] Nordberg J., and Arner E.S. Reactive oxygen species, antioxidants, and the mammalian thioredoxin system. Free Radical. Biol. Med. 31: 1287-1312, 2001.

[] Hancock J.T., Desikan R. and Neill S.J. 2001. Role of reactive oxygen species in cell signaling pathways. Biochem. Soc. Trans. 29: 345-350, 2001.

[] Wlaschek M., Briviba G.P., Stricklin G.P. Singlet oxygen may mediate the ultraviolet A-induced synthesis of interstitial collagenase.J. Invest. Dermatol. 104 , 194-198, 1995.
[] Masaki H., Atsumi T., Sakurai. Detection of hydrogen peroxide and hydroxyl radicals in murine skin fibroblast under UVB irradiation. Biochem. Biophys. Res. Commun. 206 , 474-479, 1995.

[] Jurkiewicz B.A., Buettner G.R. Ultraviolet light-induced free radical formation in skin : an electron paramagnetic resonance study. Photochem. Photobiog.59, 1-4, 1994.

[] Wills EE, AndersonTW, Beattie BL, et al. Randomized placebo-controlled trial of ultraviolet light in the treatment of superficial pressure sores. J.Amer. Geriatr. Soc 31, 131-3, 1983.

[] Naussbaum RL, Biemann I, Mustard B. Comparison of ultrasound/ultraviolet-C and laser for treatment of pressure ulcers in patients with spinal cord injury. Phys Ther 74 :812-25, 1994.

[] Kloth LC. Physical modalities in wound management : UVC, therapeutic healing and electrical stimulation. Ost. Wound. Manag 41, 18-27, 1995.

[] Ellem KAO, Culliman M, Baumann KC, et al. UVR induction of TGFa : a possible autocrine mechanism for the epidermal melanocytic response and for promotion of epidermal carcinogenes. Carcinogenesis 5 :797-801, 1988.

[] Ley KD, Ellem KAO. UVC modulation of epidermal growth factor receptor number in HeLaS3 cells. Carcinogenesis 13 :183-7, 1992.

[] Sachsenmaier C, Radler-Pohl A, Zinck R, et al. Involvement of growth factor receptors in the mammalian UVC response. Cell 78 :963-72, 1994.

[] Huang R, Wu J, et all. UV activatesgrowth factor receptors via reactive oxygen intermediates. J Cell Biol 133 :211-20, 1996.

[] Bell E, Ivarsson B, Merrill C. Production of a tissue-like structure by contraction of collagen lattices by human fibroblast of different proliferative potential in vitro. Proc Nat Acad. Science USA 76 :1274-8, 1979.

[] Gillery P, Maquart FX, Borel JP. Fibronectin dependence of the contraction of collagen lattices by human dermal fibroblasts. Exp Cell Res 167, 29-37, 1986.

[] Marks MW, Morykwas MJ, Wheatley MJ. Fibroblast mediated contraction in actinally exposed and actinically protected aging skin. Plast Reconstr Surg 86, 255-9, 1990.

[] Pieraggi MT, Julian M, Bouissou H. Fibroblast changes in cutaneous aging. Virchows Arch A pathol Anat Histolpathol 402, 275-87, 1984.

[] Morykwas m, Malcolm M, Effects of ultraviolet light on fibroblast fibronectin production and lattice contraction. Wounds, 10(4), 111-117, 1998.

[] Hidaka H., Horikoshi S., Serpone N., and Knowland J., J. Photochem. Photobiol. A, 111,205-213, 1997.

[] Matsumara Y. and Ananthaswamy H., Toxicol. Appl. Pharmacol., 195, 298-308, 2004.

[] Bernard, B.K., Osheroff, M.R.., Mennear, J.H. Toxicology and Carcinogenesis Studies of Dietary Titanium Dioxide-Coated Mica in Male and Female, Fisher 344 Rats. J. Toxicol. Environ.Health 29 : 417-429, 1990.

[] Chen, J.L., Fayerweather, W.E., Epidemiologic Study of Workers Exposed to Titanium Dioxide. J.Occup.Environ. Med. 30, 937-942, 1988.

[] Hart, G.A., Hesterberg, T.W. In vitro toxicity of respirable size particules of diatomaceous earth and crystalline silica compared with asbestos and titanium dioxide. J. Occup.Environ. Med. 40 :29-42, 1998.

[] Oberdorsen, G., Ferin, J., Lehnert, B.E. Correlation between particle size, in vitro particle persistance and lung injury. Environ. Health Perspect. 102, 173-179, 1994.

[] Sayes, C.M., Wahi, R., Kurian, P.A., Liu, Y.P., West, J.L., Ausman, K.D., Warheit, D.B., Colvin, V.L. Correlating nanoscale titanium structure with toxicity : A cytotoxicity and inflamatory response study with human dermal fibroblasts and human lung epithelial cells. Toxicol.Sci.92 :174-185, 2006.

[] Gurr, J.R., Wang A.S.S., Chen, C.H., Jan, K.Y., Ultrafine titanium dioxide particles in the absence of photoactivation can induce oxidative damage to human bronchial epithelial cells. Toxicology 213 :66-73, 2005.

[] Lee, W.A., Pernodet N., Li, B.Q., Lin, C.H., Hatchwell, E., Rafailovich, M.H., Multicomponent polymer coating to block photocatalytic activity of TiO2 nanoparticule. Chem.Commun. 4815-4817, 2007.

[] Pan, Z., Lee, W.A., Slutsky, L., Clark, R.A.F., Pernodet, N., Rafailovich M.H., Adverse effects of titanium dioxide nanoparticle on human dermal fibroblasts and how to protect cells. Small 5 no.4, 511-520, 2009.